Applied Thermal Engineering 185 (2021) 116447

Contents lists available at ScienceDirect

Applied Thermal Engineering

journal homepage: www.elsevier.com/locate/ate

Review of supercritical CO_2 technologies and systems for power generation

Martin T. White [a,*], Giuseppe Bianchi [b], Lei Chai [b], Savvas A. Tassou [b], Abdulnaser I. Sayma [a]

[a] Thermo-Fluids Research Centre, School of Mathematics, Computer Science and Engineering, City, University of London, Northampton Square, London, EC1V 0HB, UK

[b] Centre for Sustainable Energy Use in Food Chains, Institute of Energy Futures, Brunel University London, Kingston Lane, Uxbridge, Middlesex, UB8 3PH, UK

ARTICLE INFO

Keywords:
Supercritical carbon dioxide
sCO_2
Power generation
Turbomachinery
Heat exchangers
Control systems
Applications

ABSTRACT

Thermal-power cycles operating with supercritical carbon dioxide (sCO_2) could have a significant role in future power generation systems with applications including fossil fuel, nuclear power, concentrated-solar power, and waste-heat recovery. The use of sCO_2 as a working fluid offers potential benefits including high thermal efficiencies using heat-source temperatures ranging between approximately 350 °C and 800 °C, a simple and compact physical footprint, and good operational flexibility, which could realise lower levelised costs of electricity compared to existing technologies. However, there remain technical challenges to overcome that relate to the design and operation of the turbomachinery components and heat exchangers, material selection considering the high operating temperatures and pressures, in addition to characterising the behaviour of supercritical CO_2. Moreover, the sensitivity of the cycle to the ambient conditions, alongside the variable nature of heat availability in target applications, introduce challenges related to the optimal operation and control. The aim of this paper is to provide a review of the current state-of-the-art of sCO_2 power generation systems, with a focus on technical and operational issues. Following an overview of the historical background and thermodynamic aspects, emphasis is placed on discussing the current research and development status in the areas of turbomachinery, heat exchangers, materials and control system design, with priority given to experimental prototypes. Developments and current challenges within the key application areas are summarised and future research trends are identified.

1. Introduction and motivation

Since the industrial revolution, societies throughout the world have remained reliant on fossil fuels to provide heat, which is subsequently converted into electricity through thermodynamic power cycles. Unfortunately, this reliance on fossil-fuelled power generation to sustain economic growth has taken its toll on the environment through greenhouse gas emissions, leading to global warming, alongside environmental pollution. As such, over the past few decades there has been a rapid growth in the deployment of renewable energy technologies, such as solar photovoltaics and wind, which no longer rely on thermodynamic power cycles. However, to meet the need for secure, reliable, clean and sustainable energy, it is widely acknowledged that a broad portfolio of energy conversion and storage technologies will be required. This is likely to include nuclear power generation, concentrated-solar power plants, and the use of blue and green hydrogen, alongside the implementation of technologies to improve overall energy efficiency, such as waste-heat recovery, and the continued use of fossil fuels, ultimately with carbon capture and storage [1,2]. Thus, thermodynamic power cycles will likely remain a pivotal component within future energy networks.

Existing thermodynamic power cycles, such as the Rankine cycle and the Joule–Brayton cycle, typically operate with water or air respectively. However, in the drive towards higher cycle thermal efficiencies, and to overcome some of the technical challenges related to existing cycles, attention has turned to the use of alternative working fluids. As such, supercritical carbon dioxide (sCO_2) power cycles have been put forward as a promising candidate with the main advantages being high thermal efficiencies from heat sources ranging between 350 °C and 800 °C, a simple and compact physical footprint, and good operational flexibility to cope with the uncertain availability of renewable energy sources. The potential of sCO_2 is confirmed by the significant growth in research within the last decade, alongside the financial support that has been made available internationally to aid technological advancement.

This rapid growth in research, and the potential of sCO_2 power cycles, warrant a detailed review of current research activities, alongside the most promising applications and future research trends. A

* Corresponding author.
E-mail addresses: martin.white@city.ac.uk (M.T. White), giuseppe.bianchi@brunel.ac.uk (G. Bianchi), lei.chai@brunel.ac.uk (L. Chai), savvas.tassou@brunel.ac.uk (S.A. Tassou), a.sayma@city.ac.uk (A.I. Sayma).

https://doi.org/10.1016/j.applthermaleng.2020.116447
Received 30 July 2020; Received in revised form 11 November 2020; Accepted 6 December 2020
Available online 10 December 2020

number of review papers have been published prior to 2018 focusing on: cycle layouts, thermodynamics and an overview of early test loops [3]; transcritical CO_2 cycles for low-grade heat conversion [4]; and sCO_2 technology with a focus on concentrated-solar power and nuclear power applications [5]. More recently, in 2019 Liu et al. [6] provided a review of sCO_2 technology, with a detailed treatment of cycle layouts, thermodynamic modelling and optimisation, alongside a discussion of applications and some component level aspects. Yin et al. [7] provided a review of sCO_2 cycles specifically for concentrated-solar power applications, primarily covering cycle design, system thermodynamic and economic modelling, and materials. Finally, Yu et al. [8] provided a bibliometric analysis, in addition to briefly discussing applications, cycle configurations and modelling, CO_2-based mixtures, system components and experiments.

The motivation and novelty of the current review can be summarised as follows. Firstly, the rapid growth in sCO_2 technology means most published work has been conducted within the last few years since the early review papers [3–5]; this is substantiated by Fig. 1. Secondly, a significant emphasis within previous studies has been on cycle layout design, alongside thermodynamic modelling and optimisation. This review differentiates from these previous studies by focusing on practical technological challenges related to sCO_2 systems and equipment, alongside a summary of key application areas. Following a brief overview of the historical background of sCO_2 power cycles in Section 2, an overview of thermodynamic aspects is presented in Section 3 to contextualise the technical and operational issues within the thermodynamic cycle. A review of technical issues is then presented in Section 4, with emphasis on turbomachinery, heat exchangers, material options and system control. This is followed by a discussion of the key application areas in Section 5, namely fossil-fuelled and waste-heat to power generation, concentrated-solar power and nuclear, alongside a number of other notable applications. The paper concludes with a summary of the challenges facing sCO_2 power generation systems, and an outlook to the future.

2. Historical background

The real gas effects of CO_2 were investigated in the 19th century through the experimental work by Andrews who tested the validity of Boyle's law over a wide range of pressures [9]. However, it was in the mid-20th century that CO_2 began to be considered as a working fluid for power generation systems. In that period, research activities aimed at overcoming the limitations of the open Joule–Brayton and steam Rankine cycles through the use of alternative working fluids in closed loop cycles. Most of the published literature attributes the paternity of the concept of closed loop CO_2 power cycles to a 1950 Swiss patent granted to Sulzer that focused on partially-cooled condensation cycles [10].

Much of the early research on sCO_2 power systems was completed in the 1960s. Dekhtiarev suggested CO_2 as a suitable working fluid, proposing a reheated, precompression transcritical cycle operating with CO_2 [11], although the works of Feher and Angelino are more regularly cited. Feher [12] investigated a simple recuperated supercritical cycle and evaluated the sensitivity of the cycle to the operating parameters and the component performance. Within his work, the mismatch in the heat capacities between the hot and cold fluids within the recuperator was discussed, which introduces irreversibility within the cycle. Angelino [13–15] further considered both supercritical and transcritical cycles and investigated a range of different cycle layouts with a view to minimising this irreversibility.

Following the 1960s, interest in sCO_2 power cycles diminished until it was reignited by Dostal [16] who proposed the cycle for nuclear power applications. Much like the earlier works of Angelino, Dostal evaluated a range of cycles, including intercooling, reheating, recompression and precompression, concluding that the recompression cycle offers the highest thermal efficiency, whilst retaining a relatively simple cycle arrangement.

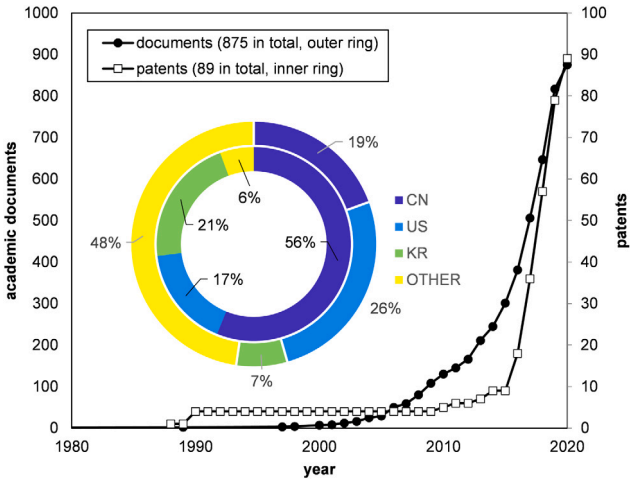

Fig. 1. Historical evolution and geographical distribution of intellectual property outputs in the field of sCO_2 power systems. Elaboration from Scopus and Espacenet world databases between January 1988 and March 2020. The doughnut charts refer to the total number of outputs in the period surveyed while their legend shows the shares in the People's Republic of China (CN), the United States of America (US), the Republic of Korea (KR) and the rest of the world (OTHER).

Since Dostal's work, there have been numerous studies investigating the merits of various cycle architectures for different applications. This is demonstrated in Fig. 1 by the steep increase in the number of academic documents (journal papers, conference proceedings, books etc.) and patents indexed in well-known databases. Research outputs have been increasing since 2006, while the number of patents has risen significantly from 2016. China (CN), United States (US) and South Korea (KR) are the top countries. This leadership results from the research and innovation programmes on sCO_2 power technology carried out in these and other countries like Japan and Australia. A detailed summary of the sCO_2 power activities with focus on the US is available in the book edited by Brun, Friedman and Dennis [17]. This is currently the most thorough reference on sCO_2 power technology.

Supercritical CO_2 is a topic that recently gained interest and appeal within many scientific conferences. Besides the tracks allocated within turbomachinery and waste-heat recovery conferences, the most established events are the International sCO_2 Power Cycles Symposium taking place in the US and the European sCO_2 conference for energy systems organised by the European sCO_2 alliance [18,19].

3. Thermodynamic aspects

The primary aim of this paper is to cover technical and operational issues, rather than covering the topic of thermodynamic cycle analysis in detail. However, it is important to contextualise the technical and operational issues within the overall thermodynamic cycle, and thus the purpose of this section is to provide only a short overview of thermodynamic aspects. For a more detailed overview, readers are referred to Friedman & Anderson [20].

3.1. *Thermodynamic behaviour of supercritical* CO_2

The operation of a closed-loop power cycle with a carefully selected working fluid could overcome some of the limitations of power plants operating with air or water. Specifically, for certain fluids, operating the cycle compression process close to the critical point allows the compression work to be significantly reduced, whilst the non-isothermal heat-transfer processes facilitate a high degree of internal heat recuperation [12,13]. The choice of working fluid is not limited to CO_2, and a

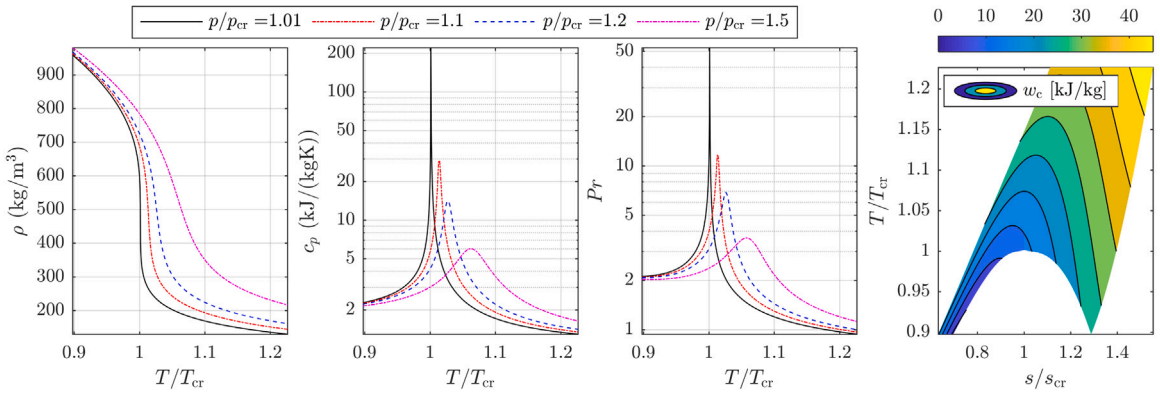

Fig. 2. Thermodynamic behaviour of sCO_2 in the vicinity of the critical point (T_{cr}, p_{cr}): (a) density ρ; (b) specific-heat capacity at constant pressure c_p; (c) Prandtl number $Pr = c_p\mu/k$; (d) specific work for an isentropic compression for a compression ratio of 2, w_c.

range of fluids have been studied [16,21,22]. However, the interest in CO_2 can be attributed to the temperature of its critical point, which is defined by a critical temperature and critical pressure of T_{cr} = 31.1 °C and p_{cr} = 73.8 bar respectively, being close to ambient conditions. This allows the low work compression process to be achieved following heat rejection down to close to ambient temperatures. Moreover, CO_2 is abundant, low cost, non-toxic, non-flammable and thermally stable at high temperatures.

The thermodynamic behaviour of CO_2 in the vicinity of critical point, and the motivation for operating the compression process close to the vicinity of the critical point, is explored in Fig. 2. These results were generated using NIST REFPROP [23] to compute the thermodynamic properties of CO_2, which is the most widely employed method; a detailed assessment of different property prediction methods is provided by White & Weiland [24]. Referring to Fig. 2, the right-hand plot reports the specific work for an isentropic compression process with a compression ratio of two. This compression ratio is representative of existing experimental sCO_2 systems (see Table 1), although similar trends are observed at other compression ratios. Noting that a low compression work increases cycle efficiency (*i.e.*, $\eta = (w_t - w_c)/q_h$, where η, w_t and q_h are the thermal efficiency, specific expansion work and heat addition respectively), the advantages of sCO_2 become apparent.

Operating under supercritical pressures, however, has implications on both cycle operation and component design. Firstly, operation pressures that are within the range of 50 to 250 bar require all parts to be designed to safely operate under both high pressures and high pressure differentials, and may also require specialist materials that can withstand harsh operating conditions, i.e., high pressure, high temperature and the occurrence of corrosion (see Section 4.3). The high pressures also lead to high densities, and consequently low volumetric-flow rates through the system. This enables compact pipework and plants with a small physical footprint, but introduces challenges in designing turbomachinery components with a high power density (see Section 4.1). There are also challenges related to starting the compression process close to the critical point. Specifically, there are significant variations in the thermodynamic properties of CO_2 in the vicinity of the critical point (see Fig. 2). The sharp drop in density from around 700 to 200 kg/m^3 around $T/T_{cr} \approx 1$ and $1 < p_{cr} < 1.2$, and the sharp spike in the specific-heat capacity around $0.98 < T/T_{cr} < 1.05$, will affect compressor operation, particularly at off-design conditions, introducing challenges related to system control to ensure steady and efficient operation (see Section 4.4). These variations also introduce challenges in compressor design and performance assessment, in addition to managing the possibility of condensation (see Section 4.1). Finally, the property variations also influence heat-exchanger design and operation. This is both from a more fundamental perspective point, where the sudden change in specific-heat capacity at constant pressure influences the effectiveness of internal heat-exchange processes, to more practical aspects relating to off-design performance (see Section 4.2).

3.2. Classification of thermodynamic power cycles

A general thermodynamic power cycle is composed of four fundamental processes, namely compression, heat addition at high pressure (p_2), expansion, and heat rejection at low pressure (p_1), and can be categorised according to whether phase change occurs within the cycle. In the Joule–Brayton cycle the cycle remains within the vapour region, whilst in the Rankine cycle the working fluid undergoes phase change in the heat-addition and heat-rejection processes.[1] Thermodynamic cycles can also be classified according to whether the operating pressures are below or above the critical pressure of the working fluid (p_{cr}). This allows three classifications, which include the subcritical ($p_1 < p_{cr}$ and $p_2 < p_{cr}$), supercritical ($p_1 > p_{cr}$ and $p_2 > p_{cr}$), and transcritical cycles ($p_1 < p_{cr}$ and $p_2 > p_{cr}$). The term supercritical Rankine cycle is often used in the context of steam and organic Rankine cycles to describe cycles in which the heat-addition takes place above p_{cr}, whilst heat-rejection occurs below p_{cr} [26,27]. However, the terms supercritical and transcritical are used here to distinguish between cycles operating with or without condensation, as used within the CO_2 research community [28]. Combining these definitions enables a general classification of thermodynamic cycles as reported in Fig. 3.

The two sCO_2 cycles of primary interest are the supercritical cycle and the transcritical cycle, which are shown by the blue and green cycles in Fig. 3 respectively. In both cycles the high pressure of the system exceeds the critical pressure. In the supercritical cycle, the low pressure of the system is also above 73.8 bar, and there is no distinction between the fluid being in a liquid or a vapour state, whilst in the transcritical cycle, the low pressure of the system is below 73.8 bar, and condensation is possible within the low-pressure heat-rejection process. Referring to the right-hand plot in Fig. 2, it is observed that the lower the compressor inlet temperature and the closer the compression process is to the saturated liquid line, the lower the compression work. This motivates the use of a transcritical cycle to maximise thermal efficiency. Consequently, this means a transcritical cycle can only be considered where it is possible to cool the CO_2 below 31.1 °C. If this is not possible, a supercritical cycle should be considered with the compression process starting close to the critical point to maximise thermal efficiency.

Alongside pure CO_2, CO_2 mixtures have been proposed for closed-loop power cycles. By doping CO_2 with another fluid the thermodynamic properties can be altered, and the critical point of the working fluid shifted. This could include the use of noble gases, alongside

[1] The cycle devised by Rankine considers an expansion from saturated vapour and while Hirn [25] proposed the superheated Rankine cycle, the term Rankine cycle is used here to refer more generally to a cycle in which phase change occurs.

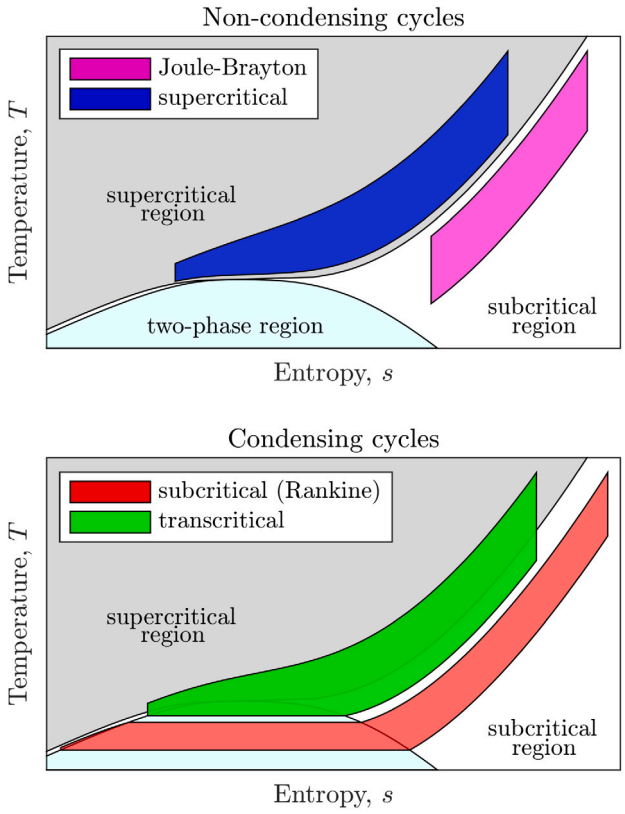

Fig. 3. Classification of thermodynamic power cycles. (For interpretation of the references to colour in this figure legend, the reader is referred to the web version of this article.)

nitrogen and oxygen, to lower the critical temperature and pressure, which could enhance thermal efficiency by allowing higher pressure ratios [29]. Alternatively, doping could increase the critical temperature, allowing condensation cycles to be realised at elevated heat sink temperatures. For this purpose, neon, SF_6 and butane have been studied for low-temperature applications (160 °C) [30], hydrocarbons for temperatures up to around 400 °C [31], and $TiCl_4$, N_2O_4 and NO_2 for applications up to 700 °C [32]. An important step in realising such cycles is to characterise the behaviour and thermal stability of CO_2 mixtures [33].

3.3. Thermodynamic modelling studies

The purpose of thermodynamic modelling is to investigate how the cycle parameters, such as the operating temperatures and pressures, affect thermodynamic cycle performance. This is done by coupling a suitable equation of state for CO_2 with a thermodynamic model of each component within the cycle and running a parametric or optimisation study to identify optimal cycles. This may be from the first-law perspective of maximising thermal efficiency [34,35], the second-law perspective of reducing internal irreversibility [36,37], or from the perspective of minimising the specific-investment cost or the levelised cost of electricity (LCOE) [38,39].

The baseline cycle for most studies is the simple recuperated cycle, be that either a supercritical or transcritical cycle, where a recuperator is used to transfer heat from the hot exhaust leaving the turbine to the cold fluid leaving the compressor (see points 2 → 3 and 5 → 6 in Fig. 4a, 4d). Within the literature the terms recuperation and regeneration are used interchangeably to describe the simple cycle; here the term recuperation is used since the internal heat recovery occurs with the use of a recuperative heat exchanger. The simple recuperated cycle can be extended to more complex layouts, which may include reheat, recompression, precompression, or any combination thereof; a few notable cycle arrangements are also reported in Fig. 4.

The reheat cycle (Fig. 4b) divides the expansion process (4 → 5 and 6 → 7), and introduces an intermediate reheating process. This increases the average temperature of heat addition, and hence cycle efficiency, and also increases the turbine exhaust temperature, which increases the potential internal heat recovery within the recuperator.

Within Dostal's work [16], the recompression cycle (Fig. 4c) was identified as a promising cycle, with the characteristics of high thermal efficiency whilst retaining a simple cycle arrangement. Within the recompression cycle, the recuperation is divided into a high-temperature recuperator (3 → 4 and 6 → 7) and a low-temperature recuperator (2 → 3 and 7 → 8), with a secondary compressor installed that operates between points 3 and 8. The purpose of this compressor is to bypass a fraction of the main flow from the heat-rejection process and main compressor, which reduces the heat-capacity rate (i.e., $\dot{m}c_p$) within the high-pressure side of the low-temperature recuperator (2 → 3). This helps offset the mismatch in the heat capacities of the hot and cold fluids within the recuperator, reducing the irreversibility compared to the simple recuperated cycle [12–15]. Today, the recompression cycle is widely considered to be a promising cycle for sCO_2 power cycles, and the improvement in thermal efficiency is expected to offset the additional cost associated with the additional components [20]. A combination of reheat and recuperation has been proposed for a large-scale sCO_2 cycle [40].

Since the individual works of Feher, Angelino and Dostal, there have been numerous studies investigating the merits of various cycle architectures for different applications. Extensive assessments of cycle layouts have been carried out by Crespi et al. [28,35]. Whilst the authors make some general observations about optimal cycle, they also note that when reporting an optimal cycle it is important to provide an indication of the operating and boundary conditions, alongside any technological limits. To this end, thermodynamic modelling and optimisation is likely to remain an important step when evaluating the performance of sCO_2 cycles for a given application.

4. Component aspects

4.1. Turbomachinery

The properties of sCO_2 introduce opportunities and challenges in turbomachinery design. The high operating pressures and densities allow compact turbomachinery components, which could allow a significant reduction in size, and hence cost, of the overall plant, but also lead to high power density turbomachinery, and, for power outputs below a few MW_e, turbomachines that must rotate at high speed to maintain high isentropic efficiency. Small diameters and higher rotational speeds are associated with increased aerodynamic losses, such as increased tip-clearance and secondary-flow losses, and introduce challenges in the design of the shaft, bearings and seals to ensure stable rotordynamic behaviour across the range of expected operating speeds. The high operating pressures and large absolute pressure difference across a single turbine stage also introduce challenges related to the mechanical design of the turbine housing and the turbine blades, and in managing axial thrust and leakage to the surroundings. This creates a complex design space in which suitable designs that meet the trade-off between aerodynamic, rotordynamic and mechanical performance need to be identified.

Within any sCO_2 system there are a minimum of two turbomachines, namely the compressor or pump and the turbine. Within more complex cycles, such as the recompression cycle, this is supplemented with an additional recompressor. Whilst the turbine, and recompressor, operate sufficiently far from the critical point that they operate with a gas-like substance, the proximity of the main compressor to the critical point and its operation with supercritical pressures, mean the main

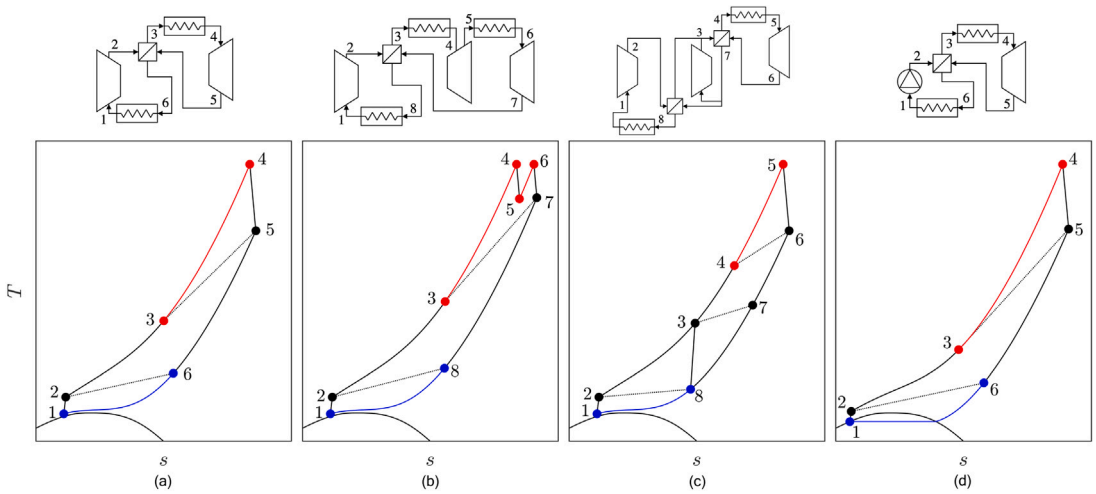

Fig. 4. Potential sCO_2 power cycles: (a) supercritical recuperated; (b) supercritical reheated–recuperated (c) supercritical recompression; (d) transcritical recuperated. The red and blue lines represent the heat-addition and heat-rejection processes respectively. (For interpretation of the references to colour in this figure legend, the reader is referred to the web version of this article.)

compressor can be referred to as a pump or compressor. For generality, the term compressor will be used here, and the term pump is reserved for condensing transcritical cycles.

Both compressors and turbines take the form of either an axial or a centrifugal/radial-inflow architecture. In the former, the flow passes through the machine parallel to the axis of rotation, whilst in the latter the flow turns through 90°. The axial design allows multiple expansion stages to be readily mounted onto the same shaft, whilst in a radial or centrifugal design the change in radius between the rotor inlet and outlet facilitates a larger enthalpy change over a single stage. For large-scale applications multi-stage axial turbomachines are favoured, while for smaller-scale applications the radial-inflow turbine and centrifugal compressor designs are preferred as they can accommodate the required pressure change over a single stage. Preliminary sizing and selection is typically completed using the maps developed by Balje [41], which relate the achievable design-point efficiency for the different turbomachinery architectures to the specific speed N_s and specific diameter D_s:

$$N_s = \frac{\omega\sqrt{\dot{V}}}{\Delta h_s^{3/4}}; \tag{1}$$

$$D_s = \frac{D\Delta h_s^{1/4}}{\sqrt{\dot{V}}}, \tag{2}$$

which relate rotational speed ω and diameter D to the isentropic enthalpy change across the machine Δh_s, and volumetric-flow rate $\dot{V}$ at either the inlet (compressor) or outlet (turbine) of the machine.

From a simple thermodynamic cycle analysis it can be shown that increasing the pressure ratio of the cycle (to a point) will increase the cycle thermal efficiency. This will increase the enthalpy change across the compressor and turbine and for a specified net power output reduce the mass- and volumetric-flow rates for both machines. Thus, more efficient cycles are likely to require smaller diameters and higher rotational speeds, which further exacerbates the issues mentioned previously [42]. Considering that the cycle thermal efficiency is sensitive to the turbomachinery efficiencies, with Allison et al. [43] suggesting a drop in compressor efficiency from 90% to 80% could lead to a drop in overall cycle efficiency of 2.0% and the same drop in turbine efficiency could lead to a drop in overall cycle efficiency of 4.4%, it is clear that turbomachinery and cycle performance are closely coupled. Thus, turbomachinery and cycle design should be tackled in unison, although even then, such studies point to optimal cycles with turbine inlet pressures between 200 and 400 bar [44], or optimal pressure ratios in the range of 2 to 5 [45]. These values are somewhat higher than existing prototypes, which were designed to minimise cost and risk [43].

Another useful chart for sCO_2 turbomachinery selection was proposed by Sienicki et al. [46] (Fig. 5). Alongside identifying the power ranges where different turbomachinery architectures are expected to be most suitable, it provides an overview of the available options for the bearings, seals, alternators and shaft arrangement. The main conclusion from this chart is that below around 10 MW_e, radial and centrifugal machines are preferred, with rotational speeds in excess of 30,000 RPM, which requires a permanent magnet rotor, and potentially multiple shafts. For large-scale sCO_2 power systems (> 100 MW_e) axial turbomachinery is preferred.

4.1.1. Turbomachinery design and simulation

Alongside experimental demonstrations, there has been a concerted effort in the design, simulation and optimisation of sCO_2 turbomachinery. The use of meanline design tools and optimisation methods to identify optimal geometries that can achieve the desired aerodynamic performance is widely applied within the field of turbomachinery, and in theory these tools can be readily applied to sCO_2 turbomachinery. These employ loss models to account for various losses, such as passage, incidence, clearance and windage losses, which are typically empirically-derived for air and steam turbomachinery. There are many examples of such studies, although a few examples include those relating to sCO_2 compressor design [47,48], turbine design [49,50], off-design turbomachinery prediction [51], and the integration of turbomachinery design models with thermodynamic cycle design [44,45]. However, a major issue facing these models is that they have not been experimentally validated for sCO_2 applications, and as demonstrated by Lee & Gurgenci [52], the choice of model can affect the results generated.

A similar statement can be made with regards to the use of computational-fluid dynamic (CFD) tools to assess sCO_2 turbomachinery performance. Arguably the turbine, and possibly a recompressor, operate sufficiently far away from the critical point such that the CO_2 behaves like an ideal gas. Thus, existing meanline models and CFD solvers may provide an adequate means to generate suitable turbomachinery designs. However, for sCO_2 turbomachinery the trade-off between aerodynamic, rotordynamic and mechanical considerations, particularly for small-scale applications, may shift the optimal design away from the conventional design space. Thus, the use of CFD to assess novel designs prior to experimentation is a useful approach. A good example of this is provided by Keep [53,54], who investigated low

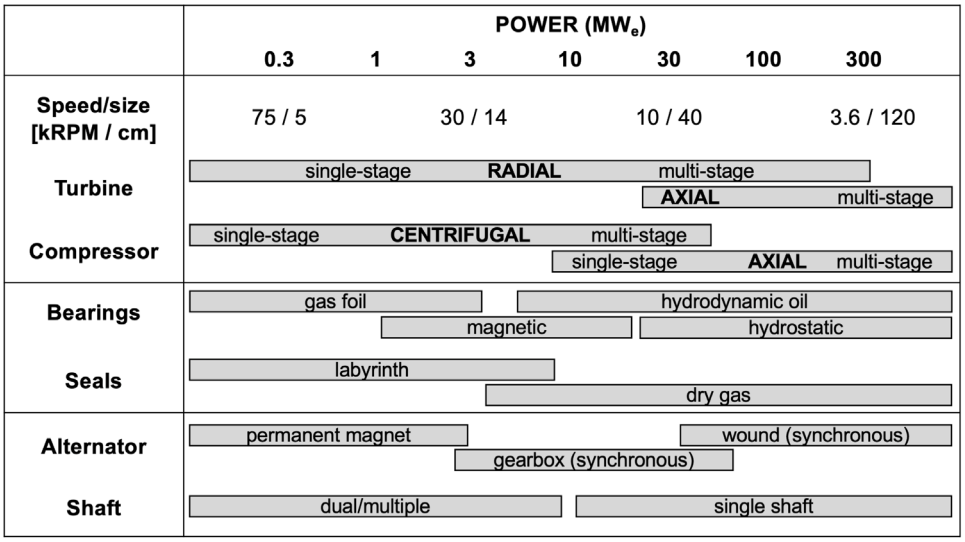

Fig. 5. Turbomachinery options for sCO_2 power cycles. *Source:* Reproduced with permission from Sienicki et al. [46].

specific-speed turbine designs and found an isentropic efficiency of 81% for a 300 kW_e radial-inflow turbine could be possible, suggesting that efficiency could be improved by modifying the rotor–stator interspace, minimising the clearance gap or using a shrouded rotor, or adding splitter blades to the rotor.

Another area that represents a challenge for scientific theory and CFD simulation is the simulation and performance prediction of sCO_2 compressors operating near the critical point. The non-linear thermodynamics of CO_2 around the critical point lead to possible real-gas effects, whilst condensation near the leading-edge of the compressor may occur. Studies have investigated real-gas models to predict the behaviour of CO_2 near the critical point [55], real-gas effects [56,57], the performance of centrifugal compressor diffusers [58], and condensation effects both numerically and experimentally in a converging–diverging nozzle [59,60]. The results suggest the time required for stable liquid droplets to form during expansion significantly reduces as the critical point is approached. Operation near the critical point also has implications for compressor stability and the prediction of off-design performance, since conventional similitude laws cannot be applied [61] and uncertainty in determining efficiency is introduced [62].

4.1.2. *Existing* sCO_2 *turbomachinery*

Given the challenging operating conditions and design space, it is critical to demonstrate that the desired turbomachinery performance can be realised in practice. To this end, a number of sCO_2 test loops have been constructed, or are currently underway. A summary of the turbomachinery designs for these test loops is provided in Table 1. Before discussing these in detail, it is worth emphasising two points. Firstly, most of the turbomachinery that has been tested to date is not representative of what would be planned for larger systems. This introduces specific challenges and considerations that might eventually be unnecessary for larger-scale plants. Nonetheless, initial testing at the laboratory-scale is a necessity given the cost and complexity of designing and constructing MW-scale test loops. Secondly, it is noted that unlike other components within the cycle, it is difficult to decouple the turbomachinery into separate compression, re-compression and expansion machines, since in many existing prototypes these machines share a common shaft, and have the same challenges. For this reason, the discussion around compression and expansion machines is combined here into a single section.

Sandia National Laboratories (SNL), in partnership with the Department of Energy and Barber Nichols, developed and tested two turbine–alternator–compressor (TAC) units, with one containing the main compressor and the other containing the recompressor of a re-compression Brayton cycle [63]. The use of a TAC unit allows all of the rotating machinery to be mounted on a single shaft. This has the advantage of simplicity, particularly for a simple cycle where there is only a single compressor and turbine, but does require the compressor and turbine to rotate at the same speed and be matched appropriately. Although in the reported test the heat input was limited, the results suggested that the turbomachinery behaved as expected, in addition to verifying the speed control algorithms, stable operation of the single-shafted TAC unit and cold startup methods [63]. However, a significant challenge identified for small-scale sCO_2 turbomachinery during the initial SNL tests arose from the need to use gas-foil bearings, owing to the high power density of the turbomachinery, which results in large shaft diameters and high shaft surface velocities. Whilst the journal bearings behaved adequately, thrust bearing failures were observed [85]. It was suggested to use smaller diameter thrust bearings, and employ additional cooling for the bearings [63]. Failure was also attributed to the Teflon coating which was unsuitable for high temperature operation. Later, this lead to low-friction coatings for gas-foil bearings being investigated to facilitate rotation during start-up and shut-down where the shaft typically rides along the foil bearing surface [85].

The turbomachinery installed within a demonstration sCO_2 test loop installed at Carleton University is also based on the SNL design [86]. More recently, the SNL test loop has been upgraded to test a turbocompressor designed by Peregrine Turbine Technologies, which consists of two centrifugal compressor stages and a single radial-inflow turbine on the shaft [64]. Although the test capabilities could not match the design point of the machine, the tests demonstrated the use of a blow-down procedure to start the compressor in the absence of a starting motor and enabled the team to resolve issues relating to the thrust and radial bearings [65]. Initial testing reported issues with both the radial and thrust bearings experiencing rubs or failure. Issues with the thrust bearing were resolved by adjusting the turbine back pressure to adjust the thrust, whilst it was hypothesised that the radial bearing failure arose from a non-uniform turbine inlet temperature and/or flow rate. To overcome this issue, the length to diameter ratio of the radial bearing was increased to increase the load capacity, resulting in successful operation.

Alongside developments at SNL, a collaboration between Bechtel Marine Propulsion Corporation and the Bettis Atomic Power Laboratory developed a 100 kW_e integrated system test (IST), for which the turbomachinery comprised of a variable speed turbine-compressor, and

Table 1
Existing sCO_2 turbomachinery designs.

Name	Power [kW_e]	Cycle[a]	T_{max} [°C]	P_{max} [bar]	PR	Type[b]	Seals	Bearings	Architecture[c]	N [kRPM]	D [mm]	$\dot{m}$ [kg/s]
SNL [63]	125	RC	537	170	1.8	TAC	Labyrinth	Gas foil	IFR CC (main)	75 75	68.1 37.3	2.7 3.5
						TAC	Labyrinth	Gas foil	IFR CC (recomp)	75 75	68.3 57.9	3.08 2.4
PTT [64,65]	–	RC	750	423		TC	Leaf	Gas	IFR, CC (x2)	118	–	5.5
IST [66,67]	100	RE	299		1.8	TC, TG	Labyrinth	Gas foil	IFR (TC, TG) CC (TC)	75 75	53 38	– –
Echogen	8000	RE	485			TC	–	–	IFR, CC	24–36	–	–
[68]						TG	Dry-gas	Tilting pad	IFR	30	–	–
SWRI/GE [69,70]	1000 (10,000)	RC	715	251	2.9	T	Dry gas, Labyrinth	Tilting pad	4-stage AT	27	–	8.41
STEP [71]	10,000	RC	715	250	2.7	T	–	–	3-stage AT	–	–	103
NET Power [72–74]	200,000 (kW_{th})	AL	1150	300		T	–	–	7-stage AT	–	–	–
TIT [75]	10	RE	277	119	1.45	TAC	–	Gas	IFR CC	100 100	35 30	1.1 1.1
KAIST	300	RE	500	200	2.67	MC	–	–	CC (twin, shrouded)	70	–	3.2
(SCIEL)						TG	–	–	IFR (shrouded)	80	–	5.05
[76,77]						TAC	–	–	–	68	–	–
KIER	1	RE	200	130	2.27	TG	–	Angular ball	IFR (PA)	200	22.6	–
[78–80]	10	S	180	130	1.65	TAC	Labyrinth	Gas foil	CC, IFR (shrouded)	70	50	–
	60	RE	392	135	1.75	TG	–	Tilting pad	1-stage AT (PA)	45	73	1.74
sCO_2-HeRo [81,82]	7	S	200	117.5	1.5	TAC	Labyrinth	Angular ball	IFR (shrouded) CC (shrouded)	50 50	66 40	0.65 0.65
I-ThERM [83,84]	50	RE	435	127	1.7	TAC	–	Angular ball	IFR turbine CC	60 60	72 55	2.1 2.1

[a]Cycle layout: simple (S), recuperated (RE), recompression (RC), Allam (AL).
[b]Letters refer to components mounted on the same shaft: turbine (T); alternator (A); compressor (C); generator (G); motor (M).
[c]Types of turbine: inward-flow radial turbine (IFR); centrifugal compressor (CC); axial turbine (AT); partial admission (PA).

a constant speed turbine-generator [66]. However, it was noted that since the turbomachinery tested is not representative of what would be planned for larger systems, the use of gas foil bearings introduced specific startup and operational procedures that would be unnecessary for larger-scale plants. A later study indicated that at peak operating power the generator-turbine and compressor-turbine operated above their predicted performance, with isentropic efficiencies of 83.6% and 85.2% at power outputs of 56.8 and 52.6 kW respectively [67]. The compressor operated with an isentropic efficiency of 72.4%, which was well above the predicted value of 58%; although the accuracy of compressor maps developed using ideal-gas assumptions in close proximity to the critical point should be considered [61]. Ultimately, the IST demonstrates that at this small-scale feasible turbomachinery components can be developed, although high windage losses were observed due to the high pressure, and subsequent high density, of the fluid within the cavity that contains the motor-generator. Moreover, much like the SNL tests, the IST tests also experienced issues relating to heating generated from the gas-foil bearings. As a result, the rotational speed was limited to 60,000 rpm to maintain safe bearing temperatures using the available cooling without exceeding the thrust load capacity of gas-foil thrust bearings [67,70].

Echogen power systems [87] have developed sCO_2 technology for waste-heat recovery applications, which has been licenced to Siemens for the oil and gas sector [88] and to General Electric for marine applications [89]. The Echogen EPS100 unit has a net power output of 8 MW_e, and, similar to the IST, the turbomachinery consists of a constant speed turbine-generator and variable speed turbine-compressor. The turbine-generator rotates at 30,000 RPM and utilises a four-pole synchronous generator and epicyclic gearbox, whilst the turbine-compressor has a nominal shaft power of 2.7 MW and is constructed from a single-stage centrifugal compressor and single-stage radial turbine. Tests reported an isentropic efficiency that exceeds 80% for the turbine-compressor, and in the range of 20 to 75% for the turbine-generator, although the turbine-generator was not tested at its design point [68].

Other significant developments in turbomachinery for sCO_2 systems within the US can be related to work under the SunShot, APOLLO and STEP projects. Under the SunShot programme a 1 MW_e-scale sCO_2 test loop has been constructed to test a multi-stage axial turbine with a net power output of 10 MW_e [70,90,91]. To minimise development costs, the tests employ a reduced mass-flow rate, through reduced area nozzle and blade passages, so the design velocities can be maintained without requiring to operate the turbine at full capacity. The design of the turbine is reported by Kalra et al. [69] and comprises of a four-stage shrouded axial turbine with a rotational speed of 27,000 RPM and an isentropic efficiency in excess of 85%, as predicted from meanline and CFD analysis. Compared to the small-scale systems, issues around high bearing and windage losses, in addition to motor control issues, are expected to be less critical in large-scale systems since existing technologies such as shaft-end seals and oil-film bearings should be suitable [70]. Having said this, there have been developments in hydrostatic bearings, which require an external sCO_2 supply but facilitate hermetic turbomachinery designs removing the need for sCO_2 shaft seals [92], hydrostatically-assisted gas foil bearing designs [93], and foil bearings for large MW-scale turbomachinery where the use of foil bearings is quoted to eliminate speed and temperature limitations and the need for liquid lubrication [94]. Other challenges related to the design of the SunShot turbine include the mechanical design of the shaft and the casing. Whilst turbine inlet conditions are similar to those of existing steam turbines, sCO_2 turbines experience higher

outlet temperatures and pressures and require a steeper temperature gradient within the shaft to allow the use of dry-gas seals [43]. Thus, the thermal management of the shaft is important to ensure an axial temperature gradient in the shaft to minimise stress in the shaft and casing [70,95]. Moore et al. [95] reported initial testing of the SunShot turbine, reaching a rotational speed of 21,000 RPM and turbine inlet conditions of 550 °C and 180 bar. The primary aim of these tests was to break in the turbine and to monitor vibrations, critical speeds and bearing temperatures, which was considered a success since stable operation was observed. Future tests expect to move towards the design point of 715 °C, 250 bar and 27,000 RPM. Under the APOLLO programme, work has been initiated on the design of the compressor for the same recompression Brayton cycle. Cich et al. [96] describe the design of the compressor assembly considering all rotordynamic and mechanical design considerations. The authors propose an arrangement where the main compressor and recompressor, which are both single-stage centrifugal machines, are positioned back-to-back and variable inlet guide vanes are utilised. Within the APOLLO programme, Hanwha Techwin and Southwest Research Institute have also been developing an integrally geared compressor–expander system, in which the turbine and compressor stages are all of the radial design and are mounted within a single integrally-geared unit [97]. The unit is designed as a 5–25 MW_e modular power block, and comprises of a two-stage main compressor, two-stage recompressor, and a four-stage turbine with reheat [43]. The aim of the STEP (Supercritical Transformational Electric Power) project is to construct and commission a 10 MW_e sCO_2 plant [71]. The turbine is based on the SunShot turbine, but the stage count is reduced from four to three, facilitating a more compact design, whilst the volute area is optimised and thermal management within the turbine enhanced. The compressor within the STEP facility is provided by Baker Hughes, and leverages both existing commercial product lines and work undertaken under the APOLLO programme [71].

The ultimate goal of the SunShot, APOLLO and STEP projects is to realise large-scale sCO_2 power plants, and thus the turbomachinery for both a 50 and a 450 MW_e plant has been proposed [40,98]. Since a limitation on the maximum shaft diameter would restrict the SunShot turbine being directly up-scaled to 50 MW_e, a six-stage axial turbine has been proposed with a 406 cm tip diameter, rotational speed of 9500 RPM and an estimated efficiency of 90.3%; for the 450 MW_e plant, a reheat recompression cycle is proposed with a dual-flow four-stage high-pressure turbine and three-stage low-pressure turbine, with predicted efficiencies of 90.6% and 91.6% respectively, all mounted on a single shaft [40]. However, the availability of large-diameter film-riding end seals was seen as a limitation, leading to dedicated tests to develop a new seal design [99]. In terms of compressor design for the 450 MW_e plant, a back-to-back arrangement was proposed consisting of a two-stage centrifugal design and a four-stage centrifugal design for the main compressor and recompressor respectively, all mounted on a single shaft [98].

NET Power are developing an oxy-fuel thermodynamic power cycle for which Toshiba are providing a turbine designed to operate with inlet conditions of 300 bar and 1150 °C [100]. The concept for the turbine design is to use proven technology as much as possible, whilst testing a scaled turbine that is representative of the final turbine used within a commercial plant. As such, Toshiba have developed a preliminary turbine design for a 500 MW_{th} system, which has subsequently been scaled for a thermal input of around 200 MW_{th} and then operated with partial admission to reduce the required thermal input to 50 MW_{th} [73]. The design comprises of a single seven-stage axial turbine [72,74], which combines proven technology for high-pressure steam turbines, namely the use of an inner and outer pressure casing, and proven gas turbine technology, such as coatings and internal cooling of the turbine blades [73]. Freed et al. [101] report on the development of a gas-turbine driven integrally-geared compressor for the plant.

Outside of the US, a number of notable sCO_2 turbomachinery prototypes have been developed. In Japan, Utamura et al. [75] developed a single-shaft TAC unit with a target net power of 10 kW and nominal rotational speed of 100,000 RPM. Compressor isentropic efficiencies between 30% and 70% are reported, although high windage losses were reported. Within the Korea Institute of Energy (KIER), three experimental loops have been developed, as described by Cho et al. [78]. The first employed a 10 kW_e TAC unit, with shrouded centrifugal compressor and radial turbine rotors to overcome thrust balancing issues, although issues with the gas foil bearings are reported. The second was used to test a 1 kW_e turbine-generator constructed from a radial turbine with partial admission and utilised commercial ball bearings. The final loop was designed for a power output of 60 kW_e. Further developments are described by Shin et al. [79]. For the 60 kW_e system, commercially available tilting-pad bearings were employed to overcome high axial and radial thrusts. However, to employ these bearings it was necessary to reduce the rotational speed, which lead to the selection of a partial-admission, single-stage axial impulse turbine with a rotational speed of 45,000 RPM. In subsequent tests, an isentropic turbine efficiency of 51% has been reported, with the authors emphasising being able to resolve bearing failure issues through the use of an axial machine as a success [80].

A collaboration between the Korea Advanced Institute of Science and Technology (KAIST) and Korean Atomic Energy Research Institute (KAERI) has led to the development of the Supercritical CO_2 Integral Experiment Loop (SCIEL). For the initial low pressure ratio tests a simple cycle was constructed with a separate motor-driven compressor and turbine-generator set, rather than using a single TAC unit, and a twin impeller centrifugal design was selected for the compressor to control thrust loads [76]. At the time, future tests were planned for higher pressure ratio tests, which would utilise an additional TAC unit constructed from a high-pressure turbine and high-pressure compressor [77]. Alongside the SCIEL, a compressor test facility, named the SCO2PE (Supercritical CO_2 Pressurising Experiment) has been constructed to test compressor operation near the critical point, which utilises a 26 kW_e canned motor pump, with a centrifugal shrouded impeller and rotational speed of 4620 RPM [62,102]. Compression efficiencies between 10 and 60% are reported for varying inlet conditions [102], although the uncertainty of calculating efficiency close to the critical point is noted [62]. Wang et al. [103] report the design of an integral test loop with a power output of 1 MW_e at the Nuclear Power Institute of China. Initially, the system will employ a TAC unit with a design speed below 30,000 RPM, although further details have not been reported.

Arguably, within Europe the development of sCO_2 turbomachinery has lagged behind developments elsewhere, although there are a few exceptions. Hacks et al. [81,82] designed a TAC unit for the H2020 sCO_2-HeRo project, which comprises of a single-stage centrifugal compressor and radial turbine, both with 2D shrouded blades; the use of shrouded impellers allows the use of seals to reduce clearance losses, whilst a 2D blade more easily permits the installation of the seals compared to a 3D blade. Whilst the optimal rotational speed for a high stage efficiency would be 200,000 RPM, the rotational speed was limited to 50,000 RPM to minimise windage losses [82]. Within the H2020 I-ThERM project, the current authors from Brunel University London, in collaboration with Enogia, have developed the High Temperature Heat To Power Conversion facility (HT2C), which utilises a TAC unit with unshrouded single-stage radial compression and expansion stages [83,84], which is currently undergoing testing. Other developments within Europe include the H2020 sCO_2-Flex project which aims to adapt fossil-fuel power plants through the use of sCO_2 and will involve the design of the turbomachinery for a 25 MW_e cycle [104], and the H2020 SCARABEUS project, within which the current authors from City, University of London are leading the conceptual design of the turbomachinery for a 100 MW_e sCO_2 CSP plant operating with CO_2 blends [105].

Table 2
High pressure heat exchangers [106,107].

Type	P_{max} [bar]	T_{max} [°C]	Maximum surface area density [m^2/m^3]
Plate and shell	100	900	200
Brazed plate-fin	120	650	1500
Diffusion-bonded plate-fin	200	400	800
Packinox plate	300	700	300
Microtube	400	650	2000
Printed circuit	500	900	5000
Shell and tube	1400	600	100

4.2. Heat exchangers

In sCO_2 systems, the heat exchangers greatly influence the overall cycle efficiency and system size and must adhere to specific operating conditions and design requirements. The primary challenge is to maintain cycle compactness and endure the high temperature and pressures. The other important challenge is to find a compromise between the heat exchanger type, cost, durability and performance. Three heat exchangers are generally involved in sCO_2 systems; the heater which absorbs heat from the heat source; the recuperator which transfers heat from the turbine exhaust to the compressor exhaust; and the cooler which rejects heat to the environment. A summary of candidate types of high pressure heat exchangers, along with an appraisal of maximum pressure, maximum temperature and maximum surface area density, is provided in Table 2.

4.2.1. Heaters

Two types of heat exchanger are typically employed as CO_2 heater, depending on the heat transfer process and heat source temperature; one is a radiant heating section combining radiation and convection processes, used in fuel-fired applications, and the other uses only convection heating, for example in waste-heat recovery applications.

For the radiant heating section, the CO_2 heater geometry is similar to that in steam cycles, but the lower turbine pressure ratio and the different thermophysical properties make the CO_2 heater design significantly different from that found in steam cycles; relatively higher mass flow rates are required for the same level of heat input, and shorter piping length to minimise the pressure drop. A representation of the heating section, proposed by Moullec [108], is shown in Fig. 6. This coal-fired boiler employed eight heat exchangers to heat the CO_2 to the maximum temperature and cool the flue gas down to about 540 °C. The main challenges in the design were to reduce the flue gas temperature to meet the capabilities of modern flue gas preheaters (typically around 370 °C), to decrease the CO_2 pressure drop to a commercially feasible level, and to maintain adequate safety margins to avoid tube overheating or unacceptably high temperatures.

For convection heat transfer only, the shell-and-tube heat exchanger is the most common type with various configuration options. The sCO_2 flows along the tubes, and the heat carrier fluid flows across the tubes from the shell side to transfer heat between the two fluids. The tubes should have good thermal conductivity to achieve the desired heat transfer rates and withstand the operating temperature and pressure [109]. The shell and tubes should withstand the thermal stresses between them and should be designed for high-cycle fatigue life. A major problem with shell-and-tube heat exchangers used as CO_2 heaters are their large physical size, leading to high capital cost due to the significant amount of material needed to contain the high-temperature, high-pressure sCO_2 environment. Therefore, compact heat exchangers are more suitable for sCO_2 heater applications, due to their large surface area to volume ratio and high heat transfer coefficient [106]. Considering that the heat carrier fluid usually operates under high temperature but low pressure, the microtube architecture and plate-fin structure are suitable for CO_2 heater applications [110]. The microtube heat exchanger can provide significantly improved performance over

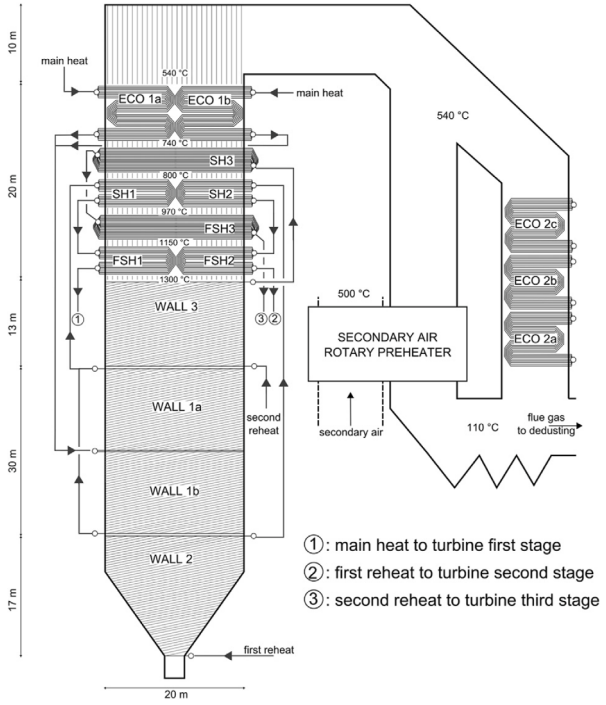

Fig. 6. Designed boiler adapted to an sCO_2 Brayton cycle [108].

a conventional shell-and-tube heat exchanger, including the ability of microtubes to withstand very high pressures. As shown in Fig. 7, microtube heat exchangers can be designed with the heat carrier fluid crossing the tube bundle, which can greatly reduce the pressure drop in the shell side. Plate-fin heat exchangers are a matrix of alternate flat plates consisting of enclosed channels and fin corrugations. The fins, such as the plain triangular, louver, perforated, wavy fin, or with vortex generators, enhance the heat transfer of the lower pressure heat carrier fluid. This sandwich construction has a naturally strain-compliant design, leading to the potential to achieve a high-cycle fatigue life. However, smaller channel dimensions are associated with some disadvantages, including higher pressure drop per unit length, propensity to fouling and the difficulty in repair in case of leakage inside the heat exchanger core [111].

4.2.2. Recuperators

Printed circuit heat exchangers (PCHEs) are the most widely adopted sCO_2 recuperators, due to their compactness and structural rigidity and reliable performance under conditions of extreme pressure and temperature [111,112]. The diffusion bonding process creates an exceptionally strong heat exchanger core as shown in Fig. 8, which consists of stacks of flat metal plates with fluid flow channels either chemically etched or pressed into them. The diffusion bonding process allows the plates to be joined together with the same strength as the parent metal. The chemically etched process allows the mechanical design to be flexible so that etching patterns can be adjusted to match the required operating temperature and pressure-drop constraints. The etched flow passages as shown in Fig. 9 are mainly categorised into four types: straight channel, zigzag (or wavy) channel, channel with S-shaped fins, and channel with airfoil fins. Since the 2000s, sCO_2 test facilities have been developed in the US, Japan, South Korea, China and the UK and the thermohydraulic performance of PCHEs has been extensively investigated. Huang et al. [113] and Kwon et al. [111] reviewed the flow and heat transfer characteristics of sCO_2 as well as available correlations for the design of PCHEs. Chai and Tassou [112] detailed characteristics and challenges relevant to PCHEs in sCO_2 Brayton cycles, including material selection, manufacture and assembly,

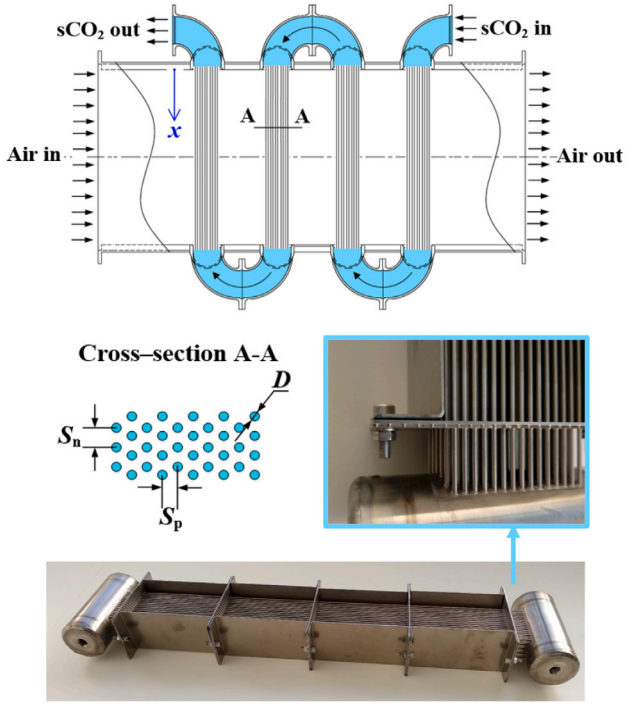

Fig. 7. Microtube CO_2 heater for exhaust waste heat recovery: the heat exchanger schematic at the top of the figure consists of four modules; each module, displayed in the picture at the bottom of the figure, is made up of microtubes whose arrangement is reported in the A–A cross-section view (courtesy of Reaction Engines Ltd.).

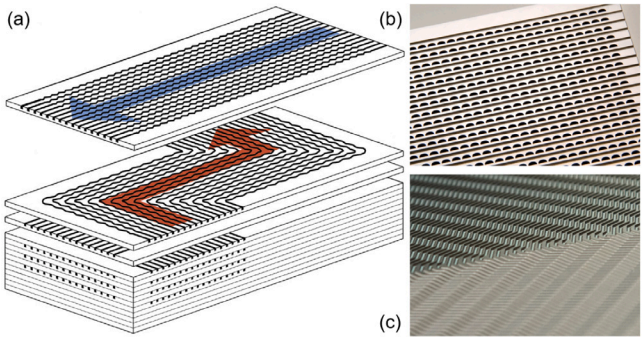

Fig. 8. (a) Typical PCHE: (b) flow paths and details of the diffusion-bonded core (c) and of an etched plate (courtesy of Heatric Meggitt UK).

thermohydraulic performance, geometric optimisation and provided suggestions for further research and development.

A summary of heat transfer and friction factor correlations for PCHEs is listed in Table 3. These correlations were proposed based on CO_2, water and helium data. It is important to note that some of the performance data used was far from the critical point so many published correlations may be subject to a high degree of uncertainty. Moreover, most of the correlations were developed for specific flow passages and using thermophysical properties corresponding to the average temperature. Therefore, they are not universal but for specific PCHE configurations.

Despite the superior heat transfer performance, a major problem caused by the non-straight channels in PCHEs is their large pressure drop, due to longer flow passages and complicated channel geometry. Another important issue is related to the pinch point, particularly in the low temperature recuperator where two heat exchangers are employed to optimise the capital and operating costs. The rapid decrease in the temperature difference between the exchanging fluids, due the large

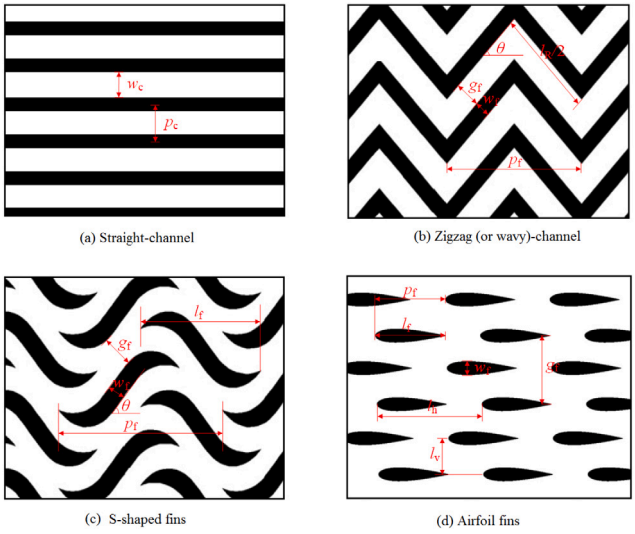

Fig. 9. Etched flow passages: (a) straight channel, (b) zigzag (or wavy) channel, (c) channel with S-shaped fins, and (d) channel with airfoil fins [112].

difference in the fluid properties of the two fluids, leads to a minimum heat transfer rate. Lastly, cleaning PCHEs is complicated due to a welded body from the core to the header. Hence, it is advisable to employ PCHEs within a limited fouling environment, or to at least use strainers.

According to [114], up to 90% of the cost of the sCO_2 Brayton cycle could be associated to heat exchangers assuming the use of PCHEs. As such, to facilitate techno-economic feasibility and the market uptake of sCO_2 power systems, alternatives to PCHE have been developed. Fourspring et al. [115] described two compact heat-transfer surfaces in the form of a recuperator. One surface employed a wire mesh as the extended heat-transfer surface, and the other surface employed a folded-wavy-fin as the extended heat-transfer surface. The recuperator employing the traditional, folded-wavy-fin heat-transfer surface can achieve the design heat-transfer rate with less than half of the allowable pressure drop. Carlson et al. [116] suggested that cast-metal heat exchangers may offer performance similar to or better than PCHEs at less than a fifth of the cost while allowing for greater flexibility in material selection and channel geometry. Chordia et al. [107] developed a microtube heat exchanger bundled together with axial separation sheets that direct flow in a strictly counter-current direction, which has the potential to meet the high temperature and high differential pressure criteria but with much lower capital cost.

4.2.3. Coolers

The operating temperatures and pressures in the cooler are lower than in the heater or recuperator, leading to less concern about structural integrity and material selection. The cooling fluid is either air or water, leading to widely different heat exchanger configurations. Their differing thermophysical properties significantly affect the heat flux in the cooler and influence the operating parameters and hence the heat transfer performance.

In air-coupled coolers, the sCO_2 operates at much higher pressure and has a significantly higher heat transfer coefficient than the cooling air, so the finned-tube heat design is appropriate for this application [109,110]. The sCO_2 flows in the array of circular or flat tubes, and the cooling air crosses the finned tubes where flat or continuous (plain, wavy, or interrupted) external fins are employed to increase the heat transfer surface area. Since the cooling sCO_2 is close to the critical point, the large variations of the thermodynamic properties can significantly affect predictions of the heat transfer and pressure drop. Therefore, the traditional Dittus–Boelter correlation [131] and

Table 3
Summary of heat-transfer correlations for printed circuit heat exchangers.

Type	Ref.	Correlation	Applicability range	Fluid
Straight channel	[117,118]	$Nu = \frac{(f/2)(Re-1000)Pr}{1+12.7(Pr^{2/3}-1)\sqrt{f/2}}$, $f = \frac{1}{4}\left(\frac{1}{1.72\log Re-1.64}\right)^2$	$2300 \le Re \le 5\times10^6$, $0.5 \le Pr \le 2000$	Helium
	[118,119]	$Nu = 3.5239\left(\frac{Re}{1000}\right)^4 - 45.148\left(\frac{Re}{1000}\right)^3 \ldots +212.13\left(\frac{Re}{1000}\right)^2 - 427.45\left(\frac{Re}{1000}\right) + 316.08$	$2300 \le Re \le 3100$	Helium
	[120]	$Nu = (0.01352 \pm 0.0094)Re^{(0.80058\pm0.0921)}$ $Nu = (3.6361\times10^{-4} \pm 7.855\times10^{-5})Re^{(1.2804\pm0.0273)}$	$1200 \le Re \le 1850$ $1850 < Re \le 2900$	Helium
		$Nu = (0.047516 \pm 0.015662)Re^{(0.633151\pm0.044606)}$ $Nu = (3.680123\times10^{-4} \pm 1.184389\times10^{-4})Re^{(1.282182\pm0.042068)}$	$1200 \le Re \le 1850$ $1850 < Re \le 2900$	
	[121]	$Nu = 0.7203Re^{0.1775}Pr^{1/3}\left(\mu/\mu_w\right)^{0.14}$, $f = 1.3383Re^{-0.5003}$	$100 < Re \le 850$	Water
Zigzag channel	[122]	$h_{hot} = 2.52Re^{0.681}$ $h_{cold} = 5.49Re^{0.625}$ $f_{hot} = \left((-1.402\times\pm0.087)\times10^{-6}\right)Re^{+(0.04495\pm0.00038)}$ $f_{cold} = \left((-1.545\pm0.099)\times10^{-6}\right)Re^{+(0.09318\pm0.0009)}$	$2800 < Re < 5800$ $6200 < Re < 12,100$ $2800 < Re < 5800$ $6200 < Re < 12,100$	CO_2
	[123]	$Nu = (0.1696 \pm 0.0144)\,Re^{0.629\pm0.009}Pr^{0.317\pm0.014}$ $f = (0.1924 \pm 0.0299)\,Re^{-0.091\pm0.016}$	$2500 < Re < 2.2\times10^4$, $0.8 < Pr < 2.2$ $3500 < Re < 2.2\times10^4$	CO_2
	[124]	$Nu = 3.255 + 0.00729(Re - 350)$ $fRe = 16.51 + 0.1627Re$ $Nu = 4.089 + 0.00365RePr^{0.58}$ $fRe = 15.78 + 0.004868Re^{0.8416} - (10.939 - 11.014v_s/v)$	$350 < Re < 800$, $Pr = 0.66$ $350 < Re < 1200$ $Re < 2500$ $Re < 2500$	Helium
	[125]	$Nu = (0.0291 \pm 0.0015)Re^{0.8138\pm0.005}$, $f = (0.2515 \pm 0.0097)Re^{-0.2013\pm0.0041}$ $Nu = (0.0188 \pm 0.0032)Re^{0.8742\pm0.0162}$, $f = (0.2881 \pm 0.0212)Re^{-0.1322\pm0.0079}$	$\theta = 32.5°$, $0.7 < Pr < 1$, $2000 < Re < 58,000$ $\theta = 40°$, $0.7 < Pr < 1$, $2000 < Re < 55,000$	CO_2
	[126]	$Nu = (0.05515 \pm 0.00160)Re^{0.69195\pm0.00559}$ $Nu = (0.09221 \pm 0.01397)Re^{0.62507\pm0.01949}$ $f = 17.639Re^{-(0.8861\pm0.0017)}$ $f = 0.019044 \pm 0.001692$	$1400 \le Re \le 2200$ $2200 < Re \le 3558$ $1400 \le Re \le 2200$ $2200 < Re \le 3558$	Helium
	[127]	$Nu = 5.05(0.02\theta + 0.003)RePr^{0.6}$	$5° \le \theta \le 15°$, $Pr \le 1$, $200 \le Re \le 550$, $4.1 \le l_R/D_h \le 12.3$	Helium
		$Nu_h = (0.71\theta + 0.289)(l_R/D)^{-0.087}\ldots \times Re^{(-0.11(\theta-0.55)^2-0.004(l_R/D)\theta+0.54)}Pr^{0.56}$, $Nu_c = (0.18\theta + 0.457)(l_R/D)^{-0.038}\ldots \times Re^{(-0.23(\theta-0.74)^2-0.004(l_R/D)\theta+0.56)}Pr^{0.58}$	$15° < \theta \le 45°$, $550 < Re \le 2000$, $Pr \le 1$, $4.1 \le l_R/D_h \le 12.3$	
		$f_{app} = \frac{15.78}{Re} + 0.0067268\exp(6.6705\theta)(l_R/D)^{-2.3833\theta+0.26648}\ldots +0.043551\theta - 0.010814$ (sharp-edged zigzag channels) $f_{app} = \frac{15.78}{Re} + 0.029311\exp(1.9216\theta)(l_R/D)^{-0.8261\theta+0.031254}\ldots +0.047659\theta - 0.028674$ (round-edged zigzag channels)	$5° \le \theta \le 45°$, $50 \le Re \le 2000$, $4.09 \le l_R/D_h \le 32.73$ $5° \le \theta \le 45°$, $50 \le Re \le 2000$, $4.09 \le l_R/D_h \le 32.73$	
S-shape fins	[123]	$Nu = (0.1740 \pm 0.0118)Re^{(0.593\pm0.007)}Pr^{(0.430\pm0.014)}$, $f = (0.4545 \pm 0.0405)Re^{(-0.340\pm0.009)}$	$3500 < Re < 2.3\times10^4$, $0.75 < Pr < 2.2$	CO_2
	[128]	$Nu_h = 0.207Re^{0.627}Pr^{0.340}$ $Nu_c = 0.253Re^{0.597}Pr^{0.349}$	$1500 < Re < 1.5\times10^4$, $1 < Pr < 3$ $100 < Re < 1500$, $2 < Pr < 11$	CO_2, Water
Airfoil fins	[129]	$Nu = 3.7 + 0.0013Re^{0.78}Pr^{0.38}$ $Nu = 0.027Re^{0}.78Pr^{0.4}$ $fRe = 0.931 + 0.028Re^{0.86}$	$Re < 2500$, $0.6 < Pr < 0.8$ $3\times10^3 < Re < 1.5\times10^5$, $0.6 < Pr < 0.8$ $Re < 1.5\times10^5$	CO_2
	[130]	$j = 0.026\left(\frac{p_t}{l_f}\right)^{-0.17}\left(\frac{w_t}{l_v}\right)^{-0.248}Re^{-0.19\left(\frac{w_t}{l_v}\right)^{-0.187}}$ $f = 0.357\left(\frac{p_t}{l_f}\right)^{-0.252}\left(\frac{w_t}{l_v}\right)^{-0.255}Re^{-0.173\left(\frac{w_t}{l_v}\right)^{-0.274}}$	$8000 < Re < 10^5$ $8000 < Re < 10^5$	CO_2

D_h: hydraulic diameter, m; f: friction factor; h: heat transfer coefficient, W/(m^{2}K); j: Colburn factor; l: length, m; l_R: relative length, m; l_v: transverse pitch, m; Re: Reynolds number; Nu: Nusselt number; p: pitch, m; p_f: longitudinal pitch, m; Pr: Prandtl number; w: width, m; w_f: width of internal channel, m; θ: fin angle; v: kinematic viscosity, m^2/s. Subscripts: in, inlet; c, cold; h, hot; f: fin; in, inlet; min: minimum.

Gnielinski correlation [117], which are not able to account for the property difference between the wall and bulk fluid temperatures, are not accurate enough to predict the heat transfer coefficient for the sCO_2. Jackson [132] summarised convective heat transfer correlations developed for fluids at supercritical pressure and compared them with approximately 2000 different experimental conditions. The correlation of Krasnoshchekov [133] showed the best performance with 98% of the sCO_2 data within 25% difference. Chai and Tassou [134] also compared their sCO_2 results with six heat transfer correlations and the Krasnoshchekov correlation again showed the best prediction. A major problem with air-coupled coolers is the pinch point, due to the one or two orders of magnitude lower heat transfer coefficient of the cooling air than the sCO_2. The temperature drop of the sCO_2 mostly takes place at the very small part of the heat exchanger [135]. The much lower density and specific heat capacity of the cooling air compared to the sCO_2 also mean the cooler requires extremely high air mass flow rates and larger heat transfer surfaces. To address these problems, the microchannel-plate fin heat exchanger as shown in Fig. 10 can be considered for the CO_2 cooler design. The microchannel-plate fin cooler has the potential to achieve better heat transfer performance than the finned-tube one and significantly reduce the overall heat exchanger size.

Fig. 10. Microchannel heat exchanger (courtesy of Danfoss).

In water-coupled CO_2 coolers, the pinch point issue is not as pronounced due to comparable density and specific heat capacity between water and sCO_2. Plate heat exchangers have been employed in water-coupled cooler applications. The corrugated plates create channels with increased flow turbulence and extended heat transfer area, which improves heat transfer performance and minimises the fouling risk. Some review papers have been published to underline this application. Ayub [136] summarised the single-phase correlations available for the design and analysis of plate heat exchangers. Abu-Khader [137] presented advances in plate heat exchanger design while Elmaaty et al. [138] reviewed plate structures and heat transfer mechanisms. It should be noted that there is no generally accepted heat transfer correlation for sCO_2 flowing between corrugated plates. Chai and Tassou [110] modified the correlation proposed by Wanniarachchi et al. [139] with a function developed by Krasnoshchekov [133] to account for the sCO_2 working close to the near-critical region in plate heat exchangers. Alongside plate heat exchangers, some newly proposed technologies employed in CO_2 heat-pump water heaters can be considered for sCO_2 cooler applications. These include fluted tube-in-tube [140], serpentine microchannel [141] and multi-twisted-tube heat exchangers [142]. They have been shown to be capable of operating at high pressures, have a high overall heat transfer coefficient and good temperature matching between water and the sCO_2 in counter-flow arrangements.

The significant variation of sCO_2 thermophysical properties in the near-critical-point region differentiates the heat transfer and flow mechanism from conventional fluids. Particularly, the abrupt increase of specific heat greatly increases the heat-transfer coefficient which reaches its peak at the pseudocritical temperature [143]. The heat transfer and flow mechanism are also influenced by geometrical and operational parameters, including channel shape and dimension, flow direction, mass flux, heat flux, inlet temperature and pressure, and heating or cooling conditions etc. [143–151]. Due to the density change, buoyancy also significantly affects the heat transfer and flow mechanism for all flow orientations at Reynolds numbers up to 10^5 [144,145,152–155]. Heat transfer can also be significantly impaired by flow acceleration, especially for high-heat-flux conditions and in mini/micro channels [156,157]. Several authors have developed empirical correlations for specific geometries; however, most have been developed for a given range of temperature, pressure, heat flux, and flow characteristics. Comparisons of various correlations for sCO_2 heat transfer showed that several correlations can be used for preliminary estimation of heat transfer in tubes, but no single correlation is able to accurately describe local heat transfer for different channel geometries [158,159].

4.3. Material considerations

Material selection for sCO_2 systems is dictated by the mechanical and thermal properties of the material, compatibility with the high-temperature and pressure CO_2 environment, and the fabrication cost of the power plant [160]. The sCO_2 environment strongly influences the evolution of ionic solubility and dissociation processes and further affects the performance of corrosion, oxidation and creep resistance of the material [161].

A brief summary of studies investigating material performance with moderate to high temperature sCO_2 is provided in Table 4. Within this the selected materials, test conditions, test characteristics and main findings are presented. However, most of these studies are limited to low sCO_2 velocity laboratory conditions, and are not the representative of the high-velocity operating conditions expected within practical sCO_2 power systems.

Key components concerning material selection are the heater, the recuperator, and the turbine. The heater involves either direct heating through the mixing of the heat carrier fluid with the sCO_2 or indirect heat transfer process between the different fluids, all of which operate at high temperature and high pressure and expose a large surface area to the heat source. A major consideration in heater design is material strength and durability. The thick-walled corrosion-resistant tubing should withstand rapid start-ups and transients, and should guarantee long thermal cycling and fatigue life under temperature and pressure containments of both sCO_2 and the heat source.

The recuperator operates under high temperature, high pressure and significant pressure differentials between the exchanging fluids which requires considerable material resistance to creep and corrosion for long service duration without any structural degradation [112]. To satisfy these requirements, most sCO_2 test facilities have employed PCHEs for heat recuperation (see Section 4.2.2). PCHEs are manufactured by photochemically machining the flow passages into flat plates followed by stacking the plates together which are then diffusion bonded. As noted by Li et al. [167], the material challenge for these heat exchangers is to withstand exposure to high temperatures and pressures for up to 60 years within a very corrosive environment involving possible oxidation, carburisation or decarburisation. Material selection also demands a balance between heat conduction performance and capital cost.

The operating conditions within the turbine bring about both high temperature and pressure drops from inlet to outlet. The concern for material selection relates to the thermal expansion during operation, the mechanical interference during startup and shutdown, the temperature limits of the seals and bearings, corrosion and other design issues. As mentioned by Wright et al. [183], sCO_2 pressures up to 300 bar and the higher density (compared to steam) can significantly influence the loading on the turbine rotor blades and necessitate higher strength alloys. The alloy choice is determined by the required strength at peak temperature, which depends on the structural design of the turbine blades and whether they are cooled. Additionally, flexible materials are usually used for seals in the turbomachinery. The sCO_2 can dissolve into these materials at high pressure and cause rapid gas decompression, leading to unique challenges for seal design.

To keep material costs low, various classes of structural alloys, including low-alloyed steels, austenitic steels, Nickel alloys, and Titanium alloys, can be employed in a power cycle for different equipment and component design. Generally, at operating temperatures lower than 650 °C, traditional stainless steel can be employed, while for operating temperatures higher than 650 °C, nickel-based or even titanium-based alloys would be required to reduce oxidation from the sCO_2 environment and achieve pressure containment without excessive material thicknesses, but at much higher capital cost [164].

4.4. Control systems

Power plants based on sCO_2 technology are widely regarded as flexible systems thanks to their capability to operate efficiently both at full and part load, and to quickly adapt to large variations in the operating conditions and at high ramp rates [184]. In the short to medium term, this is a key requirement for base-load power systems

Table 4
Representative studies of material selection for sCO_2 power system.

Reference	Materials	Test conditions	Test characteristics	Remarks
Maziasz et al. [162–164]	347SS and Alloys 120, 214, 230, 625, 740, 803, HR120 and AL20-25+Nb	650–800 °C	Creep strength	347SS cannot be used as temperature exceeds 650 °C; Alloys 214, 625, HR120 and AL20-25+Nb can have very good properties for high temperatures.
Osman et al. [165]	347SS	700 °C/54 and 221 MPa	Creep rupture	Thin foil specimens of 347SS had higher creep rates and rupture ductility than their bulk specimen counterparts.
Evans et al. [166]	Alloy 625	750 °C/100 MPa	Creep rupture	Alloy 625 is an attractive potential alloy for use in the high temperature heat exchanger.
Li et al. [167]	Alloys 800H, HX, 230 and 617	900 °C	Creep strength	Alloy 617 is the leading candidate material for the high temperature heat exchanger.
Klower et al. [168]	Alloy 617	700 °C	Creep strength	Alloy 617 can be a candidate material for 700 °C power plants.
Anderson et al. [169,170]	347SS, NF616, HCM12A and Alloy 800H	650 °C/3925 psi	Corrosion	Cr and Al had profound influence on imparting corrosion resistance.
Cao et al. [171]	316SS, 310SS and Alloy 800H	650 °C/200 bar	Corrosion	Alloy 800H exhibited the best corrosion resistance, followed by 310SS and 316SS.
Firouzdor et al. [172]	AL-6XN, Alloy PE-16, Haynes 230 and Alloy 625	650 °C/200 bar	Corrosion	Cr_2O_3 oxide layers protect the Haynes 230 and Alloy 625 from further corrosion.
Lee et al. [173,174]	Alloys 800HT, 600 and 690	550, 600 and 650 °C/200 bar	Corrosion and carburisation	The α-alumina layer results in superior carburisation resistance.
Rouillard et al. [175]	T91, 316L, 253MA® and Alloy 800	550 °C/250 bar	Corrosion	Alloy 800 were much more corrosion-resistant than T91.
Holcomb et al. [176]	347H, Alloys 625 and 282	730 °C/207 bar	Oxidation and corrosion	Little effect of pressure on the oxidation behaviour of Alloys 625 and 282; Austenitic stainless steels would be more cost effective for long term use in sCO_2 power system.
Adam et al. [177]	Alloy 800H	650 and 750 °C/200 bar	Corrosion	sCO_2 resulted in a higher density of carbides beneath the oxide scale than the air.
Gui et al. [178]	T91, VM12, Super 304H, and Sanicro 25	650 °C/150 bar	Oxidation	Super 304H and Sanicro 25 showed enhanced corrosion resistance due to the chromia-rich oxide scales formed on them.
Liang et al. [179]	T91, TP347HFG and Alloy 617	650 °C/150 bar	Oxidation	TP347HFG and 617 showed enhanced their corrosion resistance due to the chromia-rich oxide scales formed on them.
Pint et al. [180]	Fe- and Ni-based alloys	750 °C/300 bar	Oxidation	Pressure had a limited effect on oxide thickness and internal oxidation and reaction products.
Bidabadi et al. [181]	Alloy F91	550 °C/100 bar	Oxidation	Pressure affects the increase rate of carbon concentration at the oxide–alloy interface.
Kim et al. [182]	316H and Alloy 800HT	600 °C/200 bar	Corrosion	316H and Alloy 800HT exhibited reduced elongation at fracture after sCO_2 exposure; Alloy 800HT shows much greater ductility reduction and brittle failure at the bond-line.

given the increasing penetration of renewable, yet intermittent, energy sources in the global energy mix. As such, a large body of research has focused on the development of control strategies to address the part-load operation and the transient behaviour of sCO_2 systems during startup and shutdown. In this framework, the use of dynamic modelling approaches have facilitated the understanding of the transient performance of sCO_2 power equipment and systems prior to the development of the physical controls. The dynamic modelling of sCO_2 power systems has been carried out through low order models (zero and one dimensional) implemented either in ad-hoc tools (ANL's Plant Dynamics Code [185,186], MIT's SCPS and TSCYCO [187]) or in commercial ones such as Modelica/Dymola® [188–191], GT-SUITE® [192,193], ASPEN PLUS® [194,195], and Apros® [196].

Compressors and turbines are typically modelled using a map-based approach [67] in which the inputs are either from ad-hoc models (mean-line codes [197], 3D CFD [193]) or from experimental data [198]. On the other hand, the off-design performance of turbomachinery can be scaled using similarity theory [191,199]. The map-based approach is justified by the timescale of any dynamics within turbomachinery, which is significantly shorter than that of heat exchangers. As such, performance maps merely act as look-up tables to provide the boundary conditions to the equipment upstream and downstream. To account for the time variation of the revolution speed imposed by a change of load at the generator, some studies further considered the turbomachinery rotordynamic aspects [200]. Unlike the conventional map-based approaches which rely on a single non-dimensional map to describe the whole operation of the turbomachine, the strong real gas effects of CO_2 in close proximity to the critical point of CO_2 require multi-dimensional maps at different inlet conditions [187]. This holds especially for compressors working in the critical region. Alternatively, dimensionless turbomachinery performance maps, expressed in terms of flow and load coefficients, may be employed to overcome this issue [201,202].

Heat exchangers are typically modelled with a transient one-dimensional formulation of the conservation equations underpinned by semi-empirical correlations for the heat transfer coefficient and friction factor, listed in Section 4.2 [187,203]. The fine discretisation

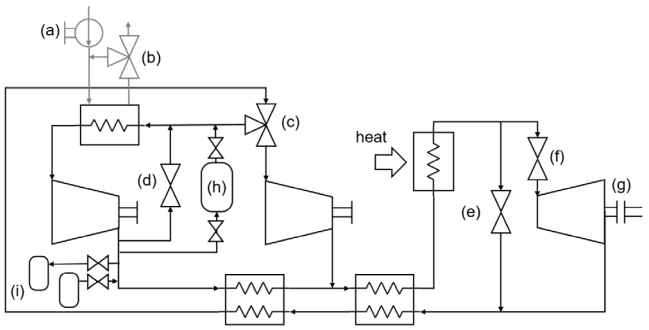

Fig. 11. Summary of control strategies reported on a recompressed cycle layout: (a) heat sink flow rate, (b) cooler bypass, (c) compressor flow split, (d) compressor bypass, (e) turbine bypass, (f) turbine throttling, (g) turbine speed, (h) single tank inventory control, (i) dual tank inventory control.

required to resolve the non-linearities of heat transfer phenomena in sCO_2 applications results in high computational costs for dynamic simulations which goes against the requirements for an appropriate control system. To overcome this shortcoming, a correction factor for the logarithmic mean temperature difference (LMTD) coupled with an iterative pressure drop calculation has been proposed to accelerate the off-design simulations in PCHE up to 350 times and with less than 5% deviation from the one-dimensional performance results [204]. In addition to this, non-model based adaptive control approaches, such as the extremum seeking one, are being explored. This method considers the sCO_2 system as a black box and relies on continuous measurements of the plant performance, e.g. turbine inlet pressure and temperature as well as net power output [205].

In addition to the specifics that are dictated by the heat source, such as reactor core cooling in nuclear applications, in a sCO_2 plant the purpose of the control system is to ensure an efficient operation of the power block without exceeding safety and operational limits. Typical limitations that apply both at part-load and transient conditions are: compressor stall/choking/two-phase operation, turbine choking, extreme CO_2 pressures and temperatures, extreme shaft rotational speeds, cooling water exit temperature not exceeding calcification threshold etc. [187]. Control systems should also aim at meeting the load demand and ramp rate, maintaining cycle efficiency and rejecting process disturbances such as heat input availability [195].

Control strategies have mainly been investigated with reference to the recompression and simple recuperated cycle layouts given the cost and efficiency advantages recalled in Section 3 as well as the availability of experimental data. The controllers implemented have mostly been proportional-integral ones (PI) since they provide zero error at the steady state and are insensitive to the higher-frequency terms of the inputs such as interferences [197,206]. However, the derivative term in the PID controllers set-up may also be tuned through the Cohen–Coon technique [207]. The operational stability of sCO_2 power systems has mainly been addressed in terms of control of the compressor inlet temperature and pressure balance at the junction points in the case of recompression cycles [208]. On the other hand, the sCO_2 performance at part-load were primarily controlled through the turbine inlet temperature [194]. A summary of control strategies is reported in Fig. 11; the scheme refers to a recompressed cycle as an example and does not relate to a specific application.

The control of the compressor inlet temperature may be achieved by acting on the heat sink at the cooler. In particular, the combined control of the heat sink flow rate (Fig. 11a) and the cooler bypass (Fig. 11b) can result in a constant temperature at the main compressor inlet, avoiding the two-phase region [187]. At part-load conditions, before using inventory control, the low temperature control may be employed to isobarically increase the compressor inlet temperature, up to a region in which the fluid density is less sensitive to pressure changes (e.g. from 32 °C to 34 °C). In this way, the CO_2 inventory withdrawal required for operation at part-load can take place without introducing significant instabilities to the system whilst still maintaining operation outside the two-phase region [209]. However, since with no inventory control the CO_2 mass in the cycle is constant, an isobaric change of compressor inlet conditions is only possible if the turbine inlet temperature is regulated at the same time as compressor inlet temperature. In the case analysed in [209], this was achieved through a reduction of the nuclear reactor power and the sodium mass flow rate, i.e. the heat input to the sCO_2 power block.

In the recompression cycle, the flow split ratio between the two compressors (Fig. 11c) was considered to maintain compressor surge margin [208]. In the simple recuperated cycle, the same control functionality can be achieved through a bypass of flow from downstream of the compressor to upstream of the cooler (Fig. 11d) [67]. The control of the recompressor flow showed marginal benefits when used for load regulation compared to the inventory control. However, the compressor flow control resulted in optimal load tracking with lower control complexity [208].

The control of the turbine inlet temperature has been addressed through multiple approaches: turbine flow bypass, turbine flow throttling, inventory control, speed control if the power turbine is on an independent shaft and/or if the generator is a synchronous permanent magnet (Fig. 11g) [204]. The turbine flow bypass (Fig. 11e) reduces the mass flow rate expanding in the turbine and was found to be a suitable strategy for fast transients and for load variations between 90% and 100% of the design value.

Inventory control implies a change of the CO_2 charge between the power loop and the storage tanks. This approach was found to be the most efficient strategy to maximise the cycle efficiency for operation between 50% and 90% of the design point as well as to increase the load by up to 110% of the nominal value [187]. The stability implications due to the withdrawals/additions of CO_2 were identified as one of the major drawbacks of inventory control. Moreover, this approach usually suffers from a slow response rate compared to the turbine bypass control. In fact, the filling and emptying processes are often driven by pressure gradients in the loop rather than through the ancillaries. As such, the key limiting factor in inventory control lies in the finite capacity of the storage tanks, whose estimation can be preliminary carried out through the approach proposed by Bitsch and Chaboseau in [210] and recalled in [211]. The location of the inventory storage tanks significantly affects the transient behaviour of the system due to the possible temporary mismatch between the compressor and turbine mass flow rates. The most common layout considers the withdrawal point downstream of the compressor and the feeding point upstream of the cooler (Fig. 11h). This layout is suitable and responsive for load reductions but suffers from a response in the case of increased load demand. A fast supply of CO_2 from the storage tanks upstream of the compressor would lead to a sudden increase in compression power for the same turbine power which may, in the worst situations, cause a shutdown of the power system. To overcome the slow response rate at increasing loads, inventory control layouts with removal and feeding points downstream of the compressor and two storage systems were also considered (Fig. 11i). In this arrangement, the turbine power is always greater than the compressor power [211]. However, an ancillary system is required to boost the inventory stored in the high-pressure cylinder beyond the compressor outlet pressure. Together with inventory control, the inertia of the sCO_2 power system may also be tuned with respect to the volume ratio between hot and cold sides of the loop. A smaller hot-to-cold side volume-ratio leads to faster startup while large ratios are advisable for continuous load requirements and fluctuating heat source and sink conditions [189].

The turbine flow throttling (Fig. 11f) was envisaged for part-load operation between 50% and 20% of the nominal power. This approach requires the coupling of turbine throttling with the flow split control in recompression cycles to ensure the operation of the compressors within their acceptable ranges. Further load reductions can be accomplished using also the turbine bypass [187].

Besides theoretical knowledge, the outcomes of transient and control studies have been exploited to develop the controls for the existing experimental facilities. Even though each test rig has its own unique features, based on the operational experience reported, similar procedures were identified. The filling process of sCO_2 loops was carried out with high-purity carbon dioxide (e.g. 99.995%), after vacuuming the loop to remove moisture and non-condensable gases. Similarly to CO_2 refrigeration systems, gaseous CO_2 should be employed during the initial charging to overcome the CO_2 triple point (5.17 bar, -56.60 °C) and prevent the formation of dry ice. Afterwards, liquid CO_2 allows faster charging rates until the saturation pressure at ambient conditions is achieved [212]. From this state, a small quantity heat is supplied to the loop, until the whole CO_2 vaporises and reaches supercritical conditions throughout the circuit (e.g. 85 bar, 38 °C [66]). The heat input during the startup phase may be supplied from different locations of the loop and may also involve a temporary shutdown of the heat rejection system [190]. At the same time, ancillary devices, such as CO_2 centrifugal pumps or air driven reciprocating gas boosters, are used to circulate a minimal flow rate to ensure the absence of two-phase spots. At the end of the start-up phase, the turbomachinery can be switched on and the heat load increased. While the turbomachinery speed ramps-up fast (e.g. 20 s from 0% to 100% of design speed [213]), the heat is supplied gradually (e.g. 50–111 K/h [66,212]) to avoid thermal stresses in the equipment and joints. From these conditions on-wards, the control strategies discussed above are used to reach the desired test conditions [214,215]. A cooling procedure in the reverse order of the start-up procedure is employed for the shutdown of the turbomachinery and eventually the whole power system.

Regarding the largest scale systems for which control literature has been published, it is worth acknowledging the STEP and Echogen research contributions. In fact, besides the performance aspects previously discussed, the architectures of these sCO_2 systems include additional loops which are paramount to fulfil functional and operational requirements. The controls of the STEP test facility are presented in [195]. The full control system consists of flow, pressure and temperature controllers for the natural gas fuelled heat source, temperature controllers for the compressor and turbine inlet temperatures, pressure-based inventory controller with split-range philosophy to prevent jittering (open/close), and net work controller to meet the power demand. The control system of the Echogen's 7.3 MW_e EPS100 unit is instead composed of: a compressor bypass valve to control the turbocompressor speed and, in turn, flow rate and pressure rise; a combination of bypass and throttle valves, and load bank resistance (simulating the grid in the study) to control the power turbine; an inventory control system downstream of the cooler to control the compressor inlet pressure [192]. In both applications all controllers were PI ones. However, the Echogen's study additionally reports the experimental validation of the model-based control system. The simulations were initialised with experimental boundary conditions at steady state and then validated against more than eight hours of transient data. When the measured turbocompressor speed was used as the boundary condition instead of the set point value, a good alignment between measurements and simulation data was reported. A key open point highlighted by Echogen, and generally applicable to any sCO_2 control research, was the need to also validate such models at startup and shutdown conditions, where different control strategies from the performance-oriented ones come into play.

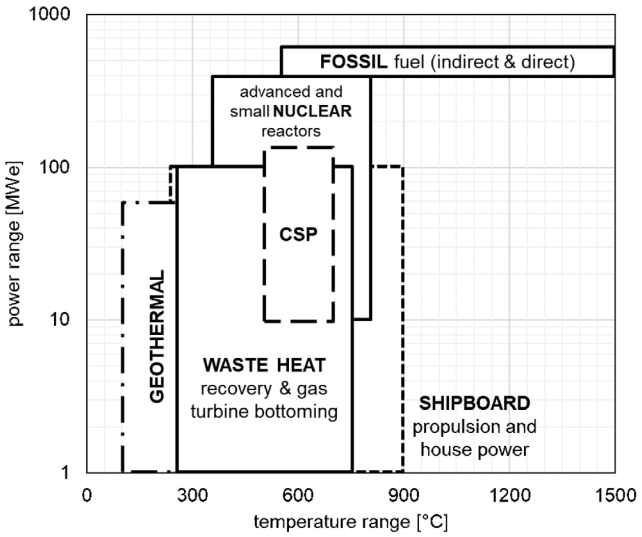

Fig. 12. Overview of sCO_2 power applications. *Source:* Elaboration from [217].

5. Applications

Supercritical CO_2 technology offers a broad potential for power generation and propulsion. An attempt to summarise the operating ranges and sizes envisaged for the main application areas is reported in Fig. 12. These application areas are elaborated on in the following subsections, whilst a summary of the main application areas is provided in Table 5, in which representative cycles, operating conditions and power ratings are presented alongside thermodynamic and economic metrics such as thermal efficiency and levelised cost of electricity (LCOE). A market analysis conducted by Sandia National Laboratories projects an LCOE for an sCO_2 system between 44.8 and 56.1 $/MWh for power ratings between 100 and 300 MW_e [216], but these values are not linked to a specific application.

5.1. Fossil fuelled and waste heat to power generation

Supercritical CO_2 power systems were originally conceived to overcome the limitations of steam power plants. Even though sCO_2 power concepts regained popularity in the early 2000s for nuclear applications, the need for operational flexibility to accommodate the increasing penetration of renewable energy sources in the global energy mix, the low footprint and the possibility to integrate a carbon capture system provided further consideration of sCO_2 cycles for base-load power generation applications.

Fossil fuelled sCO_2 power plants are commonly classified based on the heat addition method [218]: in direct heating, the CO_2 loop is an open system in which the heat input is from combustion processes involving fuels and oxidants circulating together with CO_2; in indirect heating, the sCO_2 power block is a closed loop system where heat addition and rejection take place through heat exchangers. Hence, the sCO_2 unit acts as a typical bottoming heat to power system, such as steam or organic Rankine cycles which, in turn, are the main competitors of sCO_2 technology. The bottoming cycle approach is also applicable for waste heat recovery.

5.1.1. Indirect sCO_2 heating — Heat to power

Heat to power generation through bottoming sCO_2 cycles aims at the recovery of thermal energy from the topping process to maximise the power output. This goal differs from maximising cycle efficiency, which is typical of applications in which heat is generated at a cost,

Table 5
Summary of the main application areas for sCO_2 power cycles and notable thermodynamic and economic modelling studies.

Application	Ref.	Operating conditions						Advantages	Challenges
		Cycle[a]	T_{max} [°C]	p_{max} [bar]	Power [MW_e]	LHV/HHV[†] Efficiency	LCOE/COE[*] [$/MWh][b]		
Fossil fuel (coal fired)	[108]	RH	620	300	1150	50.3%		(i) increased utilisation factor due to higher operational flexibility than steam plants; (ii) parasitic losses due to CCS compensated by high cycle efficiency; (iii) direct cooling reduces water consumption	(i) competition with ultra-supercritical steam power plants with CCS; (ii) technological gap for primary heater (aka sCO_2 boiler) and axial turbomachinery
		RH+CCS	620	300	1000	41.4%	73.1		
	[219]	RH	620	200	635	43.9%[†]	75.7		
(oxy-fuel)	[220]	AL	1150	300	846	55.1%	92	(i) integrated carbon sequestration; (ii) higher efficiency than indirect heating cycles; (iii) optimal operation at higher cycle pressure ratios than conventional sCO_2 cycles; (iv) operational flexibility; (v) low footprint; (vi) very attractive LCOE	(i) technological gap for sCO_2 oxy-combustor; (ii) CO_2 impurities; (iii) materials corrosion and erosion; (iv) turbine blade film cooling; (v) alternative control strategies; (vi) competition with other oxy-fuelled power generation concepts
(oxy-coal)	[221]	AL	1204	308	606	40.6%[†]	122.7[*]		
Waste heat (gas turbines)	[222]	PH	389	238	8.6	25.9%	40	(i) suitable for high-grade (>350 °C) concentrated waste heat sources (>1 MW_e); (ii) high efficiency; (iii) operational flexibility; (iv) low footprint	(i) competition with conventional steam and ORC systems; (ii) same techno-financial barriers as other WHR technologies; (iii) need primary heater technologies characterised by low pressure drop, resistance to corrosion and fouling, modularity etc.
	[223]	RCRH	572	154	146	47.73%			
(IC engines)	[224]	SR+ORC	320	200	0.2				
(industrial)	[38]	SR	425	200	0.9[c]	25.1%	8.3		
	[225]	SR	389	256	9.5	27.9%			
CSP	[226]	RC	580	275	82	38.4%	(6350)[d]	(i) suitable for next generation CSP systems (> 600 °C); (ii) higher efficiency should reduce size and cost of collector field; (iii) simpler, compact power block; (iv) heat exchange temperature profiles allow compact thermal-energy storage	(i) CSP LCOE not yet competitive with solar PV; (ii) need suitable heat carriers for operation at elevated temperatures; (iii) CSP plants are in regions with high ambient temperatures; (iv) demonstration required at appropriate scale
		RCPC	580	275	71	33.2%	(6510)[d]		
	[227][e]	RC	705	273	100	48.8%	59.8		
	[39]	RCPC	900	300	50	55%	(5015)[d]		
	[228]	RCPC	630	250	115	46.2%	144		
	[32][f]	RET	550	250	35	43%	135; 164		
			700	250	35	50%	135; 164		
	[229]	RC	550	250	50	46%	110		
	[230]	RCICPH	468	250	10	35.6			
Nuclear	[231]	RCRH	465	250	10	43.7%	53.6	(i) good temperature match with future Gen IV SFR and LFR reactors; (ii) increased efficiency and reduced physical footprint should reduce LCOE; (iii) good candidate for small modular reactors	(i) technology needs to be demonstrated in other applications first; (ii) need to understand interactions between sCO_2 and reactor materials (e.g., sodium, lead)
	[232]	RC+ORC	550	210	250	42.5%	(44.6)[g]		
	[233]	RC	550	250	10	36.7-44.5%	50–55		
Geothermal	[234]	S	60	119	51	5%	200	Reduced pumping work compared to indirect brine systems and better performance at shallow depths and low reservoir permeabilities	(i) more sensitive to ambient cooling conditions; (ii) operation close to the critical point means turbine designs differ to other sCO_2 systems
			86.6	160	157	5%	120		

[a]Allam (AL); carbon capture system (CCS); cost of electricity (COE); higher heating value (HHV); internal combustion (IC); levelised cost of electricity (LCOE); lower heating value (LHV); organic Rankine cycle (ORC); preheated (PH); recompression (RC); recompression with intercooling and preheating (RCICPH); recompression partially-cooled (RCPC); recompression reheating (RCRH); recuperated transcritical (RET); reheated (RH); simple (S); simple recuperated (SR).

[b]Assumed conversion rate: 1 EUR = 1.1 USD.

[c]Assuming 10 kg/s waste exhaust and plate heat exchangers as gas coolers.

[d]Overnight capital costs, $/$kW_e$.

[e]The related SunShot programme within the U.S. targets a LCOE of 60 $/MWh with a thermal efficiency in excess of 50%.

[f]The related SCARABEUS project targets a LCOE of 106 $/MWh (96 EURO/MWh) with a thermal efficiency in excess of 50%.

[g]Total product cost based on exergoeconomic assessment

i.e. nuclear or fuel combustion. With the exception of coal-fired power plants, in indirect heating applications the heat stream comes as a by-product of a main process. As such, if not recovered, that thermal energy will be otherwise wasted to the environment. For this reason, highly recuperative cycles are not preferred for waste heat recovery. Instead, split cycles, that divert part of the CO_2 flow downstream of the compressor directly to the heater rather than to the recuperators, are more suited [28,38,222].

Bottoming heat to power cycles based on steam or organic working fluids have a mature technology readiness level. A number of providers offer commercial solutions even in the kilowatt power range. In this context, even though the technology is potentially applicable to a broader spectrum of operating conditions, sCO_2 technology becomes particularly competitive for high-grade heat sources (>350 °C) and large-scale applications (>0.5 MW_e). These considerations result from the authors' experience in sCO_2 heat to power projects and business cases developed for European industry. The aforementioned market segment allows sCO_2 to tackle high temperature sources, even beyond the operating ranges of ultra-supercritical (USC) steam power cycles (600–620 °C), with favourable economies of scale and lower footprint. Potential applications for sCO_2 power units are gas turbines, reciprocating internal combustion engines and energy intensive industries.

The global gas turbine market was valued at more than $6bn in 2019. In March 2020, pre-covid-19 projections estimated a growth at a compound annual growth rate (CAGR) of 8.2% in the 2020–2026 period with the additional installed capacity of 43.7 GW worldwide [235]. The 250–500 MW segment is considered the backbone of the gas turbine power generation industry [236]. Market growth drivers are the global commitment towards clean energy outlooks (gas rather than coal, integration with renewable energy sources, upgrade or retrofit of existing equipment etc.), the renewed interest in shale gas and liquefied natural gas (LNG) as well as the decommissioning of nuclear power plants in some regions. Globally, the Asia-Pacific region has the largest market for gas turbines, with China and India being the hot spots for demand [237]. Unlike reciprocating internal combustion engines, in a gas turbine the waste heat is almost totally concentrated in the turbine exhaust, whose temperature ranges between 350 °C and 600 °C [238]. Supercritical CO_2 cycles could be employed as an alternative to current bottoming steam sections in greenfield or retrofitted combined cycle gas turbine (CCGT) power plants.

The global generator set (or genset) market was valued at over $18bn in 2019 and, before covid-19 (April 2019), it was anticipated to grow at a CAGR of 6% by 2030. The segment above 750 kVA is considered the backbone of the genset industry. The main market driver for gensets is the need for continuous and uninterrupted power supply, especially for data centres and those industries impacted by the digital revolution [239]. Genset power units are composed of an electrical generator driven by a reciprocating internal combustion engine which can be fuelled with natural gas, diesel, gasoline, biofuels etc. Out of the fuel energy input, nearly one third is wasted through the engine exhaust at temperatures ranging from 350 °C up to 670 °C [240]. Supercritical CO_2 power cycles could be employed as an alternative to the current bottoming ORC sections. However, given the size of the reciprocating internal combustion engines, the power output is expected to be below 1 MW_e. This aspect, together with a possible low capacity factor, poses serious challenges to the economic feasibility of the sCO_2 retrofit.

Recent top-down estimations of the waste-heat potential in industry indicate that the share of primary energy consumption wasted, as exhausts or effluents, that is above 300 °C is 11.4% (3367 TWh in absolute terms) of the total supply at world level and 8.7% (275 TWh) at European level [241,242]. Among the industrial sectors reviewed, the ones in which high grade waste heat has the highest share of primary energy consumption are iron and steel, non-ferrous metals (i.e. aluminium) and non-metallic minerals (i.e. glass and cement). Detailed assessments on waste-heat recovery opportunities in these sectors can be found in [243–246]. Common elements to these industrial processes are the large size of the application, the coexistence of convective and radiative mechanisms in the heat source (mostly due to furnaces), the uninterrupted nature of the process and the need to comply to emission trading systems regulations (e.g. European ETS). These aspects are in favour of a waste-heat recovery retrofit with sCO_2 systems, which unlike steam or organic Rankine cycles, would be more compact and able to fully tackle the high temperature recovery opportunity of these energy intensive industries.

5.1.2. *Indirect* sCO_2 *heating — Coal power*

According to the IEA's sustainable development scenario, coal power generation is expected to drop from 10 PWh to 2 PWh by 2040. Nonetheless, coal power still contributes to 37% of today's world electricity supply and is mostly used for base-load power generation [247]. As such, a number of initiatives are being explored to retrofit or upgrade existing coal fired power stations with sCO_2 technology, with the two key drivers being decarbonisation and flexibility. The majority of the published research has focused on cycle analysis and thermo-economic assessments, including carbon capture systems [108,219,248]. Among these works, there is strong agreement in identifying the sCO_2 'boiler' as the technological bottleneck. Compared to a steam boiler at the same duty, a coal-fired sCO_2 system has larger heat transfer surfaces due to the higher mass flow rates, lower heat transfer coefficients (3–5 kW/m^2K [249]) and lower pressure drop requirements [250]. Carbon dioxide also enters the heater near supercritical conditions and exit the heater at temperatures higher than the 620 °C of USC boilers [251]. This poses challenges in material selection and availability due to high-temperature corrosion (internal because of CO_2 and external due to the flue gas), non-stationary load profiles and different control strategies [184], as well as cost limitations.

5.1.3. *Direct* sCO_2 *heating*

Direct heating sCO_2 power cycles are open-loop internal combustion engines underpinned by variants of the Joule–Brayton cycle and in which the heat input typically results from an oxy-fuel combustion using either natural gas or syngas from a coal gasification process. Hence, this concept is applicable and is being developed both for gaseous and solid fossil fuels. The sCO_2 heater found within indirect cycles is replaced by a combustor in which the heat of the oxy-combustion is diluted with CO_2 entering the combustor after a regenerative heating at temperatures around 750 °C. The direct heating not only allows higher cycle temperatures than indirect sCO_2 cycles but can also deliver optimal performance at higher pressure ratios. As a result, at the turbine inlet (200+ bar and 1100+ °C) the working fluid has a higher power density compared to indirect heating cycles.

Besides the theoretical efficiency advantages resulting from high turbine inlet temperature and cycle pressure ratio, the most interesting aspect of these advanced cycle architectures is the capability to perform a carbon sequestration together with power conversion (i.e. without additional equipment). This is achieved thanks to the following operational features: the oxy-combustion products are primarily CO_2 and water; water can be separated downstream of the cooler; the maximum cycle pressure exceeds conventional CO_2 pipelines (110–150 bar [220]). Hence, the CO_2 generated as a product of combustion can be separated downstream of the compressor such that the CO_2 flow at the inlet of the high-pressure side of the recuperator is constant, even if the CO_2 loop is open. For this reason, this family of cycles are also referred to as semi-closed.

A breakthrough in the field of direct heating sCO_2 fossil power generation was the invention of the Allam–Fetvedt cycle, commonly referred to as the Allam cycle. The concept was patented in 2011 [252] and is being up-scaled to full-scale demonstration through initiatives led, partly or fully, by 8 Rivers Capital both for natural gas (50MW_{th} NET Power's plant in La Porte, Texas (US) [253]) and coal-fired (300 MW_e 'Allam Cycle Zero Emission Coal Power' project co-funded by US

DOE [254]) power generation. The Allam cycle is a simple regenerative, semi-closed sCO_2 cycle in which the imbalance between residual enthalpy at the low pressure turbine exhaust and the heat required to raise the temperature of the high pressure CO_2 flow prior to combustion is compensated through an external heat addition at the recuperator. This external regenerative heat is provided either by the air separation unit (ASU) in the gas-fired version of the cycle or by the coal gasifier in the coal-fired Allam cycle [73,255]. Since the invention of the Allam cycle, several investigations have been carried out in the field of direct heating sCO_2 power cycles.

Alongside thermodynamic and techno-economic studies [221,256,257], a large body or research is currently aiming to tackle the know-how and technological challenges introduced by the direct heating of CO_2 as well as the more ambitious operating conditions which characterise these cycles: CO_2 impurities due to fuel, nitrogen, water; corrosion aspects in coal gasification; CO_2 corrosion at high and low temperatures; combustion dynamics in high density flow [258–260]; turbine blade film cooling and erosion due to impurities [261]; recuperator erosion due to impurities and stress magnitude due to high cycle pressure ratios; alternative control strategies to turbine throttling [262]; materials [263]; levelised costs of electricity in comparison with other oxy-fuel power generation concepts [220].

5.2. Concentrated-solar power

A concentrated-solar power (CSP) plant uses a mirror or lens to focus the sun's rays that fall onto a given area to a much smaller receiver area in order to generate heat, which is subsequently converted into electricity through the power block. The key components of a CSP plant are the solar collector, the solar receiver and the power block, although thermal-energy storage is also a key component to decouple the availability of the sun and the demand for power. Whilst all components are important, emphasis here will be placed on the power block, for which sCO_2 is a promising candidate; for a more detailed review of CSP technology readers can refer to the literature [264,265].

Cumulatively, the global installed capacity of CSP has grown five-fold since 2010, and in that time has seen a drop in LCOE from 0.346 $/kWh to 0.182 $/kWh [266]. However, compared to other technologies CSP is still in its infancy, and is associated with higher LCOE values compared to other renewable technologies, such as solar PV (0.068 $/kWh) [266]. Much of the drop in LCOE for CSP systems can be attributed to reductions in the costs of solar collector fields, which represent around 40% of the total capital cost [267]. In contrast, there have not been significant developments in the power block technology, which remains based on the steam Rankine cycle.

The deployment of an sCO_2 power block, in place of steam, could offer a number of benefits. Firstly, sCO_2 power cycles are capable of achieving higher thermal efficiencies at temperatures relevant to CSP applications, which enables sCO_2 to produce the same amount of energy using a smaller solar field. Moreover, the possibility for more compact turbomachinery, a simpler cycle layout, and a smaller physical footprint could reduce both the thermal mass and complexity of the power block, which could improve the cycle's response time during intermittent operation, whilst the lack of phase-change within the primary heat-addition process reduces the pinch point within the primary heater and should allow for more compact thermal-energy storage systems [267,268]. Consequently, the use of sCO_2 has the potential to reduce capital, operational and maintenance costs of the power block, enabling a significant reduction in the LCOE of CSP plants. This motivation is supported by the Gen3 CSP roadmap [269], developed within the US SunShot programme, which maps out the pathway towards the next-generation of CSP systems.

Whilst space does not permit a detailed review of sCO_2-CSP systems (such a review is provided by Yin et al. [7]), thermodynamic modelling and optimisation remains an important research topic to identify optimal cycle layouts and operating conditions for CSP applications. Neises & Turchi [268] compared simple recuperated, recompression and partially-cooled cycles for CSP applications in terms of thermodynamic performance. Later the same authors considered the economic performance and concluded that the partially-cooled cycle had a LCOE that was 6.2% lower than either the simple or recompression cycle [228]. Binotti et al. [270] compared cycles for a CSP application with temperatures up to 800 °C and found that a recompression cycle with main compression inter-cooling outperformed either the recompression cycle or partially-cooled cycles. Finally, Crespi et al. [39] assessed the overnight capital costs of sCO_2 for CSP applications, with their conclusions suggesting that the partially-cooled cycle is a promising candidate when both thermodynamic performance and capital costs are considered. Their results also suggest that very complex cycles may be unsuitable, even though they have high thermal efficiencies. Ultimately, these studies point towards the recompression and partially-cooled cycles as most promising candidates sCO_2-CSP systems.

Alongside thermodynamic modelling, there is a need to demonstrate the technology at a commercial scale. Of this, the developments under the SunShot programme are the most notable, which targets a LCOE of 0.06 $/kWh for CSP systems, with a thermal efficiency of 50%, and under which a 10 MW_e sCO_2 turbine is being tested up to 750 °C and 250 bar under reduced flow conditions [70,91]. Another notable development is the Shouhang-EDF demonstration plant in China, which involves retrofitting a 10 MW_e steam power plant with a sCO_2 power block by the end of 2020. The plant employs a recompression cycle with intercooling and preheating with an estimated net efficiency of 35.6%, and while the current maximum turbine inlet temperature is limited to 468 °C, the project eventually aims to achieve higher temperatures [230].

Finally, it is worth noting that optimal locations for CSP plants are typically in hot and arid regions where there may be a limited availability of water. As such, it is necessary to rely on dry cooling for the heat-rejection process, which leads to compressor inlet temperatures in the region of 50 °C once the approach temperature in the cooler is considered. Whilst sCO_2 cycles are suitable for dry cooling [267], this increase in compressor temperature moves the compression process away from the critical point, somewhat negating the low compressor work promised by operating with sCO_2, and may also require increased compressor inlet pressures to maximise efficiency [271]. To this end, CO_2-blends have been proposed to increase the critical point of the working fluid, not only moving the compression process closer to the critical point, but also facilitating the use of a transcritical cycle. Manzolini et al. [32] studied CO_2-blends for CSP applications, and suggest that for turbine inlet temperatures of 550 and 700 °C CO_2-blends could increase thermal efficiency by 2% and reduce LCOE by 10% compared to a conventional steam cycle.

5.3. Nuclear power

Nuclear power plants generate heat through a contained and controlled nuclear reaction within a nuclear reactor core. The heat generated by this reaction is then removed from the core through a heat-transfer fluid and then converted into electricity by the power cycle. In the case of a direct power cycle, the heat-transfer fluid is the working fluid of the power cycle, whilst in an indirect cycle the heat-transfer fluid leaving the core exchanges heat with the power cycle working fluid through an additional heat-exchange process.

Currently, there are six Generation IV nuclear reactors that are being investigated for deployment within future nuclear power applications [272]. These advanced reactors employ various means to cool the core, and subsequently provide heat to the power generation system. The goal of these reactors is to realise higher core outlet temperatures (500 to 900 °C) compared to water-cooled reactors (≈ 300 °C) [3]. This increases the thermal efficiency and reduces the cost

of the power block. Each of the six Gen IV reactors provide different core outlet temperatures and heat across a limited range. The gas-cooled fast reactor, and very high-temperature reactor, provide core outlet temperatures in excess of 850 °C and employ a closed-loop helium Brayton cycle for the power generation cycle. However, the high operating temperatures present challenges in material selection. For this reason, the work of Dostal [16] was conducted with the focus of identifying power cycles that could provide comparable efficiencies at lower temperatures. The conclusion was that sCO_2 cycles operating with a maximum temperature of 550 °C could achieve comparable efficiencies to a helium Brayton cycle operating at a temperature of 850 °C, making sCO_2 a promising candidate for any reactor with core outlet temperatures in excess of 500 °C. Of the remaining Gen IV nuclear reactors, the sodium-cooled fast reactor (SFR) and lead-cooled fast reactor (LFR) are the most promising applications for sCO_2 cycles. Sienicki & Moisseytsev [273] note that both reactors provide core outlet temperatures in the region of 500 to 550 °C, and that the temperature match between the temperature rise of the heat-transfer fluid in the primary heater and across the turbine are well matched. This enables sCO_2 cycles to achieve higher efficiencies than an equivalent steam cycle, whilst having a smaller footprint, leading a potential reduction in capital cost and LCOE. This is supported by Li et al. [5] who considered LFRs to be a new frontier for research.

Within the aforementioned references a detailed review of the historical developments [273], and of thermodynamic and techno-economic modelling [5] of sCO_2 cycles for nuclear applications can be found. This is further expanded on in the recent paper by Wu et al. [274]. For this reason, these topics are not covered in detail here. Instead an overview of the main developments within a few notable research groups are summarised.

Within the US, most developments can be related to work at the Argonne National Laboratory, which considered sCO_2 cycles for both sodium- and lead-cooled fast reactors. Moisseytsev & Sienicki [275] reported the design of a LFR, named the secure transportable autonomous reactor with liquid metal coolant (STAR-LM), which coupled the reactor to a sCO_2 recompression cycle. At the design point, the turbine inlet temperature is 540 °C, whilst the power cycle has a net power output of 179 MW_e and estimated cycle thermal efficiency of 45%. Later, Sienicki et al. [276] reported on the design of a smaller reactor, referred to as SSTAR, with a net power output of 20 MW_e. The system employs a direct heat exchange between the lead coolant and the CO_2, and with a turbine inlet of 550 °C could obtain a thermal cycle efficiency of 44%. A major consideration during the development on SSTAR was to focus on a small reactor that is suitable for international deployment, which should allow non-fuel cycle states and developing nations to help meet future energy demands in a sustainable manner [276]. This sentiment is supported by the IEA's 2015 nuclear technology roadmap [277], which suggests that the development of small modular reactors could extend the market for nuclear technology, whilst also helping to address financing barriers. Thus, it could be argued that the small modular reactor market could be a good proving ground for sCO_2 technology. Alongside studies relating to LFRs, Chang et al. [278] reports the pre-conceptual design of a SFR coupled to a recompression sCO_2 cycle with a net power of 95 MW_e. Simulations estimate that for a turbine inlet temperature of 471.5 °C a cycle thermal efficiency of 39.1% could be obtained. A later study found that more complex power cycle layouts did not improve on this efficiency, but reducing the minimum temperature to 20 °C, and operating a condensation cycle, could improve the efficiency by up to 4%; although this would have implications for the required heat sink [34]. Finally, Sienicki & Moisseytsev [273] report the detailed design of a 100 MW_e small modular SFR reactor with a turbine inlet temperature of 517 °C with an estimated cycle thermal efficiency of 42.3%.

Within the Korea Advanced Institute of Science and Technology researchers have investigated the use of sCO_2 power cycles with SFRs [279], in addition to water-cooled reactors [280] and high-temperature gas-cooled reactors [281]. Alongside this, Yu et al. [282] reports the design a micro modular reactor, named KAIST MMR, in which the core is directly cooled by the supercritical CO_2 and the intermediate heat exchanger is removed. The KAIST MMR is designed to have a thermal power of 36.2 MW_{th} and a 20-year lifetime without refuelling. Within Tokyo Institute of Technology there was also interest in sCO_2 cycles for application within gas-cooled reactors, with the replacement of helium with sCO_2 [283] reducing temperatures down from 850 °C to 650 °C whilst retaining a similar thermal efficiency; thus echoing the findings of Dostal [16]. In particular, a partial pre-cooling cycle with a turbine inlet temperature of 650 °C and cycle thermal efficiency of 45.8% was proposed. Later, Muto & Kato [284] investigated a dual expansion cycle for fast reactors and high-temperature gas-cooled reactors.

Within China, Li et al. [233] proposed a conceptual design for a 10 MW_e LFR, integrated with a recompression sCO_2 cycle. Alongside thermo-economic modelling, which predicted a thermal efficiency in the range of 36.7 and 44.5% and cost of electricity between 50 and 55 $/MWh for a turbine inlet temperature of 550 °C, the authors presented a conceptual design for the reactor core, intermediate heat-transfer system and the auxiliary systems.

Within Europe there have been a few studies focusing on sCO_2 cycles for nuclear applications. In France, sCO_2 was being considered as a power cycle for the advanced sodium technological reactor for industrial demonstration (ASTRID) project [285,286]. For the plant, which has a total thermal power of 1500 MW_{th}, simulations suggested that a net plant efficiency of 42.2% could be obtained for turbine inlet conditions of 25 MPa and 515 °C [286]. However, as of the August 2019 the ASTRID programme has been cancelled [287]. There have also been developments within the Czech Republic. Specifically, the SUSEN test loop has been developed, which was constructed with a view towards testing sCO_2 components with applications focused on gas-cooled fast reactors [288]. This test loop was also utilised within the sCO_2-HeRo project, which focused on the proof of concept for a small-scale heat removal safety back-up system for a light-water reactor [289]. A final notable study explored the suitability of sCO_2 power cycles for the DEMO demonstration power plant, which investigated fusion applications within Europe [290]. Although, it seems steam is still the power cycle of choice for that plant [291], recent simulations suggest that sCO_2 cycles may outperform steam providing that the heat-source temperature is above 460 °C [292].

Finally, it is worth noting that most of experimental prototypes mentioned within this paper have been developed with nuclear applications in mind; albeit with the removal of a nuclear heat source. To this end, the challenge facing the implementation of sCO_2 technologies within all nuclear applications is the successful demonstration of the technology at an industrial scale, which must be obtained before nuclear power plants utilising sCO_2 can be realised. Moreover, as summarised by Wu et al. [274], specific challenges relating to nuclear applications include: (i) understanding the interaction between the sCO_2 system and the reactor coolant system; (ii) understanding the effect of the dynamic behaviour of the reactor core on the sCO_2 cycle; and (iii) conducting a comprehensive safety analysis.

5.4. Other applications

Supercritical CO_2 power cycles could also find use in a range of other applications. For example, there have been studies investigating the use of sCO_2 as a bottoming cycle for molten carbonate fuel cells [293–296]. Another promising area is geothermal. Within existing geothermal plants, a brine solution is pumped deep underground where it extracts heat from the surrounding rock and is heated up to around 100 to 200 °C. The hot brine is then returned to the surface where it is converted to electricity by a power block, which is typically a closed-loop organic Rankine cycle (ORC) with indirect heating between the hot brine and the organic fluid. Therefore, sCO_2 power cycles could replace the ORC system [30,297], whilst the second, and perhaps more

interesting option, is the operation of a closed-loop direct cycle where the brine is replaced with sCO_2 and the hot, high-pressure CO_2 leaving the well is expanded within a turbine. This direct cycle can lead to more effective geothermal extraction, whilst due to a stronger thermosiphon effect the pumping power required to drive the cycle is reduced [234]. Adams et al. [298] investigated the use of CO_2 as the heat-carrier fluid, and then later compared direct sCO_2 cycles with indirect brine-based systems using either an ORC or sCO_2 power block [297]. They concluded that direct sCO_2 cycles produced more power at lower reservoir depths, significantly more power at higher reservoir depths, and that for indirect systems a transcritical sCO_2 power block could outperform an ORC system operating with the refrigerant R245fa. Within the US, GreenFire Energy are developing the ECO2G, which is a direct closed-loop sCO_2 system for geothermal applications [299]. Recently, they demonstrated the technology as the Coso Geothermal Field, although emphasis was placed on testing the heat exchanger technology operating with sCO_2, and hence an expansion valve was used in place of the turbine [300]. Glos et al. [234] conducted a preliminary assessment of closed-loop direct sCO_2 cycles considering thermodynamic modelling, turbine design and a preliminary cost assessment. Their results suggest that LCOEs of 0.20 and 0.12 $/kWh could be obtained for 52 and 157 MW_e systems respectively for installation at brownfield sites where there are existing wells. A final potential application could be as a power block for use within the marine industry, either as part of the ship propulsion system or for on-board power. Within the sCO_2 technology roadmap prepared by Mendez & Rochau [217], the authors noted that the US Navy is interested in gas turbine-generator sets with a power rating between 20 and 30 MW_e, which could be a promising application for sCO_2 technology. The US Navy has previously explored the use of Echogen's sCO_2 system within marine applications, with the results suggesting fuel consumption could be reduced by 20% [301].

6. Summary and future trends

Power cycles operating with supercritical carbon dioxide (sCO_2) have advantages of high thermal efficiencies using heat-source temperatures ranging between approximately 350 °C and 800 °C, a simple and compact physical footprint and good operational flexibility. These advantages make them promising candidates for future energy applications where their adoption could lower levelised costs of electricity compared to existing technologies. The significant amount of research on sCO_2 power systems has led to multiple component development campaigns and experimental test facilities aimed at demonstrating technical feasibility and investigating component operational issues. However, there remain significant hurdles to overcome, one of which is the successful demonstration of the technology at an appropriate industrial scale. The following subsections summarise the current status within the context of the main areas discussed within this paper.

6.1. Turbomachinery

- Turbomachinery for sCO_2 applications has yet to be successfully demonstrated at a sufficient level to allow commercialisation. However, there are a number of on-going projects that aim to demonstrate turbomachinery at an industrial-scale (i.e., ≥ 10 MW_e), although these are not yet fully operational.
- For large industrial-scale applications the required turbomachinery may differ from the turbomachinery tested within existing test rigs. Therefore, there is uncertainty in how much of the experimental work carried out to date can be readily transposed to full-scale plants.
- For small-scale applications (i.e., <1 MW_e), turbomachinery design is challenging due to high rotational speeds, high pressures, and the trade-off between aerodynamic, rotordynamic and mechanical performance. Although radial turbomachinery, often constructed as single-shaft turbine–alternator–compressor (TAC) unit, is most common, axial turbines and the use of separate shafts have been proposed. Existing small-scale systems have also experienced significant challenges relating to bearing and windage losses, which need to be overcome.
- Most experimental test rigs operate with conservative pressure ratios and some use commercial components to minimise costs and development risk. Once existing turbomachinery designs have been demonstrated, there remains an opportunity for further research and development to extend beyond the existing design boundaries.
- To fully realise the performance benefits of the sCO_2 cycle, operating the compressor close to the critical point is desirable. However, this introduces challenges related to droplet formation, real-gas effects and unstable compressor operation, which require further investigation to characterise compressor operation near the critical point and introduce suitable design solutions.
- The design and simulation of sCO_2 turbomachinery is reliant on empirical loss models and computational fluid dynamics (CFD) tools that were not developed for sCO_2 applications. Experimental tests are necessary to provide suitable validation data and, if necessary, introduce modifications to existing tools.

6.2. Heat exchangers

- For the heat transfer and flow mechanisms, the influence of buoyancy effects should be considered for the development of empirical correlations and the design of sCO_2 heat exchangers. Further unique universal correlations are expected to cover a wide range of test parameters and demonstrate the local heat transfer performance. Heat exchanger optimisation is also an important field, which requires specific attention not only for the individual heat exchanger but also the system as a whole.
- Each application imposes unique constraints on heater design. The thermohydraulic challenges confront requirements of very high heat flux, and high temperature and pressure differentials between the heat source and sCO_2. Further work is needed to develop designs and manufacturing processes that lead to relatively low cost, high-performance heaters that can withstand thermal cycling and fatigue and can satisfy environmental constraints in different applications.
- Challenges facing the recuperator are the requirements to withstand high-temperature pressure differentials and flow passage design that maximises heat transfer performance and reduces pressure drop.
- For air-coupled coolers, reduction of the heat exchanger size can be achieved by reducing tube diameter and tube spacing. Challenges include enhancement of the heat transfer performance on the air cooling side and optimisation of the tube circuitry to alleviate pinch point problems, and minimise pressure drop and footprint. For water-coupled coolers, important considerations are to improve heat transfer performance, reduce pressure drop on the sCO_2 side and the risk of leakage between the two fluids during operation.

6.3. Materials

- Material selection for different applications requires a combination of strength and environmental compatibility under conditions of high temperature and pressure in the sCO_2 system and high temperature heat sources.
- More information is required on material strength and durability in realistic high-velocity operating conditions and accounting for impurities in the working fluid to develop material databases and standards.

- More information is required on costs as well as on availability, manufacturability and fabrication issues, especially for welding and diffusion bonding of metals for sCO_2 applications.
- Optimisation methods based on cost-performance for material selection and specific research to develop high-temperature materials and coatings suitable for sCO_2 environments are required for the development and deployment of cost effective systems.

6.4. Control systems

Transient modelling and control are key to advanced design and efficient operation of sCO_2 power systems. They allow to fully exploit the load flexibility potential of the power generation system and assess important operational aspects such as safety. State-of-the-art research on sCO_2 controls has focused on a limited number of cycle layouts mostly regulated by proportional integral (PI) controllers in which the power block is considered as a standalone item despite being part of a broader, interconnected energy system. The investigation and development of overarching control architectures based on multi-variable control approaches that integrate the power block with the heat source and heat sink can provide opportunities for better integration and synergistic operation of the overall energy system.

6.5. Applications

- For fossil fuelled applications, using the CO_2 stream as a heat carrier of an oxy-fuel combustion not only allows high cycle efficiency (up to 55.1% based on lower heating value of natural gas), but inherently provides the capability to further sequestrate the CO_2 generated from combustion. These features have triggered a strong industrial interest that are leading to the first full-scale demonstrations of sCO_2 Allam–Fetvedt power cycles. However, the high cycle pressure ratios and turbine inlet temperatures of direct-fired sCO_2 introduce challenges related to combustion in high-density flows, turbine film cooling, material erosion and corrosion.
- For waste-heat recovery or indirect heating applications, the following conclusions are drawn: (1) unless costs are significantly reduced, sCO_2 is primarily competitive for applications beyond 0.5 MW_e and heat-source temperatures above 350 °C; (2) there is a need for high temperature sCO_2 heat exchangers that are able to deal with: high temperature CO_2 corrosion issues; fouling, back-pressure and other thermo-structural challenges imposed by the flue gas; and economic constraints imposed to materials selection and lifetime; (3) sCO_2 power technology will face the same barriers as other waste-heat recovery technologies employed in industry as bottoming power cycles such as: project financing challenges due to high capital cost; return on investment; disturbance of existing plant operations; space requirements and safety concerns.
- For concentrated solar power (CSP) applications, the goal is to develop systems that can achieve levelised costs of electricity that are competitive with solar photovoltaic (PV). Demonstration plants are under construction as part of the SunShot and STEP programmes in the US and the Shouhang-EDF plant in China. Alongside this, there is a need for suitable heat carriers that can realise higher turbine inlet temperatures, and challenges in realising the performance benefits of sCO_2 in regions with high ambient temperatures.
- The resurgence of interest in sCO_2 technology was primarily driven from the perspective of nuclear power applications, and conceptual designs for Gen IV nuclear reactors that integrate sCO_2 power cycles have been developed. However, due to cost and safety considerations related to nuclear power, sCO_2 technology will first need to be successfully demonstrated in other applications.

Declaration of competing interest

The authors declare that they have no known competing financial interests or personal relationships that could have appeared to influence the work reported in this paper.

Acknowledgements

The research presented in this paper has received funding from the European Union's Horizon 2020 research and innovation programme under grant agreements: No. 680599 – I-ThERM and No. 814985 – SCARABEUS. Aspects of the work are also funded by the Engineering and Physical Sciences Research Council (EPSRC) of the UK under research grants: EP/P004636/1 – OPTEMIN, EP/P009131/1 – NextORC, EP/K011820/1 – RCUK CSEF. The manuscript reports all the relevant data to support the understanding of the results. More detailed information and data, if required, can be obtained by contacting the corresponding author of the paper.

References

[1] European Commission, The Strategic Energy Technology (SET) Plan, Tech. Rep., European Commission, Brussels, Belgium, 2018, p. 84, http://dx.doi.org/10.1017/CBO9781107415324.004.
[2] IRENA, Global Renewables Outlook: Energy Transformation 2050, Tech. Rep., International Renewable Energy Agency, Abu Dhabi, 2020, p. 292.
[3] Y. Ahn, S.J. Bae, M. Kim, S.K. Cho, S. Baik, J.I. Lee, J.E. Cha, Review of supercritical CO_2 power cycle technology and current status of research and development, Nucl. Eng. Technol. 47 (6) (2015) 647–661, http://dx.doi.org/10.1016/j.net.2015.06.009.
[4] J. Sarkar, Review and future trends of supercritical CO_2 Rankine cycle for low-grade heat conversion, Renew. Sustain. Energy Rev. 48 (8) (2015) 434–451, http://dx.doi.org/10.1016/j.rser.2015.04.039.
[5] M.J. Li, H.H. Zhu, J.Q. Guo, K. Wang, W.Q. Tao, The development technology and applications of supercritical CO_2 power cycle in nuclear energy, solar energy and other energy industries, Appl. Therm. Eng. 126 (2017) 255–275, http://dx.doi.org/10.1016/j.applthermaleng.2017.07.173.
[6] Y. Liu, Y. Wang, D. Huang, Supercritical CO_2 Brayton cycle: A state-of-the-art review, Energy 189 (12) (2019) 115900, http://dx.doi.org/10.1016/j.energy.2019.115900.
[7] J.M. Yin, Q.Y. Zheng, Z.R. Peng, X.R. Zhang, Review of supercritical CO_2 power cycles integrated with CSP, Int. J. Energy Res. 44 (2020) 1337–1369, http://dx.doi.org/10.1002/er.4909.
[8] A. Yu, W. Su, X. Lin, N. Zhou, Recent trends of supercritical CO_2 Brayton cycle: Bibliometric analysis and research review, Nucl. Eng. Technol. (2020) http://dx.doi.org/10.1016/j.net.2020.08.005, in press.
[9] J. Rowlinson, The work of Thomas Andrews and James Thomson on the liquefaction of gases, Notes Rec. R. Soc. Lond. 57 (2) (2003) 143–159, http://dx.doi.org/10.1098/rsnr.2003.0202.
[10] G. Sulzer, Verfahren zur Erzeugung von Arbeit aus Warme, Vol. 269599, Swiss Patent, 1950.
[11] V. Dekhtiarev, On designing a large, highly economical carbon dioxide power installation, Elecrtichenskie Stantskii 5 (5) (1962) 1–6.
[12] E.G. Feher, The supercritical thermodynamic power cycle, Energy Convers. 8 (2) (1968) 85–90, http://dx.doi.org/10.1016/0013-7480(68)90105-8.
[13] G. Angelino, Perspectives for the liquid phase compression gas turbine, J. Eng. Gas Turbines Power 89 (2) (1967) 229–236, http://dx.doi.org/10.1115/1.3616657.
[14] G. Angelino, Carbon dioxide condensation cycles for power production, J. Eng. Gas Turbines Power 90 (3) (1968) 287–295, http://dx.doi.org/10.1115/1.3609190.
[15] G. Angelino, Real gas effects in carbon dioxide cycles, in: ASME 1969 Gas Turbine Conference and Products Show, March 10-13, Cleveland, Ohio, USA, 1969, http://dx.doi.org/10.1115/69-GT-102, V001T01A071.
[16] V. Dostal, A Supercritical Carbon Dioxide Cycle for Next Generation Nuclear Reactors (Phd), Massachusetts Institute of Technology, 2004, p. 317.
[17] K. Brun, P. Friedman, R. Dennis, Fundamentals and Applications of Supercritical Carbon Dioxide (sCO_2) Based Power Cycles, Woodhead Publishing, 2017.
[18] The European sCO_2 Research & Development Alliance, 2020, https://sco2.eu, Accessed: 2020-06-10.
[19] Supercritical CO_2 Power Cycles Symposium, 2018, http://sco2symposium.com/, Accessed: 2020-06-10.
[20] P. Friedman, M. Anderson, Thermodynamics, in: K. Brun, P. Friedman, R. Dennis (Eds.), Fundamentals and Applications of Supercritical Carbon Dioxide (SCO_2) Based Power Cycles, Woodhead Publishing, 2017, pp. 41–66, http://dx.doi.org/10.1016/B978-0-08-100804-1.00003-7, Ch. 3.

[21] G. Angelino, C. Invernizzi, Real gas Brayton cycles for organic working fluids, Proc. Inst. Mech. Eng. A 215 (1) (2001) 27–38, http://dx.doi.org/10.1243/0957650011536543.

[22] A. Rovira, J. Muñoz-Antón, M.J. Montes, J.M. Martínez-Val, Optimization of Brayton cycles for low-to-moderate grade thermal energy sources, Energy 55 (6) (2013) 403–416, http://dx.doi.org/10.1016/j.energy.2013.03.094.

[23] E. Lemmon, M. Huber, M. McLinden, NIST Standard Reference Database 23: Reference Fluid Thermodynamic and Transport Properties-REFPROP, National Institute of Standards and Technology, Gaithersburg, 2013.

[24] C.W. White, N.T. Weiland, Evaluation of property methods for modeling direct-supercritical CO_2 power cycles, J. Eng. Gas Turbines Power 140 (1) (2018) 011701, http://dx.doi.org/10.1115/1.4037665.

[25] L. Lombardi, E. Carnevale, A. Corti, A review of technologies and performances of thermal treatment systems for energy recovery from waste, Waste Manage. 37 (2015) 26–44, http://dx.doi.org/10.1016/j.wasman.2014.11.010.

[26] H. Chen, D.Y. Goswami, E.K. Stefanakos, A review of thermodynamic cycles and working fluids for the conversion of low-grade heat, Renew. Sustain. Energy Rev. 14 (9) (2010) 3059–3067.

[27] S. Lecompte, E. Ntavou, B. Tchanche, G. Kosmadakis, A. Pillai, D. Manolakos, M. de Paepe, Review of experimental research on supercritical and transcritical thermodynamic cycles designed for heat recovery application, Appl. Sci. 9 (2019) 2571, http://dx.doi.org/10.3390/app9122571.

[28] F. Crespi, G. Gavagnin, D. Sánchez, G.S. Martínez, Supercritical carbon dioxide cycles for power generation: A review, Appl. Energy 195 (2017) 152–183, http://dx.doi.org/10.1016/j.apenergy.2017.02.048.

[29] W.S. Jeong, J.I. Lee, Y.H. Jeong, Potential improvements of supercritical recompression CO_2 Brayton cycle by mixing other gases for power conversion system of a SFR, Nucl. Eng. Des. 241 (6) (2011) 2128–2137, http://dx.doi.org/10.1016/j.nucengdes.2011.03.043.

[30] T.M. Conboy, S.A. Wright, D.E. Ames, T.G. Lewis, CO_2-Based Mixtures as Working Fluids for Geothermal Turbines, Tech. Rep., Sandia National Laboratories, 2012, pp. SAND2012–4905.

[31] C.M. Invernizzi, T. van der Stelt, Supercritical and real gas Brayton cycles operating with mixtures of carbon dioxide and hydrocarbons, Proc. Inst. Mech. Eng. A 226 (5) (2012) 682–693, http://dx.doi.org/10.1177/0957650912444689.

[32] G. Manzolini, M. Binotti, D. Bonalumi, C. Invernizzi, P. Iora, CO_2 mixtures as innovative working fluid in power cycles applied to solar plants. Techno-economic assessment, Sol. Energy 181 (3) (2019) 530–544, http://dx.doi.org/10.1016/j.solener.2019.01.015.

[33] G. Di Marcoberardino, C. Invernizzi, P. Iora, A. Ayub, D. Di Bona, P. Chiesa, M. Binotti, G. Manzolini, Experimental and analytical procedure for the characterization of innovative working fluids for power plants applications, Appl. Therm. Eng. 178 (9) (2020) 115513, http://dx.doi.org/10.1016/j.applthermaleng.2020.115513.

[34] A. Moisseytsev, J.J. Sienicki, Investigation of alternative layouts for the supercritical carbon dioxide Brayton cycle for a sodium-cooled fast reactor, Nucl. Eng. Des. 239 (7) (2009) 1362–1371, http://dx.doi.org/10.1016/j.nucengdes.2009.03.017.

[35] F. Crespi, G. Gavagnin, D. Sánchez, G.S. Martínez, Analysis of the thermodynamic potential of supercritical carbon dioxide cycles: A systematic approach, J. Eng. Gas Turbines Power 140 (5) (2018) 051701, http://dx.doi.org/10.1115/1.4038125.

[36] R.V. Padilla, Y.C. Soo Too, R. Benito, W. Stein, Exergetic analysis of supercritical CO_2 Brayton cycles integrated with solar central receivers, Appl. Energy 148 (6) (2015) 348–365, http://dx.doi.org/10.1016/j.apenergy.2015.03.090.

[37] X. Wang, Y. Yang, Y. Zheng, Y. Dai, Exergy and exergoeconomic analyses of a supercritical CO_2 cycle for a cogeneration application, Energy 119 (2017) 971–982, http://dx.doi.org/10.1016/j.energy.2016.11.044.

[38] M. Marchionni, G. Bianchi, S.A. Tassou, Techno-economic assessment of Joule-Brayton cycle architectures for heat to power conversion from high-grade heat sources using CO_2 in the supercritical state, Energy 148 (2018) 1140–1152, http://dx.doi.org/10.1016/j.energy.2018.02.005.

[39] F. Crespi, D. Sanchez, T. Sanchez, G.S. Martinez, Integral techno-economic analysis of supercritical carbon dioxide cycles for concentrated solar power, in: Proceedings of the ASME Turbo Expo 2018: Turbomachinery Technical Conference and Exposition, Vol. 9, 11-15 June, Oslo, Norway, 2018, pp. GT2018–77106, http://dx.doi.org/10.1115/GT2018-77106.

[40] R.A. Bidkar, A. Mann, R. Singh, E. Sevincer, S. Cich, M. Day, C.D. Kulhanek, A.M. Thatte, A.M. Peter, D. Hofer, J. Moore, Conceptual designs of 50MW_e and 450MW_e supercritical CO_2 turbomachinery trains for power generation from coal. Part 1: cycle and turbine, in: The 5th International Supercritical CO_2 Power Cycles Symposium, 28-31 March, San Antonio, Texas, U.S., 2016.

[41] O. Balje, Turbomachines: A Guide to Design, Selection and Theory, Wiley, Chichester, U.K., 1981, p. 513.

[42] N. Holaind, G. Bianchi, M. De Miol, S.S. Saravi, S.A. Tassou, A. Leroux, H. Jouhara, Design of radial turbomachinery for supercritical CO_2 systems using theoretical and numerical CFD methodologies, Energy Procedia 123 (2017) 313–320, http://dx.doi.org/10.1016/j.egypro.2017.07.256.

[43] T.C. Allison, J. Moore, R. Pelton, J. Wilkes, B. Ertas, Turbomachinery, in: K. Brun, P. Friedman, R. Dennis (Eds.), Fundamentals and Applications of Supercritical Carbon Dioxide (SCO_2) Based Power Cycles, Woodhead Publishing, 2017, pp. 147–215, http://dx.doi.org/10.1016/B978-0-08-100804-1.00007-4.

[44] A. Uusitalo, A. Ameli, T. Turunen-Saaresti, Thermodynamic and turbomachinery design analysis of supercritical Brayton cycles for exhaust gas heat recovery, Energy 167 (2019) 60–79, http://dx.doi.org/10.1016/j.energy.2018.10.181.

[45] A. Romei, P. Gaetani, A. Giostri, G. Persico, The role of turbomachinery performance in the optimization of supercritical carbon dioxide power systems, J. Turbomach. (2020) 1–39, http://dx.doi.org/10.1115/1.4046182, (Accepted).

[46] J.J. Sienicki, A. Moisseytsev, R.L. Fuller, S.A. Wright, P.S. Pickard, Scale dependencies of supercritical carbon dioxide Brayton cycle technologies and the optimal size for a next-step supercritical CO_2 cycle demonstration, in: The 3rd International Symposium on Supercritical CO_2 Power Cycles, 24-25 May, Boulder, Colorado, U.S., 2011.

[47] A. Ameli, A. Afzalifar, T. Turunen-Saaresti, J. Backman, Centrifugal compressor design for near-critical point applications, J. Eng. Gas Turbines Power 141 (3) (2019) 031016, http://dx.doi.org/10.1115/1.4040691.

[48] S.K. Cho, S.J. Bae, Y. Jeong, J. Lee, J.I. Lee, Direction for high-performance supercritical CO_2 centrifugal compressor design for dry cooled supercritical CO_2 Brayton cycle, Appl. Sci. 9 (2019) 4057, http://dx.doi.org/10.3390/app9194057.

[49] J. Qi, T. Reddell, K. Qin, K. Hooman, I.H. Jahn, Supercritical CO_2 radial turbine design performance as a function of turbine size parameters, J. Turbomach. 139 (8) (2017) 081008, http://dx.doi.org/10.1115/1.4035920.

[50] S.I. Salah, M.A. Khader, M.T. White, A.I. Sayma, Mean-line design of a supercritical CO_2 micro axial turbine, Appl. Sci. (Switzerland) 10 (15) (2020) 1–20, http://dx.doi.org/10.3390/app10155069.

[51] S. Son, Y. Jeong, S.K. Cho, J.I. Lee, Development of supercritical CO_2 turbomachinery off-design model using 1D mean-line method and deep neural network, Appl. Energy 263 (1) (2020) 114645, http://dx.doi.org/10.1016/j.apenergy.2020.114645.

[52] S. Lee, H. Gurgenci, A comparison of three methodological approaches for meanline design of supercritical CO_2 radial inflow turbines, Energy Convers. Manage. 206 (January) (2020) 112500, http://dx.doi.org/10.1016/j.enconman.2020.112500.

[53] J. Keep, On the Design of Small to Medium Scale Radial Inflow Turbines for the Supercritical CO_2 Brayton Cycle (Phd), The University of Queensland, 2018.

[54] J.A. Keep, I.H. Jahn, Numerical loss investigation of a small scale, low specific speed supercritical CO_2 radial inflow turbine, J. Eng. Gas Turbines Power 141 (9) (2019) 091003, http://dx.doi.org/10.1115/1.4043430.

[55] A. Ameli, A. Afzalifar, T. Turunen-Saaresti, J. Backman, Effects of real gas model accuracy and operating conditions on supercritical CO_2 compressor performance and flow field, J. Eng. Gas Turbines Power 140 (6) (2018) 062603, http://dx.doi.org/10.1115/1.4038552.

[56] N.D. Baltadjiev, C. Lettieri, Z.S. Spakovszky, An investigation of real gas effects in supercritical CO_2 centrifugal compressors, J. Turbomach. 137 (9) (2015) 091003, http://dx.doi.org/10.1115/1.4029616.

[57] S.S. Saravi, S.A. Tassou, An investigation into sCO_2 compressor performance prediction in the supercritical region for power systems, Energy Procedia 161 (2019) 403–411, http://dx.doi.org/10.1016/j.egypro.2019.02.098.

[58] S.S. Saravi, S.A. Tassou, Diffuser performance of centrifugal compressor in supercritical CO_2 power systems, Energy Procedia 161 (2019) 438–445, http://dx.doi.org/10.1016/j.egypro.2019.02.079.

[59] C. Lettieri, D. Yang, Z. Spakovszky, An investigation of condensation effects in supercritical carbon dioxide compressors, J. Eng. Gas Turbines Power 137 (8) (2015) 082602, http://dx.doi.org/10.1115/1.4029577.

[60] C. Lettieri, D. Paxson, Z. Spakovszky, P. Bryanston-Cross, Characterization of nonequilibrium condensation of supercritical carbon dioxide in a de laval nozzle, J. Eng. Gas Turbines Power 140 (4) (2018) 041701, http://dx.doi.org/10.1115/1.4038082.

[61] J. Lewis, E.M. Clementoni, T.L. Cox, Effect of compressor inlet pressure on cycle performance for a supercritical carbon dioxide brayton cycle, in: The 6th International Supercritical CO_2 Power Cycles Symposium, 27-29 March, Pittsburgh Pennsylvania, 2018, http://dx.doi.org/10.1115/GT2018-75182.

[62] J. Lee, S. Baik, S.K. Cho, J.E. Cha, J.I. Lee, Issues in performance measurement of CO_2 compressor near the critical point, Appl. Therm. Eng. 94 (2) (2016) 111–121, http://dx.doi.org/10.1016/j.applthermaleng.2015.10.063.

[63] S.A. Wright, T.M. Conboy, G.E. Rochau, Break-even power transients for two simple recuperated S-CO_2 Brayton cycle test configurations, in: The 3rd International Symposium on Supercritical CO_2 Power Cycles, 24-25 May, Boulder, Colorado, U.S., 2011.

[64] J. Pasch, D. Stapp, Testing of a new turbocompressor for supercritical carbon dioxide closed brayton cycles, in: Proceedings of the ASME Turbo Expo 2018: Turbomachinery Technical Conference and Exposition, Vol. 9, 11-15 June, Oslo, Norway, 2018, pp. GT2018–77044, http://dx.doi.org/10.1115/GT2018-77044.

[65] L. Rapp, D. Stapp, Experimental testing of a 1mw SCO2 turbocompressor, in: 3rd European Supercritical CO_2 Conference, 19-20 September, Paris, France, 2019, http://dx.doi.org/10.17185/duepublico/48910.

[66] E.M. Clementoni, T.L. Cox, C.P. Sprague, Startup and operation of a supercritical carbon dioxide Brayton cycle, J. Eng. Gas Turbines Power 136 (7) (2014) 071701, http://dx.doi.org/10.1115/1.4026539.

[67] E.M. Clementoni, T.L. Cox, M.A. King, Off-nominal component performance in a supercritical carbon dioxide Brayton cycle, J. Eng. Gas Turbines Power 138 (1) (2016) 011703, http://dx.doi.org/10.1115/1.4031182.

[68] T.J. Held, Initial test results of a megawatt-class supercritical CO_2 heat engine, in: The 4th International Symposium on Supercritical CO_2 Power Cycles, 9-10 September, Pittsburgh, Pennsylvania, USA, 2014.

[69] C. Kalra, D. Hofer, E. Sevincer, J. Moore, K. Brun, Development of high efficiency hot gas turbo-expander for optimized CSP supercritical CO_2 power block operation, in: The 4th International Symposium on Supercritical CO_2 Power Cycles, 9-10 September, Pittsburgh, Pennsylvania, USA, 2014, http://dx.doi.org/10.1017/CBO9781107415324.004.

[70] T.C. Allison, J. Jeffrey Moore, D. Hofer, M.D. Towler, J. Thorp, Planning for successful transients and trips in a 1 MW_e-Scale High-Temperature sCO_2 test loop, J. Eng. Gas Turbines Power 141 (6) (2019) 061014, http://dx.doi.org/10.1115/1.4041921.

[71] J. Marion, M. Kutin, A. McClung, J. Mortzheim, R. Ames, The STEP 10 MWe sCO_2 pilot plant demonstration, in: Proceedings of the ASME Turbo Expo 2019: Turbomachinery and Technical Conference, 17-21 June, Pheonix, Arizona, U.S., 2019, pp. GT2019–91917, http://dx.doi.org/10.1115/GT2019-91917.

[72] Y. Iwai, M. Itoh, Y. Morisawa, S. Suzuki, D. Cusano, M. Harris, Development approach to the combustor of gas turbine for oxyfuel, supercritical CO2 cycle, in: Proceedings of the ASME Turbo Expo 2015: Turbine Technical Conference and Exposition, 15-19 June, Montreal, Canada, 2015, pp. GT2015–43160, http://dx.doi.org/10.1115/GT2015-43160.

[73] R. Allam, S. Martin, B. Forrest, J. Fetvedt, X. Lu, D. Freed, G.W. Brown, T. Sasaki, M. Itoh, J. Manning, Demonstration of the Allam cycle: An update on the development status of a high efficiency supercritical carbon dioxide power process employing full carbon capture, Energy Procedia 114 (2017) 5948–5966, http://dx.doi.org/10.1016/j.egypro.2017.03.1731.

[74] S. Suzuki, Y. Iwai, M. Itoh, Y. Morisawa, P. Jain, Y. Kobayashi, High pressure combustion test of gas turbine combustor for 50MWth supercritical CO_2 demonstration power plant on Allam cycle, in: Proceedings of the International Gas Turbine Congress 2019 Tokyo, 17-22 November, Tokyo, Japan, 2019, p. 232.

[75] M. Utamura, H. Hasuike, K. Ogawa, T. Yamamoto, T. Fukushima, T. Watanabe, T. Himeno, Demonstration of supercritical CO_2 closed regenerative Brayton cycle in a bench scale experiment, in: Proceedings of ASME Turbo Expo 2012, 11-15 June, Copenhagen, Denmark, 2012, pp. 155–164.

[76] Y. Ahn, J. Lee, S.G. Kim, J.I. Lee, J.E. Cha, S.W. Lee, Design consideration of supercritical CO_2 power cycle integral experiment loop, Energy 86 (6) (2015) 115–127, http://dx.doi.org/10.1016/j.energy.2015.03.066.

[77] J.E. Cha, S.W. Bae, J. Lee, S.K. Cho, J.I. Lee, J.H. Park, Operation results of a closed supercritical CO_2 simple Brayton cycle, in: The 5th International Supercritical CO_2 Power Cycles Symposium, 28-31 March, San Antonio, Texas, U.S., 2016.

[78] J. Cho, H. Shin, H.-S. Ra, G. Lee, C. Rho, B. Lee, Y.-J. Baik, Development of the supercritical carbon dioxide power cycle experimental loop in KIER, in: Proceedings of ASME Turbo Expo 2016: Turbomachinery Technical Conference and Exposition, 13-17 June, Seoul, South Korea, 2016, pp. GT2016–57460.

[79] H. Shin, J. Cho, Y.J. Baik, J. Cho, C. Roh, H.S. Ra, Y. Kang, J. Huh, Partial admission, axial impulse type turbine design and partial admission radial turbine test for SCO2 cycle, in: Proceedings of the ASME Turbo Expo, Vol. 9, 26-30 June, Charlotte, NC, U.S., 2017, pp. GT2017–64349, http://dx.doi.org/10.1115/GT2017-64349.

[80] J. Cho, H. Shin, J. Cho, H.S. Ra, C. Roh, B. Lee, G. Lee, B. Choi, Y.J. Baik, Development and operation of supercritical carbon dioxide power cycle test loop with axial turbo-generator, in: Proceedings of ASME Turbo Expo 2018: Turbomachinery Technical Conference and Exposition, Vol. 9, 11-15 June, Oslo, Norway, 2018, pp. GT2018–76488, http://dx.doi.org/10.1115/GT2018-76488.

[81] A. Hacks, S. Schuster, H.J. Dohmen, F.K. Benra, D. Brillert, Turbomachine design for supercritical carbon dioxide within the sco2-hero.eu project, J. Eng. Gas Turbines Power 140 (12) (2018) 121017, http://dx.doi.org/10.1115/1.4040861.

[82] A.J. Hacks, A. Vojacek, H.J. Dohmen, D. Brillert, Experimental investigation of the sCO2-HeRo compressor, in: 2nd European Supercritical CO_2 Conference, 30-31 August, Essen, Germany, 2018, p. 115, http://dx.doi.org/10.17185/duepublico/46088.

[83] D.M. Miol, G. Bianchi, G. Henry, N. Holaind, S.A. Tassou, A. Leroux, Design of a single-shaft compressor, generator, turbine for small-scale supercritical CO_2 systems for waste heat to power conversion applications, in: 2nd European Supercritical CO_2 Conference, 30-31 August, Essen, Germany, 2018, p. 112, http://dx.doi.org/10.17185/duepublico/46086.

[84] G. Bianchi, S.S. Saravi, R. Loeb, K.M. Tsamos, M. Marchionni, A. Leroux, S.A. Tassou, Design of a high-temperature heat to power conversion facility for testing supercritical CO_2 equipment and packaged power units, Energy Procedia 161 (2019) 421–428, http://dx.doi.org/10.1016/j.egypro.2019.02.109.

[85] M. Walker, D. Fleming, J. Pasch, Gas foil bearing coating behavior in environments relevant to S-CO2 power system turbomachinery, in: The 6th International Supercritical CO_2 Power Cycles Symposium, 27-29 March, Pittsburgh, Pennsylvania, 2018.

[86] R. Dupuis, A. Gonis, H. Saari, Development of a dynamic model for a 250 kW supercritical CO_2 simple regenerative Brayton cycle plant, in: Proceedings of Montreal 2018 Global Power and Propulsion Forum, 7-9 May, Montreal, Canada, 2018, pp. GPPS–NA–2018–0192.

[87] Echogen, Echogen power systems, 2020, https://www.echogen.com/ [Last accessed: 05/06/2020].

[88] Siemens Energy, Siemens waste heat to power system, 2020, https://new.siemens.com/global/en/products/energy/power-generation/power-plants/echogen-technology.html [Last accessed: 27/07/2020].

[89] General Electric, 2020, https://www.geaviation.com/sites/default/files/echogen-datasheet.pdf [Last accessed: 23/10/2020].

[90] J. Moore, K. Brun, N. Evans, C. Kalra, Development of 1 MWe supercritical CO_2 test loop, in: Proceedings of the ASME Turbo Expo 2015: Turbine Technical Conference and Exposition, Vol. 9, 15-19 June, Montreal, Canada, 2015, pp. GT2015–43771, http://dx.doi.org/10.1115/GT2015-43771.

[91] J.J. Moore, S. Cich, M. Towler, T. Allison, J. Wade, D. Hofer, Commissioning of a 1 MWe supercritical CO_2 test loop, in: The 6th International Supercritical CO_2 Power Cycles Symposium, 27-29 March, Pittsburgh Pennsylvania, 2018.

[92] J.L. Preuss, Application of hydrostatic bearings in supercritical CO_2 turbomachinery, in: The 5th International Supercritical CO_2 Power Cycles Symposium, 29-31 March, San Antonio, Texas, U.S., 2016.

[93] P. Chapman, Advanced gas foil bearing design for supercritical CO_2 power cycles, in: The 5th International Supercritical CO_2 Power Cycles Symposium, 28-31 March, San Antonio, Texas, U.S., 2016, pp. 1–15.

[94] J.C.H. Heshmat, J. Walton, Technology readiness of 5th and 6th generation compliant foil bearing for 10 MWE s-CO_2 turbomachinery systems, in: The 6th International Supercritical CO_2 Power Cycles Symposium, 27-29 March, Pittsburgh, Pennsylvania, 2018.

[95] J.J. Moore, S. Cich, M. Day-Towler, D. Hofer, J. Mortzheim, Testing of a 10 MWe supercritical CO_2 turbine, in: 47th Turbomachinery & 34th Pump Symposia, 17-20 September, Houston, Texas, U.S., 2018.

[96] S.D. Cich, J. Moore, J.P. Mortzheim, D. Hofer, Design of a supercritical CO_2 compressor for use in a 10 MWe power cycle, in: The 6th International Supercritical CO_2 Power Cycles Symposium, 27-29 March, Pittsburgh Pennsylvania, 2018, pp. 1–16.

[97] J. Wilkes, T. Allison, K. Wygant, R. Pelton, Application of an Integrally Geared Compander to a sCO2 Recompression Brayton Cycle, in: The 5th International Supercritical CO_2 Power Cycles Symposium, 28-31 March, San Antonio, Texas, U.S., 2016.

[98] R.A. Bidkar, G. Musgrove, M. Day, C.D. Kulhanek, T. Allison, A.M. Peter, D. Hoger, J. Moore, Conceptual designs of 50MW_e and 450MW_e supercritical CO_2 turbomachinery trains for power generation from coal. Part 2: compressors, in: The 5th International Supercritical CO_2 Power Cycles Symposium, 28-31 March, San Antonio, Texas, U.S., 2016.

[99] A. Rimpel, S. Antonio, J. Wilkes, N. Smith, J. Wilkes, T. Allison, C. Wolfe, S. Lawson, P. Manager, Test rig design for large supercritical CO_2 turbine seals, in: The 6th International Supercritical CO_2 Power Cycles Symposium, 27-29 March, Pittsburgh Pennsylvania, 2018.

[100] R.J. Allam, M.R. Palmer, G.W. Brown, J. Fetvedt, D. Freed, H. Nomoto, M. Itoh, N. Okita, C. Jones, High efficiency and low cost of electricity generation from fossil fuels while eliminating atmospheric emissions, including carbon dioxide, Energy Procedia 37 (2013) 1135–1149, http://dx.doi.org/10.1016/j.egypro.2013.05.211.

[101] D. Freed, B. Forrest, T. Patel, J. Duffney, A gas turbine-driven, integrally gear compressor solution: Enabling the carbon capture of the sCO_2 Allam cycle power plant, in: The 6th International Supercritical CO_2 Power Cycles Symposium, 27-29 March, Pittsburgh Pennsylvania, 2018.

[102] S.J. Bae, Y. Ahn, J. Lee, S.G. Kim, S. Baik, J.I. Lee, Experimental and numerical investigation of supercritical CO_2 test loop transient behavior near the critical point operation, Appl. Therm. Eng. 99 (4) (2016) 572–582, http://dx.doi.org/10.1016/j.applthermaleng.2016.01.075.

[103] J. Wang, Y. Huang, J. Zang, G. Liu, Preliminary design considerations of a MW_e scale supercritical CO_2 integral test loop, in: Proceedings of ASME Turbo Expo 2016: Turbomachinery Technical Conference and Exposition, 13-17 June, Seoul, South Korea, 2016, pp. GT2016–56426.

[104] sCO2-Flex, 2020, https://www.sco2-flex.eu/ [Last accessed: 08/06/2020].

[105] M. Binotti, G. Di Marcoberardino, P. Iora, C. Invernizzi, G. Manzolini, Supercritical carbon dioxide/alternative fluid blends for efficiency upgrade of solar power plant, in: 3rd European Supercritical CO_2 Conference, 19-20 September, Paris, France, 2019, p. 141, http://dx.doi.org/10.17185/duepublico/48892.

[106] W. Kays, Compact heat exchangers-Guidance for engineers, WS Atkins Consultants Ltd, 2000.

[107] L. Chordia, M.A. Portnoff, E. Green, High Temperature Heat Exchanger Design and Fabrication for Systems with Large Pressure Differentials, Tech. Rep., United States, 2017, http://dx.doi.org/10.2172/1349235.

[108] Y. Le Moullec, Conceptual study of a high efficiency coal-fired power plant with CO_2 capture using a supercritical CO_2 Brayton cycle, Energy 49 (2013) 32–46, http://dx.doi.org/10.1016/j.energy.2012.10.022.

[109] K. Thulukkanam, Heat Exchanger Design Handbook, CRC press, 2013.

[110] L. Chai, S.A. Tassou, Modelling and performance analysis of heat exchangers for supercritical CO_2 power systems, in: 5th Sustainable Thermal Energy Management International Conference, 14-16 May, Hangzhou, China, 2019.

[111] J.S. Kwon, S. Son, J.Y. Heo, J.I. Lee, Compact heat exchangers for supercritical CO_2 power cycle application, Energy Convers. Manage. 209 (2020) 112666, http://dx.doi.org/10.1016/j.enconman.2020.112666.

[112] L. Chai, S.A. Tassou, A review of printed circuit heat exchangers for helium and supercritical CO_2 Brayton cycles, Therm. Sci. Eng. Prog. 18 (2020) 100543, http://dx.doi.org/10.1016/j.tsep.2020.100543.

[113] C. Huang, W. Cai, Y. Wang, Y. Liu, Q. Li, B. Li, Review on the characteristics of flow and heat transfer in printed circuit heat exchangers, Appl. Therm. Eng. 153 (2019) 190–205, http://dx.doi.org/10.1016/j.applthermaleng.2019.02.131.

[114] D. Fleming, J. Pasch, T. Conboy, M. Carlson, Testing platform and commercialization plan for heat exchanging systems for SCO2 power sycles, in: Proceedings of ASME Turbo Expo 2013: Turbomachinery Technical Conference and Exposition, Vol. V008T34A012, 3-7 June 3–7, San Antonio, Texas, US, 2013, http://dx.doi.org/10.1115/GT2013-95125.

[115] P. Fourspring, J. Nehrbauer, S. Sullivan, J. Nash, Testing of compact recuperators for a supercritical CO_2 Brayton power cycle, in: The 4th International Symposium on Supercritical CO_2 Power Cycles, 9-10 September, Pittsburgh, Pennsylvania, USA, 2014.

[116] M.D. Carlson, Sandia progress on advanced heat exchangers for sCO_2 Brayton cycles, Tech. Rep., Sandia National Lab (SNL-NM), Albuquerque, NM, United States, 2014, URL https://www.osti.gov/servlets/purl/1221560.

[117] V. Gnielinski, New equations for heat and mass transfer in the turbulent flow in pipes and channels, NASA STI/Recon Tech. Rep. A 41 (1) (1975) 8–16.

[118] S.K. Mylavarapu, X. Sun, R.E. Glosup, R.N. Christensen, M.W. Patterson, Thermal hydraulic performance testing of printed circuit heat exchangers in a high-temperature helium test facility, Appl. Therm. Eng. 65 (1) (2014) 605–614, http://dx.doi.org/10.1016/j.applthermaleng.2014.01.025.

[119] J. Abraham, E. Sparrow, J. Tong, Heat transfer in all pipe flow regimes: laminar, transitional/intermittent, and turbulent, Int. J. Heat Mass Transfer 52 (3) (2009) 557–563, http://dx.doi.org/10.1016/j.ijheatmasstransfer.2008.07.009.

[120] M. Chen, X. Sun, R.N. Christensen, S. Shi, I. Skavdahl, V. Utgikar, P. Sabharwall, Experimental and numerical study of a printed circuit heat exchanger, Ann. Nucl. Energy 97 (2016) 221–231, http://dx.doi.org/10.1016/j.anucene.2016.07.010.

[121] J.-W. Seo, Y.-H. Kim, D. Kim, Y.-D. Choi, K.-J. Lee, Heat transfer and pressure drop characteristics in straight microchannel of printed circuit heat exchangers, Entropy 17 (5) (2015) 3438—3457, http://dx.doi.org/10.3390/e17053438.

[122] K. Nikitin, Y. Kato, L. Ngo, Printed circuit heat exchanger thermal–hydraulic performance in supercritical CO_2 experimental loop, Int. J. Refrig. 29 (5) (2006) 807–814, http://dx.doi.org/10.1016/j.ijrefrig.2005.11.005.

[123] T.L. Ngo, Y. Kato, K. Nikitin, T. Ishizuka, Heat transfer and pressure drop correlations of microchannel heat exchangers with S-shaped and zigzag fins for carbon dioxide cycles, Exp. Therm Fluid Sci. 32 (2) (2007) 560–570, http://dx.doi.org/10.1016/j.expthermflusci.2007.06.006.

[124] I.H. Kim, H.C. No, Physical model development and optimal design of PCHE for intermediate heat exchangers in HTGRs, Nucl. Eng. Des. 243 (2012) 243–250, http://dx.doi.org/10.1016/j.nucengdes.2011.11.020.

[125] S.G. Kim, Y. Lee, Y. Ahn, J.I. Lee, CFD Aided approach to design printed circuit heat exchangers for supercritical CO_2 Brayton cycle application, Ann. Nucl. Energy 92 (2016) 175–185, http://dx.doi.org/10.1016/j.anucene.2016.01.019.

[126] M. Chen, X. Sun, R.N. Christensen, I. Skavdahl, V. Utgikar, P. Sabharwall, Pressure drop and heat transfer characteristics of a high-temperature printed circuit heat exchanger, Appl. Therm. Eng. 108 (2016) 1409–1417, http://dx.doi.org/10.1016/j.applthermaleng.2016.07.149.

[127] S.-J. Yoon, J. O'Brien, M. Chen, P. Sabharwall, X. Sun, Development and validation of nusselt number and friction factor correlations for laminar flow in semi-circular zigzag channel of printed circuit heat exchanger, Appl. Therm. Eng. 123 (2017) 1327–1344, http://dx.doi.org/10.1016/j.applthermaleng.2017.05.135.

[128] N. Tsuzuki, M. Utamura, T.L. Ngo, Nusselt number correlations for a microchannel heat exchanger hot water supplier with S-shaped fins, Appl. Therm. Eng. 29 (16) (2009) 3299–3308, http://dx.doi.org/10.1016/j.applthermaleng.2009.05.004.

[129] S.H. Yoon, H.C. NO, G.B. Kang, Assessment of straight, zigzag, S-shape, and airfoil PCHEs for intermediate heat exchangers of HTGRs and SFRs, Nucl. Eng. Des. 270 (2014) 334–343, http://dx.doi.org/10.1016/j.nucengdes.2014.01.006.

[130] W. Chu, X. Li, T. Ma, Y. Chen, Q. Wang, Study on hydraulic and thermal performance of printed circuit heat transfer surface with distributed airfoil fins, Appl. Therm. Eng. 114 (2017) 1309–1318, http://dx.doi.org/10.1016/j.applthermaleng.2016.11.187.

[131] R. Winterton, Where did the Dittus and Boelter equation come from?, Int. J. Heat Mass Transfer 41 (4) (1998) 809–810, http://dx.doi.org/10.1016/S0017-9310(97)00177-4.

[132] J. Jackson, Fluid flow and convective heat transfer to fluids at supercritical pressure, Nucl. Eng. Des. 264 (2013) 24–40, http://dx.doi.org/10.1016/j.nucengdes.2012.09.040.

[133] E. Krasnoshchekov, Experimental study of heat exchange in carbon dioxide in the supercritical range at high temperature drops, High Temp. 4 (1966) 375–382.

[134] L. Chai, S.A. Tassou, Effect of cross-section geometry on the thermohydraulic characteristics of supercritical CO_2 in minichannels, Energy Procedia 161 (2019) 446–453, http://dx.doi.org/10.1016/j.egypro.2019.02.077.

[135] L. Chai, K.M. Tsamos, S.A. Tassou, Modelling and evaluation of the thermo-hydraulic performance of finned-tube supercritical carbon dioxide gas coolers, Energies 13 (5) (2020) 1031, http://dx.doi.org/10.3390/en13051031.

[136] Z.H. Ayub, Plate heat exchanger literature survey and new heat transfer and pressure drop correlations for refrigerant evaporators, Heat Transfer Eng. 24 (5) (2003) 3–16, http://dx.doi.org/10.1080/01457630304056.

[137] M.M. Abu-Khader, Plate heat exchangers: Recent advances, Renew. Sustain. Energy Rev. 16 (4) (2012) 1883–1891, http://dx.doi.org/10.1016/j.rser.2012.01.009.

[138] T.M. Abou Elmaaty, A. Kabeel, M. Mahgoub, Corrugated plate heat exchanger review, Renew. Sustain. Energy Rev. 70 (2017) 852–860, http://dx.doi.org/10.1016/j.rser.2016.11.266.

[139] A.S. Wanniarachchi, U. Ratnam, B.E. Tilton, K. Dutta-Roy, Approximate correlations for chevron-type plate heat exchangers, 1995.

[140] Y. Zhu, Y. Huang, S. Lin, C. Li, P. Jiang, Study of convection heat transfer of CO_2 at supercritical pressures during cooling in fluted tube-in-tube heat exchangers, Int. J. Refrig. 104 (2019) 161–170, http://dx.doi.org/10.1016/j.ijrefrig.2019.03.033.

[141] B.M. Fronk, S. Garimella, Water-coupled carbon dioxide microchannel gas cooler for heat pump water heaters: Part I - Experiments, Int. J. Refrig. 34 (1) (2011) 7–16, http://dx.doi.org/10.1016/j.ijrefrig.2010.05.004.

[142] Y. Yang, M. Li, K. Wang, Y. Ma, Study of multi-twisted-tube gas cooler for CO_2 heat pump water heaters, Appl. Therm. Eng. 102 (2016) 204–212, http://dx.doi.org/10.1016/j.applthermaleng.2016.03.123.

[143] H.-K. Oh, C.-H. Son, New correlation to predict the heat transfer coefficient in-tube cooling of supercritical CO_2 in horizontal macro-tubes, Exp. Therm Fluid Sci. 34 (8) (2010) 1230–1241, http://dx.doi.org/10.1016/j.expthermflusci.2010.05.002.

[144] S.M. Liao, T.S. Zhao, Measurements of heat transfer coefficients from supercritical carbon dioxide flowing in horizontal mini/micro channels, Trans. Amer. Soc. Mech. Eng. J. Heat Transfer 124 (3) (2002) 413–420, http://dx.doi.org/10.1115/1.1423906.

[145] S.M. Liao, T.S. Zhao, An experimental investigation of convection heat transfer to supercritical carbon dioxide in miniature tubes, Int. J. Heat Mass Transfer 45 (25) (2002) 5025–5034, http://dx.doi.org/10.1016/S0017-9310(02)00206-5.

[146] S.H. Yoon, J.H. Kim, Y.W. Hwang, Heat transfer and pressure drop characteristics during the in-tube cooling process of carbon dioxide in the supercritical region, Int. J. Refrig. 26 (8) (2003) 857–864, http://dx.doi.org/10.1016/S0140-7007(03)00096-3.

[147] C. Dang, E. Hihara, In-tube cooling heat transfer of supercritical carbon dioxide. Part 1. Experimental measurement, Int. J. Refrig. 27 (7) (2004) 736–747, http://dx.doi.org/10.1016/j.ijrefrig.2004.04.018.

[148] C. Dang, E. Hihara, In-tube cooling heat transfer of supercritical carbon dioxide. Part 2. Comparison of numerical calculation with different turbulence models, Int. J. Refrig. 27 (7) (2004) 748–760, http://dx.doi.org/10.1016/j.ijrefrig.2004.04.017.

[149] X.L. Huai, S. Koyama, T.S. Zhao, An experimental study of flow and heat transfer of supercritical carbon dioxide in multi-port mini channels under cooling conditions, Chem. Eng. Sci. 60 (12) (2005) 3337–3345, http://dx.doi.org/10.1016/j.ces.2005.02.039.

[150] X.L. Huai, S. Koyama, Heat transfer characteristics of supercritical CO_2 flow in small-channeled structures, Exp. Heat Transfer 20 (1) (2007) 19–33, http://dx.doi.org/10.1080/08916150600977424.

[151] C.H. Son, S.J. Park, An experimental study on heat transfer and pressure drop characteristics of carbon dioxide during gas cooling process in a horizontal tube, Int. J. Refrig. 29 (4) (2006) 539–546, http://dx.doi.org/10.1016/j.ijrefrig.2005.10.010.

[152] N.M. Schnurr, Heat transfer to carbon dioxide in the immediate vicinity of the critical point, J. Heat Transfer 91 (1) (1969) 16–20, http://dx.doi.org/10.1115/1.3580086.

[153] G.A. Adebiyi, W.B. Hall, Experimental investigation of heat transfer to supercritical pressure carbon dioxide in a horizontal pipe, Int. J. Heat Mass Transfer 19 (7) (1976) 715–720, http://dx.doi.org/10.1016/0017-9310(76)90123-X.

[154] S.R. Pidaparti, J.A. McFarland, M.M. Mikhaeil, Investigation of buoyancy effects on heat transfer characteristics of supercritical carbon dioxide in heating mode, J. Nucl. Eng. Radiat. Sci. 1 (3) (2015) 031001, http://dx.doi.org/10.1115/1.4029592.

[155] K. Tanimizu, R. Sadr, Experimental investigation of buoyancy effects on convection heat transfer of supercritical CO_2 flow in a horizontal tube, Heat Mass Transfer 52 (4) (2016) 713–726, http://dx.doi.org/10.1007/s00231-015-1580-9.

[156] P.X. Jiang, Y. Zhang, C.R. Zhao, R.F. Shi, Convection heat transfer of CO_2 at supercritical pressures in a vertical mini tube at relatively low Reynolds numbers, Exp. Therm Fluid Sci. 32 (8) (2008) 1628–1637, http://dx.doi.org/10.1016/j.expthermflusci.2008.05.006.

[157] P.X. Jiang, Y. Zhang, Y.J. Xu, R.F. Shi, Experimental and numerical investigation of convection heat transfer of CO_2 at supercritical pressures in a vertical tube at low Reynolds numbers, Int. J. Therm. Sci. 47 (8) (2008) 998–1011, http://dx.doi.org/10.1016/j.ijthermalsci.2007.08.003.

[158] L. Cheng, G. Ribatski, J.R. Thome, Analysis of supercritical CO_2 cooling in macro- and micro-channels, Int. J. Refrig. 31 (8) (2008) 1301–1316, http://dx.doi.org/10.1016/j.ijrefrig.2008.01.010.

[159] L.F. Cabeza, A. de Gracia, A.I. Fernández, . Supercritical CO_2 as heat transfer fluid: A review, Appl. Therm. Eng. 125 (2017) 799–810, http://dx.doi.org/10.1016/j.applthermaleng.2017.07.049.

[160] B. Pint, R. Brese, High-temperature materials, in: K. Brun, P. Friedman, R. Dennis (Eds.), Fundamentals and Applications of Supercritical Carbon Dioxide (SCO_2) Based Power Cycles, Woodhead Publishing, 2017, pp. 67–104, http://dx.doi.org/10.1016/B978-0-08-100804-1.00004-9, Ch. 4.

[161] V. Badescu, G.C. Lazaroiu, L. Barelli, Power Engineering: Advances and Challenges, Part A: Thermal, Hydro and Nuclear Power, CRC Press, 2018.

[162] P.J. Maziasz, R.W. Swindeman, Selecting and developing advanced alloys for creep-resistance for microturbine recuperator applications, J. Eng. Gas Turbines Power 125 (1) (2002) 310–315, http://dx.doi.org/10.1115/1.1499729.

[163] P.J. Maziasz, B.A. Pint, R.W. Swindeman, K.L. More, E. Lara-Curzio, Selection, development and testing of stainless steels and alloys for high-temperature recuperator applications, in: Proceedings of ASME Turbo Expo 2003, 2003, pp. 763–771, http://dx.doi.org/10.1115/GT2003-38762.

[164] P. Maziasz, B. Pint, J. Shingledecker, N. Evans, Y. Yamamoto, K. More, E. Lara-Curzio, Advanced alloys for compact, high-efficiency, high-temperature heat-exchangers, Int. J. Hydrogen Energy 32 (16) (2007) 3622–3630, http://dx.doi.org/10.1016/j.ijhydene.2006.08.018.

[165] H. Osman, A. Borhana, M. Tamin, Material parameters for creep rupture of austenitic stainless steel foils, J. Mater. Eng. Perform. 23 (8) (2014) 2858–2863, http://dx.doi.org/10.1007/s11665-014-1070-0.

[166] N.D. Evans, P.J. Maziasz, J.P. Shingledecker, Y. Yamamoto, Microstructure evolution of alloy 625 foil and sheet during creep at 750 °C, Mater. Sci. Eng. A 498 (1) (2008) 412–420, http://dx.doi.org/10.1016/j.msea.2008.08.017.

[167] X. Li, D. Kininmont, R. Le Pierres, S.J. Dewson, Alloy 617 for the high temperature diffusion-bonded compact heat exchangers, in: Proceedings of ICAPP, Vol. 8, 2008, pp. 282–288.

[168] J. Klöwer, R. Husemann, M. Bader, Development of nickel alloys based on alloy 617 for components in 700 °C power plants, Procedia Eng. 55 (2013) 226–231, http://dx.doi.org/10.1016/j.proeng.2013.03.247.

[169] M. Anderson, G. Nellis, M. Corradini, Materials, Turbomachinery and Heat Exchangers for Supercritical CO_2 Systems, Tech. Rep., United States, 2012, http://dx.doi.org/10.2172/1053848.

[170] K. Sridharan, M. Anderson, G. Cao, J. Jelinek, V. Firouzdor, T. Allen, Corrosion testing of materials in high temperature supercritical carbon-dioxide environment, in: The 3rd International Symposium on Supercritical CO_2 Power Cycles, 24-25 May, Boulder, Colorado, USA, 2011.

[171] G. Cao, V. Firouzdor, K. Sridharan, M. Anderson, T. Allen, Corrosion of austenitic alloys in high temperature supercritical carbon dioxide, Corros. Sci. 60 (2012) 246–255, http://dx.doi.org/10.1016/j.corsci.2012.03.029.

[172] V. Firouzdor, K. Sridharan, G. Cao, M. Anderson, T. Allen, Corrosion of a stainless steel and nickel-based alloys in high temperature supercritical carbon dioxide environment, Corros. Sci. 69 (2013) 281–291, http://dx.doi.org/10.1016/j.corsci.2012.11.041.

[173] H.J. Lee, H. Kim, S.H. Kim, C. Jang, Corrosion and carburization behavior of chromia-forming heat resistant alloys in a high-temperature supercritical-carbon dioxide environment, Corros. Sci. 99 (2015) 227–239, http://dx.doi.org/10.1016/j.corsci.2015.07.007.

[174] H.J. Lee, G.O. Subramanian, S.H. Kim, C. Jang, Effect of pressure on the corrosion and carburization behavior of chromia-forming heat-resistant alloys in high-temperature carbon dioxide environments, Corros. Sci. 111 (2016) 649–658, http://dx.doi.org/10.1016/j.corsci.2016.06.004.

[175] F. Rouillard, F. Charton, G. Moine, Corrosion behavior of different metallic materials in supercritical carbon dioxide at 550 °C and 250 bars, Corrsion 67 (9) (2011) 095001–095001–7, http://dx.doi.org/10.5006/1.3628683.

[176] G.R. Holcomb, C. Carney, O.N. Doğan, Oxidation of alloys for energy applications in supercritical CO_2 and H_2O, Corros. Sci. 109 (2016) 22–35, http://dx.doi.org/10.1016/j.corsci.2016.03.018.

[177] B. Adam, L. Teeter, J. Mahaffey, M. Anderson, L. Árnadóttir, J.D. Tucker, Effects of corrosion in supercritical CO_2 on the microstructural evolution in 800h alloy, Oxid. Met. 90 (3–4) (2018) 453–468, http://dx.doi.org/10.1007/s11085-018-9852-7.

[178] Y. Gui, Z. Liang, Q. Zhao, Corrosion and carburization behavior of heat-resistant steels in a high-temperature supercritical carbon dioxide environment, Oxid. Met. 92 (1–2) (2019) 123–136, http://dx.doi.org/10.1007/s11085-019-09917-x.

[179] Z. Liang, Y. Gui, Y. Wang, Q. Zhao, Corrosion performance of heat-resisting steels and alloys in supercritical carbon dioxide at 650 °C and 15 MPa, Energy 175 (2019) 345–352, http://dx.doi.org/10.1016/j.energy.2019.03.014.

[180] B.A. Pint, J. Lehmusto, M.J. Lance, J.R. Keiser, Effect of pressure and impurities on oxidation in supercritical CO_2, Mater. Corros. 70 (8) (2019) 1400–1409, http://dx.doi.org/10.1002/maco.201810652.

[181] M.H.S. Bidabadi, Y. Zheng, A. Rehman, L. Yang, C. Zhang, H. Chen, Zhi-GangYang, Effect of CO_2 gas pressure on composition, growth rate, and structure of duplex oxide formed on 9cr steel at 550°C, Corros. Sci. 163 (2020) 108252, http://dx.doi.org/10.1016/j.corsci.2019.108252.

[182] S.H. Kim, J.-H. Cha, C. Jang, I. Sah, Microstructure and tensile properties of diffusion bonded austenitic fe-based alloys—before and after exposure to high temperature supercritical- CO_2 , Metals 10 (4) (2020) 480, http://dx.doi.org/10.3390/met10040480.

[183] I.G. Wright, B.A. Pint, J.P. Shingledecker, D. Thimsen, Materials considerations for supercritical CO_2 turbine cycles, in: Proceedings of ASME Turbo Expo 2013: Turbomachinery Technical Conference and Exposition, 3-7 June 3–7, San Antonio, Texas, US, 2013, http://dx.doi.org/10.1115/GT2013-94941.

[184] A. Cagnac, M. Mecheri, S. Bedogni, Configuration of a flexible and efficient sCO_2 cycle for fossil power plant, in: 3rd European Supercritical CO_2 Conference, 19-20 September, Paris, France, 2019, http://dx.doi.org/10.17185/duepublico/48907.

[185] A. Moisseytsev, J.J. Sienicki, Modeling of the SNL S-CO_2 loop with ANL plant dynamics code, in: Plant Systems, Structures, and Components; Safety and Security; Next Generation Systems; Heat Exchangers and Cooling Systems, vol. 2, 2012, pp. 641–650, http://dx.doi.org/10.1115/ICONE20-POWER2012-54548.

[186] A. Moisseytsev, J. Sienicki, Simulation of IST turbomachinery power-neutral tests with the ANL plant dynamics code, in: The 6th International Symposium on Supercritical CO_2 Power Cycles, 27-29 March, Pittsburgh Pennsylvania, 2018.

[187] T.Q. Trinh, Dynamic Response of the Supercritical CO_2 Brayton Recompression Cycle to Various System Transients (Ph.D. thesis), Massachusetts Institute of Technology, 2009.

[188] G. Xiao, K. Xing, J. Zhang, Y. Le Moullec, P. Zhou, T. Yang, M. Ni, K. Cen, Heat transfer characteristics of sCO_2 and dynamic simulation model of sCO_2 loop, in: 3rd European Supercritical CO_2 Conference, 19-20 September, Paris, France, 2019, http://dx.doi.org/10.17185/duepublico/48881.

[189] R. Singh, A.S. Rowlands, S.A. Miller, Effects of relative volume-ratios on dynamic performance of a direct-heated supercritical carbon-dioxide closed Brayton cycle in a solar-thermal power plant, Energy 55 (2013) 1025–1032, http://dx.doi.org/10.1016/j.energy.2013.03.049.

[190] M.T. Luu, D. Milani, R. McNaughton, A. Abbas, Dynamic modelling and start-up operation of a solar-assisted recompression supercritical CO_2 Brayton power cycle, Appl. Energy 199 (2017) 247–263, http://dx.doi.org/10.1016/j.apenergy.2017.04.073.

[191] R. Singh, S.A. Miller, A.S. Rowlands, P.A. Jacobs, Dynamic characteristics of a direct-heated supercritical carbon-dioxide Brayton cycle in a solar thermal power plant, Energy 50 (2013) 194–204, http://dx.doi.org/10.1016/j.energy.2012.11.029.

[192] V.K. Avadhanula, T.J. Held, Transient modeling of a supercritical CO_2 power cycle and comparison with test data, in: Oil and Gas Applications; Supercritical CO2 Power Cycles; Wind Energy, vol. 9, 2017, http://dx.doi.org/10.1115/GT2017-63279, V009T38A007.

[193] M. Marchionni, S.S. Saravi, G. Bianchi, S.A. Tassou, Modelling and performance analysis of a supercritical CO_2 system for high temperature industrial heat to power conversion at off-design conditions, in: 3rd European Supercritical CO_2 Conference, 19-20 September, Paris, France, 2019, pp. 281–289, http://dx.doi.org/10.17185/duepublico/48908, 133.

[194] M.T. Luu, D. Milani, R. McNaughton, A. Abbas, Analysis for flexible operation of supercritical CO_2 Brayton cycle integrated with solar thermal systems, Energy 124 (2017) 752–771, http://dx.doi.org/10.1016/j.energy.2017.02.040.

[195] P. Mahapatra, S.E. Zitney, J. Albright, E.A. Liese, Advanced regulatory control of a 10 MW_e supercritical CO_2 recompression Brayton cycle towards improving power ramp rates, in: The 6th International Symposium on Supercritical CO_2 Power Cycles, 27-29 March, Pittsburgh Pennsylvania, 2018.

[196] E. Hakkarainen, T. Sihvonen, J. Lappalainen, Dynamic modelling and simulation of CSP plant based on supercritical carbon dioxide closed Brayton cycle, AIP Conf. Proc. 1850 (1) (2017) 070004, http://dx.doi.org/10.1063/1.4984418.

[197] M. Marchionni, G. Bianchi, A. Karvountzis-Kontakiotis, A. Pesyridis, S.A. Tassou, An appraisal of proportional integral control strategies for small scale waste heat to power conversion units based on organic Rankine cycle, Energy 163 (2018) 1062–1076, http://dx.doi.org/10.1016/j.energy.2018.08.156.

[198] S.A. Wright, R.F. Radel, M.E. Vernon, P.S. Pickard, G.E. Rochau, Operation and Analysis of a Supercritical CO_2 Brayton Cycle, Tech. Rep., United States, 2010, http://dx.doi.org/10.2172/984129.

[199] J.J. Dyreby, S.A. Klein, G.F. Nellis, D.T. Reindl, Modeling off-design operation of a supercritical carbon dioxide Brayton cycle, in: The 3rd International Symposium on Supercritical CO_2 Power Cycles, 24-25 May, Boulder, Colorado, USA, 2011.

[200] A. Moisseytsev, K. Kulesza, J. Sienicki, et al., Control System Options and Strategies for Supercritical CO_2 Cycles, Tech. Rep., Argonne National Lab (ANL), Argonne, IL, United States, 2009.

[201] J.J. Dyreby, S.A. Klein, G.F. Nellis, D.T. Reindl, Modeling off-design and part-load performance of supercritical carbon dioxide power cycles, in: Supercritical CO2 Power Cycles; Wind Energy; Honors and Awards, vol. 8, 2013, http://dx.doi.org/10.1115/GT2013-95824.

[202] S. Modekurti, J. Eslick, B. Omell, D. Bhattacharyya, D.C. Miller, S.E. Zitney, Design, dynamic modeling, and control of a multistage CO2 compression system, Int. J. Greenh. Gas Control 62 (2017) 31–45, http://dx.doi.org/10.1016/j.ijggc.2017.03.009.

[203] M. Marchionni, L. Chai, G. Bianchi, S.A. Tassou, Numerical modelling and transient analysis of a printed circuit heat exchanger used as recuperator for supercritical CO_2 heat to power conversion systems, Appl. Therm. Eng. 161 (2019) 114190, http://dx.doi.org/10.1016/j.applthermaleng.2019.114190.

[204] J. Kwon, J.I. Lee, Development of accelerated PCHE off-design performance model for optimizing power system control strategies in s-CO_2 system, in: The 6th International Symposium on Supercritical CO_2 Power Cycles, 27-29 March, Pittsburgh Pennsylvania, 2018.

[205] R. Singh, M.P. Kearney, C. Manzie, Extremum-seeking control of a supercritical carbon-dioxide closed Brayton cycle in a direct-heated solar thermal power plant, Energy 60 (2013) 380–387, http://dx.doi.org/10.1016/j.energy.2013.08.001.

[206] A. Heifetz, R. Vilim, Turbine bypass, mass inventory, and mixed-mode generator power control of s-CO_2 recompression cycle, Nucl. Technol. 189 (3) (2015) 268–277, http://dx.doi.org/10.13182/NT13-113.

[207] A. Vojacek, T. Melichar, P. Hajek, F. Doubek, T. Hoppe, Experimental investigations and simulations of the control system in supercritical CO_2 loop, in: 3rd European Supercritical CO_2 Conference, 19-20 September, Paris, France, 2019, http://dx.doi.org/10.17185/duepublico/48916.

[208] M.T. Luu, D. Milani, R. McNaughton, A. Abbas, Advanced control strategies for dynamic operation of a solar-assisted recompression supercritical CO_2 Brayton power cycle, Appl. Therm. Eng. 136 (2018) 682–700, http://dx.doi.org/10.1016/j.applthermaleng.2018.03.021.

[209] N. Carstens, Dynamic Response and Safety Implications for Supercritical CO_2 Brayton Cycles Coupled to Gen-IV Reactors (Ph.D. thesis), Massachusetts Institute of Technology, 2007.

[210] D. Bitsch, J. Chaboseau, Paper 11: Power level control of a closed loop gas turbine, by natural transfer of gas between the loop and auxiliary tanks, in: Nuclear Gas Turbines, pp. 111–115, http://dx.doi.org/10.1680/ngt.44678.0014.

[211] B.S. Oh, J.I. Lee, Study of autonomous control system for s-CO_2 power cycle, in: 3rd European Supercritical CO_2 Conference, 19-20 September, Paris, France, 2019, pp. 345–352, http://dx.doi.org/10.17185/duepublico/48913, 145.

[212] A.J. Hacks, T. Freutel, M. Strätz, A. Vojacek, F. Hecker, J. Starflinger, D. Brillert, Operational experiences and design of the sCO2-HERO loop, in: 3rd European Supercritical CO_2 Conference, 19-20 September, Paris, France, 2019, p. 132, http://dx.doi.org/10.17185/duepublico/48906.

[213] B.S. Oh, S.G. Kim, S.K. Cho, J.I. Lee, Start up modeling of s-CO_2 cooled KAIST micro modular reactor using extended turbomachinery performance map, in: 2nd European Supercritical CO_2 Conference, 30-31 August, Essen, Germany, 2018, http://dx.doi.org/10.17185/duepublico/46096.

[214] K.J. Kimball, K.D. Rahner, J.P. Nehrbauer, E.M. Clementoni, Supercritical carbon dioxide Brayton cycle development overview, in: Proceedings of ASME Turbo Expo 2013: Turbomachinery Technical Conference and Exposition, Vol. V008T34A005, 3-7 June, San Antonio, Texas, US, 2013, http://dx.doi.org/10.1115/GT2013-94268.

[215] E. Clementoni, T. Cox, M. King, Initial transient power operation of a supercritical carbon dioxide Brayton cycle with thermal-hydraulic control, in: The 5th International Supercritical CO_2 Power Cycles Symposium, 28-31 March, San Antonio, Texas, U.S., 2016, pp. 29–31, URL http://sco2symposium.com/papers2016/Testing/060paper.pdf.

[216] T.E. Drennen, sCO_2 Brayton system market analysis, Tech. Rep., Sandia National Laboratories, Albuquerque, New Mexico, 2020, pp. SAND2020–3248.

[217] C. Mendez, G. Rochau, sCO_2 Brayton Cycle: Roadmap to sCO_2 Power Cycles NE Commercial Applications, Tech. Rep. SAND-2018-6187, Sandia National Laboratories, Albuquerque, New Mexico, 2018, http://dx.doi.org/10.2172/1452896.

[218] M. Poerner, A. Rimpel, Waste heat recovery, in: K. Brun, P. Friedman, R. Dennis (Eds.), Fundamentals and Applications of Supercritical Carbon Dioxide (SCO_2) Based Power Cycles, Woodhead Publishing, 2017, pp. 255–267, http://dx.doi.org/10.1016/B978-0-08-100804-1.00010-4.

[219] S. Park, J. Kim, M. Yoon, D. Rhim, C. Yeom, Thermodynamic and economic investigation of coal-fired power plant combined with various supercritical CO_2 Brayton power cycle, Appl. Therm. Eng. 130 (2018) 611–623, http://dx.doi.org/10.1016/j.applthermaleng.2017.10.145.

[220] N. Ferrari, L. Mancuso, J. Davison, P. Chiesa, E. Martelli, M.C. Romano, Oxy-turbine for power plant with CO_2 capture, Energy Procedia 114 (2017) 471–480, http://dx.doi.org/10.1016/j.egypro.2017.03.1189.

[221] N.T. Weiland, C.W. White, Techno-economic analysis of an integrated gasification direct-fired supercritical CO_2 power cycle, Fuel 212 (2018) 613–625, http://dx.doi.org/10.1016/j.fuel.2017.10.022.

[222] S.A. Wright, C.S. Davidson, W.O. Scammell, Thermo-economic analysis of four sCO_2 waste heat recovery power systems, in: The 5th International Supercritical CO_2 Power Cycles Symposium, 28-31 March, San Antonio, Texas, U.S., 2016.

[223] Z. Bai, G. Zhang, Y. Yang, Z. Wang, Design performance simulation of a supercritical CO_2 cycle coupling with a steam cycle for gas turbine waste heat recovery, J. Energy Resour. Technol. 141 (10) (2019) http://dx.doi.org/10.1115/1.4043391.

[224] J. Song, X. Li, K. Wang, C.N. Markides, Parametric optimisation of a combined supercritical CO_2 (s-CO_2) cycle and organic rankine cycle (ORC) system for internal combustion engine (ICE) waste-heat recovery, Energy Convers. Manage. 218 (2020) 112999, http://dx.doi.org/10.1016/j.enconman.2020.112999.

[225] O. Kizilkan, Performance assessment of steam Rankine cycle and sCO_2 Brayton cycle for waste heat recovery in a cement plant: A comparative study for supercritical fluids, Int. J. Energy Res. http://dx.doi.org/10.1002/er.5138.

[226] V.T. Cheang, R.A. Hedderwick, C. McGregor, Benchmarking supercritical carbon dioxide cycles against steam Rankine cycles for concentrated solar power, Sol. Energy 113 (2015) 199–211, http://dx.doi.org/10.1016/j.solener.2014.12.016.

[227] J. Schmitt, J. Wilkes, T. Allison, J. Bennett, K. Wygant, R. Pelton, Lowering the levelized cost of electricity of a concentrating solar power tower with a supercritical carbon dioxide power cycle, in: Proceedings of ASME Turbo Expo 2017: Turbomachinery Technical Conference and Exposition, Vol. 9, 26-30 June, Charlotte, NC, U.S., 2017, pp. GT2017–64958, http://dx.doi.org/10.1115/GT2017-64958.

[228] T. Neises, C. Turchi, Supercritical carbon dioxide power cycle design and configuration optimization to minimize levelized cost of energy of molten salt power towers operating at 650 °C, Sol. Energy 181 (January) (2019) 27–36, http://dx.doi.org/10.1016/j.solener.2019.01.078.

[229] A.S. Alsagri, A. Chiasson, M. Gadalla, Viability assessment of a concentrated solar power tower with a supercritical CO_2 Brayton cycle power plant, J. Sol. Energy Eng. 141 (10) (2019) 051006, http://dx.doi.org/10.1115/1.4043515.

[230] Y.L. Moullec, Z. Qi, J. Zhang, P. Zhou, Z. Yang, W. Chen, X. Wang, S. Wang, Shouhang-EDF 10mwe supercritical CO_2 cycle + CSP demonstration project, in: 3rd European Supercritical CO_2 Conference, 19-20 September, Paris, France, 2019, p. 120, http://dx.doi.org/10.17185/duepublico/48884.

[231] M.J. Li, Y.J. Jie, H.H. Zhu, G.J. Qi, M.J. Li, The thermodynamic and cost-benefit-analysis of miniaturized lead-cooled fast reactor with supercritical CO_2 power cycle in the commercial market, Prog. Nucl. Energy 103 (2018) 135–150, http://dx.doi.org/10.1016/j.pnucene.2017.11.015.

[232] C. Wu, S. sen Wang, J. Li, Exergoeconomic analysis and optimization of a combined supercritical carbon dioxide recompression Brayton/organic flash cycle for nuclear power plants, Energy Convers. Manage. 171 (2018) 936–952, http://dx.doi.org/10.1016/j.enconman.2018.06.041.

[233] M.J. Li, J.L. Xu, F. Cao, J.Q. Guo, Z.X. Tong, H.H. Zhu, The investigation of thermo-economic performance and conceptual design for the miniaturized lead-cooled fast reactor composing supercritical CO_2 power cycle, Energy 173 (2019) 174–195, http://dx.doi.org/10.1016/j.energy.2019.01.135.

[234] S. Glos, S. Grotkamp, M. Wechsung, Assessment of performance and costs of CO_2 based next level geothermal power (NLGP) systems, in: 3rd European Supercritical CO_2 Conference, 19-20 September, Paris, France, 2019, p. 109, http://dx.doi.org/10.17185/duepublico/48876.

[235] Global Market Insights, Gas turbine market, 2020, www.gminsights.com/industry-analysis/gas-turbine-market, [Last Accessed: 2020-06-10].

[236] S. Slade, C. Palmer, Worldwide gas turbine forecasts, 2020, www.mtt-eu.com/wp-content/uploads/WORLDWIDE-GAS-TURBINE-FORECAST-Turbomachinery-Magazine.pdf, [Last accessed: 2020-06-10].

[237] Mordorintelligence, Gas turbine market, 2020, www.mordorintelligence.com/industry-reports/gas-turbine-market, [Last accessed: 2020-06-10].

[238] F.J. Brooks, GE gas turbine performance characteristics, 2020, http://ncad.net/Advo/CinerNo/ge6581b.pdf, [Last accessed: 2020-06-10].

[239] Global Market Insights, Global gas generator sets market, 2020, www.gminsights.com/industry-analysis/gas-generator-sets-market?utm_source=prnewswire.com&utm_medium=referral&utm_campaign=Paid_prnewswire, [Last accessed: 2020-06-10].

[240] L. Shi, G. Shu, H. Tian, S. Deng, A review of modified organic Rankine cycles (ORCs) for internal combustion engine waste heat recovery (ICE-whr), Renew. Sustain. Energy Rev. 92 (2018) 95–110, http://dx.doi.org/10.1016/j.rser.2018.04.023.

[241] C. Forman, I.K. Muritala, R. Pardemann, B. Meyer, Estimating the global waste heat potential, Renew. Sustain. Energy Rev. 57 (2016) 1568–1579, http://dx.doi.org/10.1016/j.rser.2015.12.192.

[242] G. Bianchi, G.P. Panayiotou, L. Aresti, S.A. Kalogirou, G.A. Florides, K. Tsamos, S.A. Tassou, P. Christodoulides, Estimating the waste heat recovery in the European Union industry, Energy Ecol. Environ. 4 (5) (2019) 211–221, http://dx.doi.org/10.1007/s40974-019-00132-7.

[243] D. Brough, H. Jouhara, The aluminium industry: A review on state-of-the-art technologies, environmental impacts and possibilities for waste heat recovery, Int. J. Thermofluids 1–2 (2020) 100007, http://dx.doi.org/10.1016/j.ijft.2019.100007.

[244] S. Karellas, A.-D. Leontaritis, G. Panousis, E. Bellos, E. Kakaras, Energetic and exergetic analysis of waste heat recovery systems in the cement industry, Energy 58 (2013) 147–156, http://dx.doi.org/10.1016/j.energy.2013.03.097.

[245] H. Zhang, H. Wang, X. Zhu, Y.-J. Qiu, K. Li, R. Chen, Q. Liao, A review of waste heat recovery technologies towards molten slag in steel industry, Appl. Energy 112 (2013) 956–966, http://dx.doi.org/10.1016/j.apenergy.2013.02.019.

[246] H. Jouhara, N. Khordehgah, S. Almahmoud, B. Delpech, A. Chauhan, S.A. Tassou, Waste heat recovery technologies and applications, Therm. Sci. Eng. Prog. 6 (2018) 268–289, http://dx.doi.org/10.1016/j.tsep.2018.04.017.

[247] IEA, Electricity generation by fuel and scenario, 2018-2040, 2020, https://www.iea.org/data-and-statistics/charts/electricity-generation-by-fuel-and-scenario-2018-2040, Accessed: 2020-06-10.

[248] Z. Li, X. Liu, Y. Shao, W. Zhong, Research and development of supercritical carbon dioxide coal-fired power systems, J. Therm. Stresses (2020) 1–30, http://dx.doi.org/10.1007/s11630-020-1282-6.

[249] J. Xu, C. Liu, E. Sun, J. Xie, M. Li, Y. Yang, J. Liu, Perspective of s-CO_2 power cycles, Energy 186 (2019) 115831, http://dx.doi.org/10.1016/j.energy.2019.07.161.

[250] D. Thimsen, P. Weitzel, Challenges in designing fuel-fired sCO_2 heaters for closed sCO_2 Brayton cycle power plants, in: The 5th International Supercritical CO_2 Power Cycles Symposium, 28-31 March, San Antonio, Texas, U.S., 2016.

[251] M. Mecheri, Y.L. Moullec, Supercritical CO_2 Brayton cycles for coal-fired power plants, Energy 103 (2016) 758–771, http://dx.doi.org/10.1016/j.energy.2016.02.111.

[252] R.J. Allam, M. Palmer, G.W. Brown, et al., System and method for high efficiency power generation using a carbon dioxide circulating working fluid, 2011, Patent US20110179799A1.

[253] D. Freed, B. Forrest, N. Rafati, J. Fetvedt, M. McGroddy, R. Allam, Progress update on the Allam cycle: Commercialization of Net Power and the Net Power demonstration facility, in: 14th Greenhouse Gas Control Technologies Conference Melbourne, 2018, pp. 21–26, URL https://papers.ssrn.com/sol3/papers.cfm?abstract_id=3366370#references-widget.

[254] Rivers Capital, Allam Cycle Zero Emission Coal Power Plant, Tech. Rep., 2019, DOE Grant Proposal 89243319CFE000015, URL https://netl.doe.gov/coal/tpg/coalfirst/DirectSupercriticalCo2.

[255] R.J. Allam, J.E. Fetvedt, B.A. Forrest, D.A. Freed, The oxy-fuel, supercritical CO_2 allam cycle: New cycle developments to produce even lower-cost electricity from fossil fuels without atmospheric emissions, in: Proceedings of ASME Turbo Expo 2014: Turbomachinery Technical Conference and Exposition, Vol. V03BT36A016, 16-20 June, Düsseldorf, Germany, 2014, pp. GT2014–26952, http://dx.doi.org/10.1115/GT2014-26952.

[256] J. Luo, O. Emelogu, T. Morosuk, G. Tsatsaronis, Exergy-based investigation of a coal-fired allam cycle, E3S Web Conf. 137 (2019) 01018, http://dx.doi.org/10.1051/e3sconf/201913701018.

[257] M. Penkuhn, G. Tsatsaronis, Exergy analysis of the Allam cycle, in: The 5th International Supercritical CO_2 Power Cycles Symposium, 28-31 March, San Antonio, Texas, U.S., 2016.

[258] D.T. Banuti, L. Shunn, S. Bose, D. Kim, Large eddy simulations of oxy-fuel combustors for direct-fired supercritical CO_2 power cycles, in: The 6th International Symposium on Supercritical CO_2 Power Cycles, 27-29 March, Pittsburgh Pennsylvania, 2018.

[259] H. Abdul-Sater, J. Lenertz, C. Bonilha, X. Lu, J. Fetvedt, A CFD simulation of coal syngas oxy-combustion in a high-pressure supercritical CO_2 environment, in: Proceedings of ASME Turbo Expo 2017: Turbomachinery Technical Conference and Exposition, Vol. V04AT04A051, 26-30 June, Charlotte, North Carolina, US, 2017, http://dx.doi.org/10.1115/GT2017-63821.

[260] S. Barak, O. Pryor, E. Ninnemann, S. Neupane, S. Vasu, X. Lu, B. Forrest, Ignition delay times of oxy-syngas and oxy-methane in supercritical CO_2 mixtures for direct-fired cycles, J. Eng. Gas Turbines Power 142 (2) (2020) http://dx.doi.org/10.1115/1.4045743.

[261] A. Rogalev, E. Grigoriev, S. Osipov, N. Rogalev, The design approach for supercritical CO_2 gas turbine, AIP Conf. Proc. 2189 (1) (2019) 020018, http://dx.doi.org/10.1063/1.5138630.

[262] N. Weiland, R. Dennis, R. Ames, S. Lawson, P. Strakey, Fossil energy, in: K. Brun, P. Friedman, R. Dennis (Eds.), Fundamentals and Applications of Supercritical Carbon Dioxide (sCO_2) Based Power Cycles, Woodhead Publishing, 2017, pp. 293–338, http://dx.doi.org/10.1016/B978-0-08-100804-1.00012-8, Ch. 12.

[263] P. Strakey, O. Dogan, G. Holcomb, G. Richards, Technology needs for fossil fuel supercritical CO_2 power systems, in: The 4th International Symposium on Supercritical CO_2 Power Cycles, 9-10 September, Pittsburgh, Pennsylvania, USA, 2014.

[264] M.T. Islam, N. Huda, A.B. Abdullah, R. Saidur, A comprehensive review of state-of-the-art concentrating solar power (CSP) technologies: Current status and research trends, Renew. Sustain. Energy Rev. 91 (8) (2018) 987–1018, http://dx.doi.org/10.1016/j.rser.2018.04.097.

[265] Abengoa Energia, D5.1 - Report on Best Available Technologies (BAT) for Central Receiver Systems, Tech. Rep., SCARABEUS project, 2019, p. 69.

[266] IRENA, Renewable power generation costs in 2019, Tech. Rep., International Renewable Energy Agency, Abu Dhabi, 2020, p. 144.

[267] C.S. Turchi, J. Stekli, P.C. Bueno, Concentrating solar power, in: K. Brun, P. Friedman, R. Dennis (Eds.), Fundamentals and Applications of Supercritical Carbon Dioxide (sCO_2) Based Power Cycles, Woodhead Publishing, 2017, pp. 269–292, http://dx.doi.org/10.1016/B978-0-08-100804-1.00011-6.

[268] T. Neises, C. Turchi, A comparison of supercritical carbon dioxide power cycle configurations with an emphasis on CSP applications, Energy Procedia 49 (2014) 1187–1196, http://dx.doi.org/10.1016/j.egypro.2014.03.128.

[269] M. Mehos, C. Turchi, J. Vidal, M. Wagner, Z. Ma, C. Ho, W. Kolb, C. Andraka, Z. Ma, A. Kruizenga, Concentrating Solar Power Gen3 Demonstration Roadmap, Tech. Rep., NREL/TP-5500-67464 National Renewable Energy Laboratory, Golden, Colorado, U.S., 2017, p. 127.

[270] M. Binotti, M. Astolfi, S. Campanari, G. Manzolini, P. Silva, Preliminary assessment of sCO_2 cycles for power generation in CSP solar tower plants, Appl. Energy 204 (2017) 1007–1017, http://dx.doi.org/10.1016/j.apenergy.2017.05.121.

[271] J. Dyreby, S. Klein, G. Nellis, D. Reindl, Design considerations for supercritical carbon dioxide brayton cycles with recompression, J. Eng. Gas Turbines Power 136 (10) (2014) 101701, http://dx.doi.org/10.1115/1.4027936.

[272] Generation IV International Forum (GIF), Technology Roadmap Update for Generation IV Nuclear Energy Systems, Tech. Rep., Nuclear Energy Agency, 2014, pp. 1–66.

[273] J.J. Sienicki, A. Moisseytsev, Nuclear power, in: K. Brun, P. Friedman, R. Dennis (Eds.), Fundamentals and Applications of Supercritical Carbon Dioxide (sCO_2) Based Power Cycles, Woodhead Publishing, 2017, pp. 339–391, http://dx.doi.org/10.1016/B978-0-08-100804-1.00013-X.

[274] P. Wu, Y. Ma, C. Gao, W. Liu, J. Shan, Y. Huang, J. Wang, D. Zhang, X. Ran, A review of research and development of supercritical carbon dioxide Brayton cycle technology in nuclear engineering applications, Nucl. Eng. Des. 368 (March) (2020) 110767, http://dx.doi.org/10.1016/j.nucengdes.2020.110767.

[275] A. Moisseytsev, J. Sienicki, Development of a Plant Dynamics Computer Code for Analysis of a Supercritical Carbon Dioxide Brayton Cycle Energy Converter Coupled to a Natural Circulation Lead-Cooled Fast Reactor, Tech. Rep., Argonne National Laboratory, Argonne, Illinois, 2006, pp. ANL–06/27.

[276] J. Sienicki, A. Moisseytsev, W. Yang, D. Wade, A. Nikiforova, P. Hanania, H. Ruy, K. Kulesaz, S. Kim, Status Report on the Small Secure Transportable Autonomous Reactor (Sstar)/lead-Cooled Fast Reactor (LFT) and Supporting Reserach and Development, Tech. Rep., Argonne National Laboratory, Argonne, Illinois, 2008, pp. ANL–GenIV–089.

[277] International Energy Agency, Technology Roadmap: Nuclear Energy, Tech. Rep., International Energy Agency, 2015, pp. 1–57.

[278] Y. Chang, P. Finck, C. Grandy, Advanced Burner Test Reactor Preconceptual Design Report, Tech. Rep., Argonne National Laboratory, Argonne, Illinois, 2006, pp. ANL–ABR–1.

[279] Y. Ahn, J.I. Lee, Study of various Brayton cycle designs for small modular sodium-cooled fast reactor, Nucl. Eng. Des. 276 (9) (2014) 128–141, http://dx.doi.org/10.1016/j.nucengdes.2014.05.032.

[280] H.J. Yoon, Y. Ahn, J.I. Lee, Y. Addad, Potential advantages of coupling supercritical CO_2 Brayton cycle to water cooled small and medium size reactor, Nucl. Eng. Des. 245 (2012) 223–232, http://dx.doi.org/10.1016/j.nucengdes.2012.01.014.

[281] S.J. Bae, J. Lee, Y. Ahn, J.I. Lee, Preliminary studies of compact Brayton cycle performance for small modular high temperature gas-cooled reactor system, Ann. Nucl. Energy 75 (2014) 11–19, http://dx.doi.org/10.1016/j.anucene.2014.07.041.

[282] H. Yu, D. Hartanto, J. Moon, Y. Kim, A conceptual study of a supercritical CO_2-cooled micro modular reactor, Energies 8 (12) (2015) 13938–13952, http://dx.doi.org/10.3390/en81212405.

[283] Y. Kato, T. Nitawaki, Y. Muto, Medium temperature carbon dioxide gas turbine reactor, Nucl. Eng. Des. 230 (2004) 195–207, http://dx.doi.org/10.1016/j.nucengdes.2003.12.002.

[284] Y. Muto, Y. Kato, Optimal cycle scheme of direct cycle supercritical CO_2 gas turbine for nuclear power generation systems, in: Challenges on Power Engineering and Environment - Proceedings of the International Conference on Power Engineering 2007, ICOPE 2007, 2007, pp. 86–92.

[285] N. Alpy, L. Cachon, D. Haubensack, J. Floyd, N. Simon, L. Gicquel, G. Rodriguez, G. Avakian, Gas cycle testing opportunity with ASTRID, the French SFR prototype, in: The 3rd International Symposium on Supercritical CO_2 Power Cycles, 24-25 May, Boulder, Colorado, U.S., 2011.

[286] J. Floyd, N. Alpy, A. Moisseytsev, D. Haubensack, G. Rodriguez, J. Sienicki, G. Avakian, A numerical investigation of the sCO_2 recompression cycle off-design behaviour, coupled to a sodium cooled fast reactor, for seasonal variation in the heat sink temperature, Nucl. Eng. Des. 260 (7) (2013) 78–92, http://dx.doi.org/10.1016/j.nucengdes.2013.03.024.

[287] Reuters, France drops plans to build sodium-cooled nuclear reactor, 2020, https://www.reuters.com/article/us-france-nuclearpower-astrid/france-drops-plans-to-build-sodium-cooled-nuclear-reactor-idUSKCN1VK0MC [Last accessed: 16/06/2020].

[288] P. Hajek, O. Frybort, Experimental loop s-CO2 SUSEN, in: The 4th International Symposium on Supercritical CO_2 Power Cycles, 9-10 September, Pittsburgh, Pennsylvania, USA, 2014, http://dx.doi.org/10.1017/CBO9781107415324.004, arXiv:arXiv:1011.1669v3.

[289] A. Vojacek, A. Hacks, T. Melichar, O. Frybort, P. Hájek, Challenges in supercritical CO_2 power cycle technology and first operational experience at CVR, in: 2nd European Supercritical CO_2 Conference, 30-31 August, Essen, Germany, 2018, p. 100, http://dx.doi.org/10.17185/duepublico/46075.

[290] J.I. Linares, A. Cantizano, B.Y. Moratilla, V. Martín-Palacios, L. Batet, Supercritical CO_2 Brayton power cycles for DEMO (demonstration power plant) fusion reactor based on dual coolant lithium lead blanket, Energy 98 (2016) 271–283, http://dx.doi.org/10.1016/j.energy.2016.01.020.

[291] A. Rovira, C. Sánchez, M.J. Montes, M. Muñoz, Proposal of optimized power cycles for the DEMO power plant (EUROfusion), Fusion Eng. Des. 148 (May) (2019) 111290, http://dx.doi.org/10.1016/j.fusengdes.2019.111290.

[292] J. Stepanek, S. Entler, J. Syblik, L. Vesely, V. Dostal, P. Zacha, Parametric study of S-CO2 cycles for the DEMO fusion reactor, Fusion Eng. Des. 160 (September) (2020) 111992, http://dx.doi.org/10.1016/j.fusengdes.2020.111992.

[293] D. Sánchez, J.M. Muñoz De Escalona, R. Chacartegui, A. Muñoz, T. Sánchez, A comparison between molten carbonate fuel cells based hybrid systems using air and supercritical carbon dioxide Brayton cycles with state of the art technology, J. Power Sources 196 (9) (2011) 4347–4354, http://dx.doi.org/10.1016/j.jpowsour.2010.09.091.

[294] S.J. Bae, Y. Ahn, J. Lee, J.I. Lee, Various supercritical carbon dioxide cycle layouts study for molten carbonate fuel cell application, J. Power Sources 270 (2014) 608–618, http://dx.doi.org/10.1016/j.jpowsour.2014.07.121.

[295] A. Baronci, G. Messina, S.J. McPhail, A. Moreno, Numerical investigation of a MCFC (molten carbonate fuel cell) system hybridized with a supercritical CO_2 Brayton cycle and compared with a bottoming organic Rankine cycle, Energy 93 (2015) 1063–1073, http://dx.doi.org/10.1016/j.energy.2015.07.082.

[296] M. Mehrpooya, P. Bahramian, F. Pourfayaz, M.A. Rosen, Introducing and analysis of a hybrid molten carbonate fuel cell-supercritical carbon dioxide Brayton cycle system, Sustain. Energy Technol. Assess. 18 (2016) 100–106, http://dx.doi.org/10.1016/j.seta.2016.10.003.

[297] B.M. Adams, T.H. Kuehn, J.M. Bielicki, J.B. Randolph, M.O. Saar, A comparison of electric power output of CO_2 plume geothermal (CPG) and brine geothermal systems for varying reservoir conditions, Appl. Energy 140 (2015) 365–377, http://dx.doi.org/10.1016/j.apenergy.2014.11.043.

[298] B.M. Adams, T.H. Kuehn, J.M. Bielicki, J.B. Randolph, M.O. Saar, On the importance of the thermosiphon effect in CPG (CO_2 plume geothermal) power systems, Energy 69 (2014) 409–418, http://dx.doi.org/10.1016/j.energy.2014.03.032.

[299] B.S. Higgins, M.P. Muir, A.D. Eastman, C.M. Oldenburg, L. Pan, Process modeling of a closed-loop SCO_2 geothermal power cycle, in: The 5th International Supercritical CO_2 Power Cycles Symposium, 29-31 March, San Antonio, Texas, U.S., 2016, http://dx.doi.org/10.1007/s13398-014-0173-7.2, arXiv:arXiv:1011.1669v3.

[300] A. Amaya, J. Scherer, J. Muir, M. Patel, B. Higgins, GreenFire energy closed-loop geothermal demonstration using supercritical carbon dioxide as working fluid, in: 45th Workshop on Geothermal Reservoir Engineering, 10-12 February, Stanford, California, U.S., 2020, pp. SGP–TR–21.

[301] M. Persichilli, A. Kacludis, E. Zdankiewicz, T. Held, Supercritical CO_2 power cycle developments and commercialization: Why sCO_2 can displace steam, in: Power-Gen India & Central Asia, 19-21 April, New Delhi, India, 2012.